Silicon detectors: From the early days to the ATLAS and CMS upgrades in the HL-LHC era

Ioannis Kopsalis

HEPHY – Institute of High Energy Physics
Academy of Sciences, Vienna
Austria

Outline and Overview

- **Introduction: Examples of silicon detectors from the early days**
- **Interaction of particles with matter – detector parameters**

  - Interaction of radiation/particles with detector material

  - Parameters characterising detectors
- **Basics of silicon detectors**

  - Principle of operation, material properties, the silicon ionization chamber (pn junction)

- **The ATLAS and CMS inner detectors**
- **Tracking detector requirements for the HL-LHC**
- **Layout of the new inner tracker (ITk)**

  - The concept of the ITk pixel and strip detector, pixel and strip sensors, strip modules

  - Radiation damage in silicon sensors
- **The High-Granularity Timing Detector in ATLAS**
- **New sensor technologies (LGADs, DMAPS etc)**
- **Summary**

The very early days of solid state detectors

- **Idea of solid state ionization chamber and first successful prototypes**
  - 1943: P.J. von Heerden, Utrecht (AgCl)
  - 1949: K.G. McKay, Bell labs (Ge – pn junction)
  - 1955 – 1965: Si mono-crystals available → surface barrier detectors at several labs (Oak Ridge, Chalk River, CEA), motivation nuclear particle spectrometers
  - 1961: G. Dearnaley, Harwell: first segmented detector, a pixel detector !
  - 1970: first strip detectors: Argonne, Fermi lab, Karlsruhe, Southampton for nuclear physics experiments
  - 1970: CCD: W.S. Boyle and G.E. Smith, Bell labs

- **Several companies in the US and Europe for detector fabrication (> 7 in 1975)**

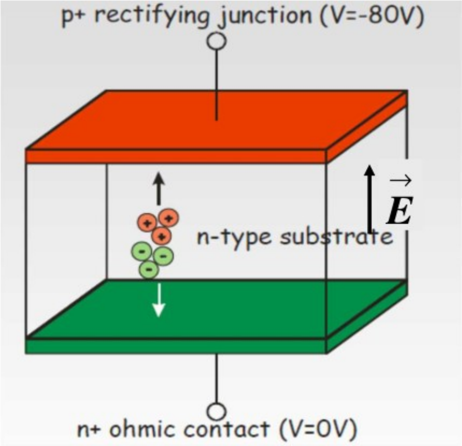

- **Typical values for Si:**
  - voltage: 50 – 500 V
  - thickness: 0.05 – 1 mm
  - signal: 1e/h-pair/3.6 eV → mip 25000 charges/0.3 mm
  - collection time: 5-50 ns
  - diffusion: few μm
  - sensitive to light ≤ 1 μm, X-rays 0.2 – 20 keV, charged particles

Si-strip detector telescope at CERN NA-11/32

- **NA-11/32 experiment (The ACCMOR Collab.):**
  - spectrometer for the study of hadronic reactions
  - lifetimes D_+, D_0, D_S, …
  - hadronic production of charm particles
- **Demonstrated excellent performance of Si strip and pixel (CCDs) detectors**

Model of NA11 spectrometer, L~30 m

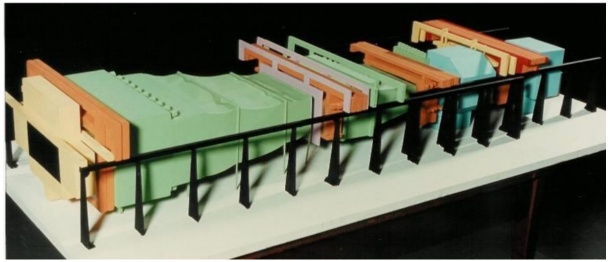

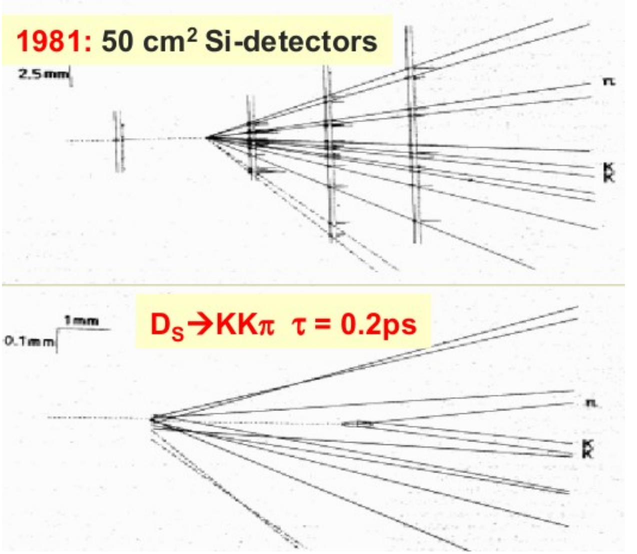

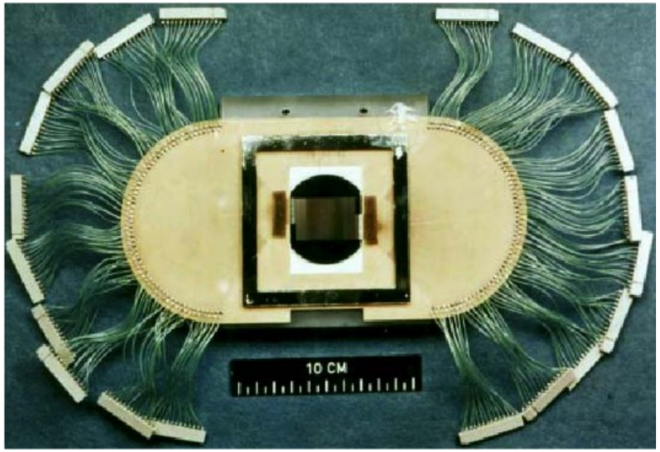

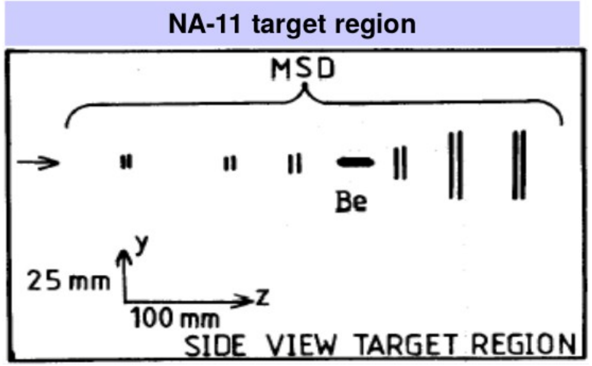

- **1981: 6 planes Si-strip detectors:**
  - 24x36 mm², 1200 strips/sensor
  - strip pitch 20 μm, 280 μm thick
  - position resolution 5.4 μm
  - total < 2000 channels
  - 100% efficiency (all channels working)

Top-quark discovery

- **Silicon strip detector, essential for the discovery of the top-quark at FNAL (1994) and also for the LEP Higgs limit**
- **CDF vertex detector at Tevatron**

  - Si area of ~11 m^2 and $4{\cdot}10^5$ readout channels

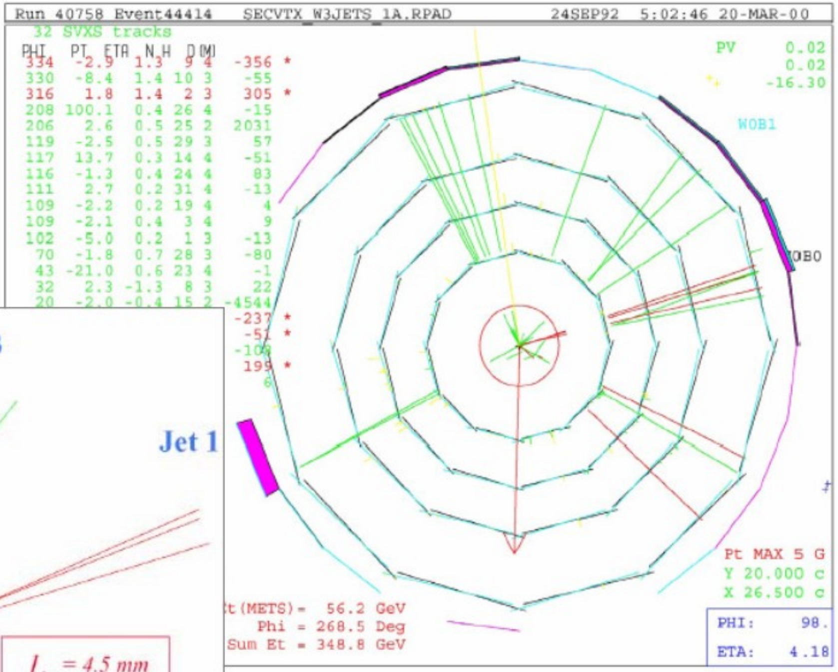

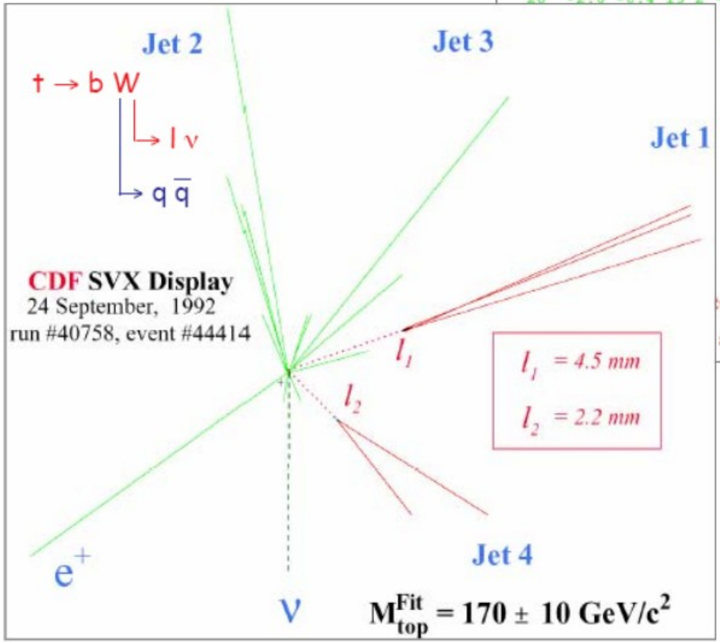

- **Today: CMS at LHC (CERN)**

  - Si area ~200 m^2 and $9.65{\cdot}10^7$ readout channels

CCDs: VXD3 vertex detector for SLD@SLC

- **VXD3 at SLD**

  - Installed in 1995, CCD pixel detector,

  307 Mpixels (ATLAS: 80 Mpixels !)

  - Layer thickness 0.4% X_0 (multiple scattering)

  - 1^{st} layer < 3 cm from beam

  - 8 μm impact parameter resolution

  - The best performing vertex detector operating so far with respect to resolution and material budget

  - Reference point for ILC vertex detectors

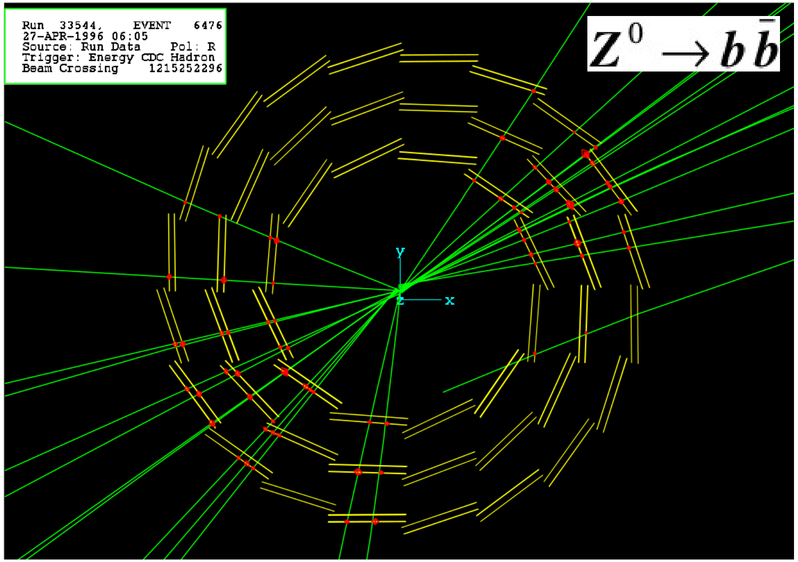

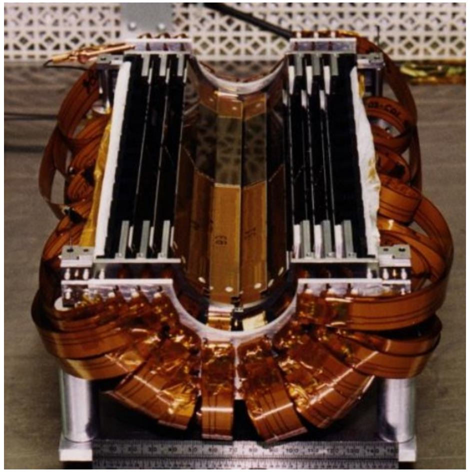

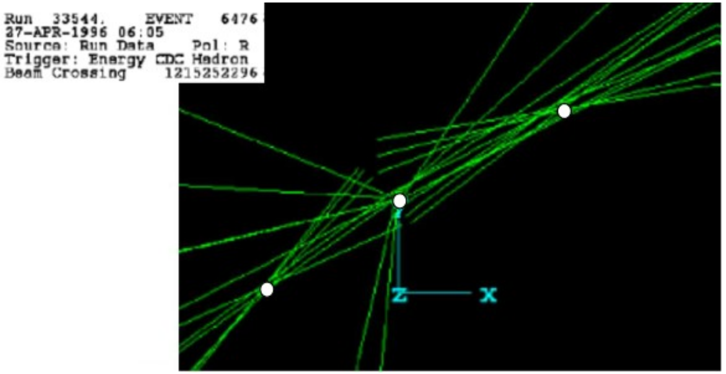

- **Leading contribution by C. Damerell (RAL PPD group) et al. in collab. with SLD@SLC**

Detection of charged particles

- dE/dx = energy loss via Coulomb scattering of electrons – ionisation:
  - mean energy loss <dE/dx> - Bethe-Bloch formula vs β
  - energy loss is a statistical process
  - discrete scattering with different results depending on “intensity” of scattering
  - primary ionisation (poisson distributed, large fluctuations per reaction)
  - secondary ionisation (mainly by high energetic primary electrons, if the energy is very high → δ - electrons)
- From dE/dx (MIP):
  - Si: 110 (e-h)/μm, 3.6 eV/(e-h) pair
  - Ge: 260 (e-h)/μm, 2.9 eV/(e-h) pair
- “Healthy” signal which can be well processed by electronics

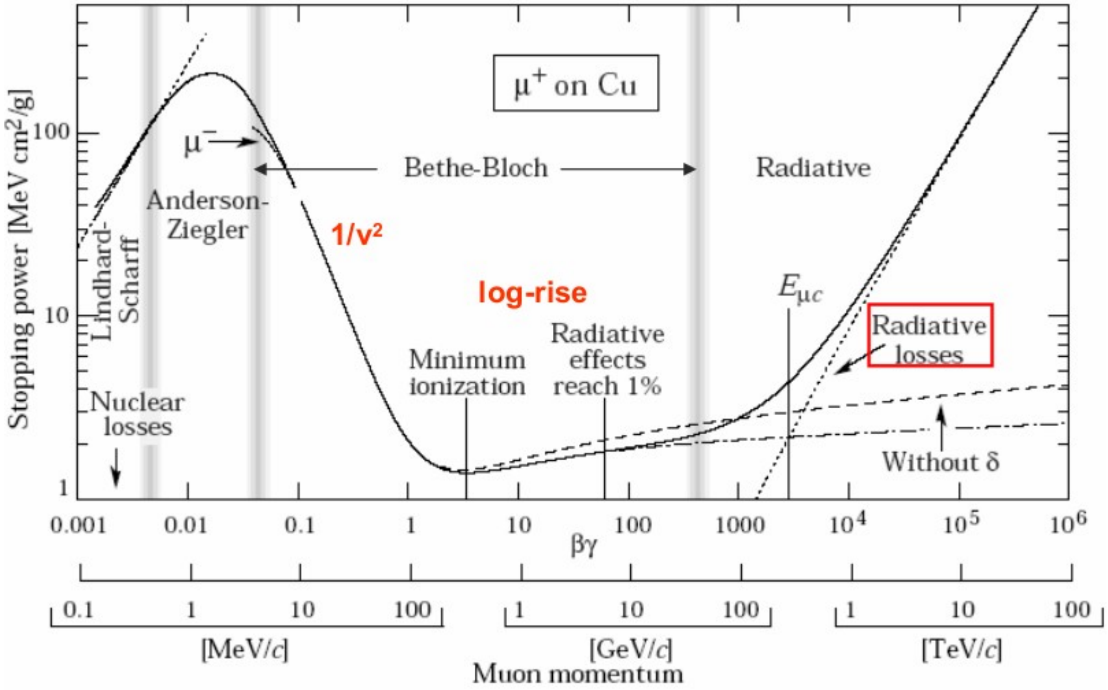

Fig. 27.1: Stopping power ($= \langle -dE/dx \rangle$) for positive muons in copper as a function of $\beta\gamma = p/Mc$ over nine orders of magnitude in momentum

Detection of charged particles

- **Fluctuations in dE/dx distribution (thin detectors)**

  - The variation width within the energy transfer of the reactions leads to large energy loss variation

  - A broad maximum: collisions with little energy loss

  - A long tail: few collisions with large energy loss

  - Straggling functions in silicon for 500 MeV pions, normalized to unity at the most probable value Δ_p/x

  - Shape of energy loss distribution depends on thickness of detector

  - For very thin detectors < 1 – 2 μm finite probability of zero signal !

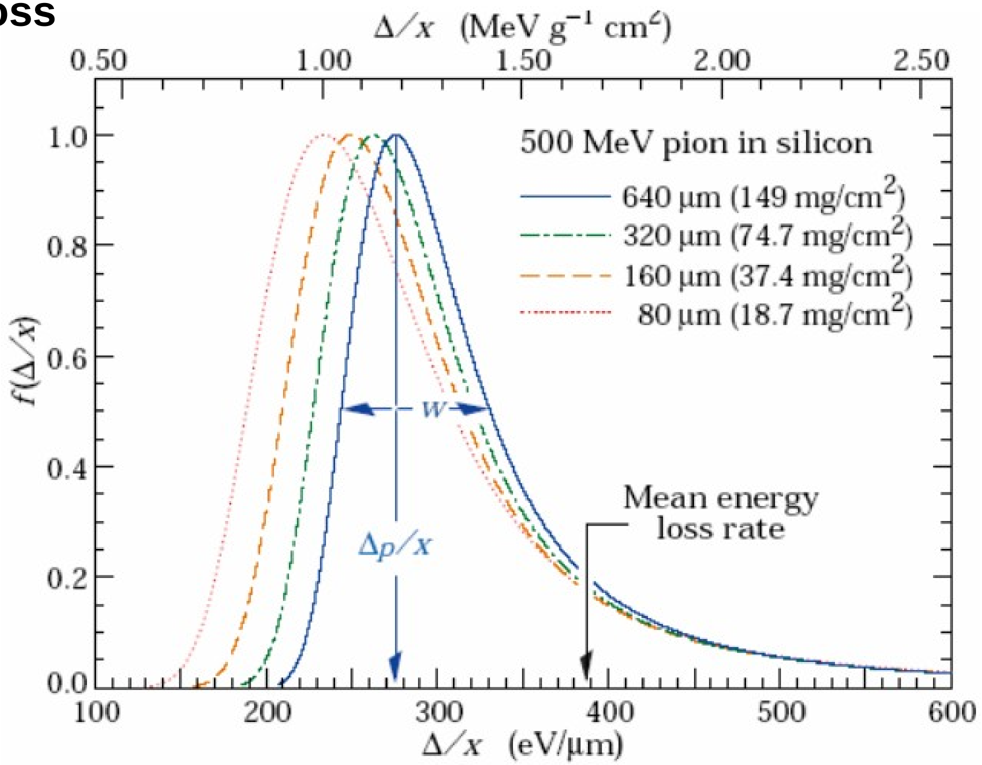

H. Bichsel, Rev. Mod. Phys. 60(1988)663

Detector characterisation

- **System = (detector) ⊗ (readout) ⊗ (calibration) ⊗ (analysis) → has to be understood !**
- **Generic detector:**

  - radiation/particle → interaction/energy deposit → signal light/charge → collect charge/signal formation → signal processing → data recording → calibration → analysis
- **Efficiency:**

  - acceptance: (recorded events) / (emitted by source): [geometry x efficiency]

  - efficiency/sensitivity: (recorded events / particles passing detector)

  - peak efficiency: (recorded events in acc. window / particles passing detector)
- **Response (resolution):**

  - spectrum from mono-energetic resolution
- **Response to 661 keV γs**

  - Ge-detector

  - organic scintillator

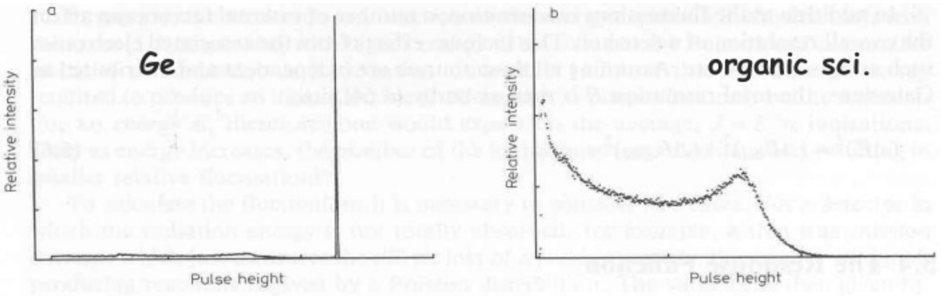

Fig. 5.2a, b. The response functions of two different detectors for 661 keV gamma rays. **(a)** shows the response of a germanium detector which has a large photoelectric cross section relative to the Compton scattering cross section at this energy. A large photopeak with a relatively small continuous Compton distribution is thus observed. **(b)** is the response of an organic scintillator detector. Since this material has a low atomic number Z, Compton scattering is predominant and only this distribution is seen in the response function

Detector characterisation

- **Response (resolution):**

  - good detector aims for Gaussian response (with little non-Gaussian tails)

  - calibration by N events with energy E

  - mean: $< S >= \frac{1}{N}\sum_{i}^{N} S_i, \quad \delta < S >= \sigma / \sqrt{N}$

  - rms resolution (σ): $\sigma^2 = \frac{1}{N-1}\sum_{i}^{N}(S_i - < S >)^2, \quad \delta(\sigma) = \sigma / \sqrt{2N}$

  - for Gauss f.: $\Gamma = 2\sqrt{2\ln 2}\,\sigma = 2.355\sigma$ **, (for box with width α:** $\sigma = a / \sqrt{12}$ **)**

  - <S> is not always the best choice: eg Landau distribution: σ → ∞ ,

  (median, truncated mean, are sometimes better choices !)

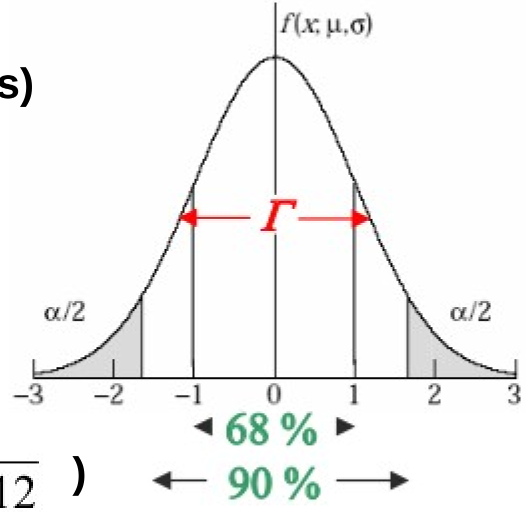

- **Calibration:** $< S >= f(E) \cong c \times E + ped$

$$\sigma = g(E), \; \sigma / E \cong c_{calib} + c_{stat} / \sqrt{E} + c_{noise} / E \; (e.g.\ for\ \ energy\ \ measurement)$$

  - c, ped … calibration constants depend on position, time etc

  - if c(E) … non-linear response

Detector characterisation

- **Time response:**

  - delay time: time between particle passage (event) and signal formation

  - dead time: minimum time distance that events can be recorded separately (depends on properties of detector and electronics, “integrating” or “dead” and on resolution criteria)

  - pile up effects: overlapping events cause a degradation of performance

  - time resolution: accuracy with which “event-time” can be measured

- **Example for counting losses due to dead time τ:**

  - n … true interaction rate [sec^{-1}]

  - m … recorded count rate [sec^{-1}]

  - τ … system dead time [sec]

$$n = \frac{m}{1 - m \times \tau}$$

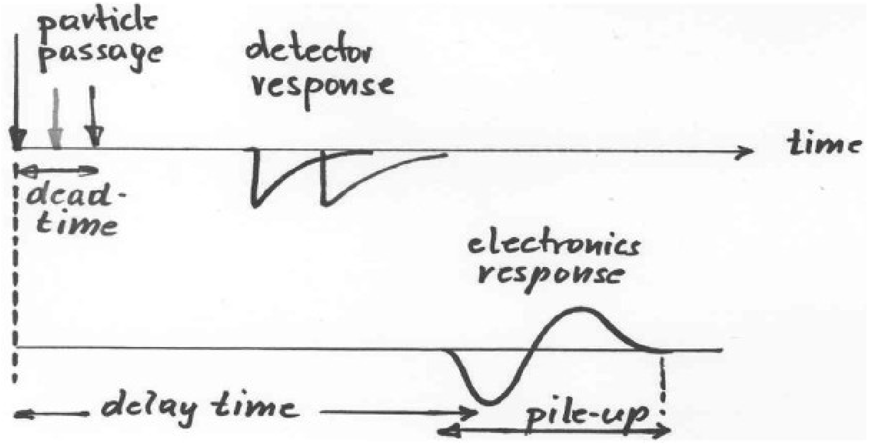

Principle of operation

- Silicon detectors are ionization chambers

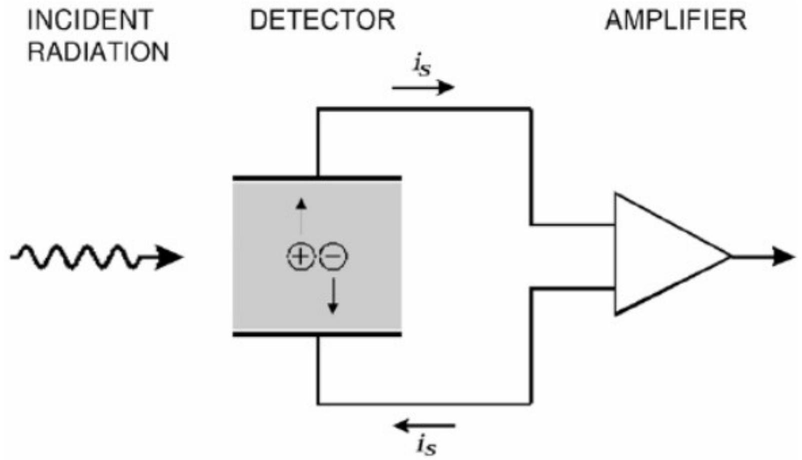

- Any material which allows charge collection can be used for an ionization chamber
- Energy required to "ionize" (produce one charge pair):

  - ~30 eV for gases and liquids

  - 1-5 eV for solid state detectors

  - few meV to break up cooper pairs
- Advantages of silicon detectors: efficient, high density, room temperature operation, highly developed μ-technology, robust, well suited for μ-electronics readout, ...

Charge carrier mobility in silicon

- Mobility μ: electrons and holes drift under the influence of electric field E
  - for low fields (Si < 5 kV/cm)
  - $\vec{v} = \mu\vec{E}$, μ … mobility
  - for high fields v ~ 10^7 cm/s
  - charge collection times for 300 μm Si detector: O (10ns)
- Drift in magnetic field
  - Lorentz angle: $tan\theta = \mu_{Hall} \cdot B_T$
  - Hall mobility, $\mu_{Hall(e)}$ = 1650 $cm^2/V\cdot s$, $\mu_{Hall(h)}$ = 310 $cm^2/V\cdot s$

    → 30º for 4 Tesla field, e^- have 165 μm shift for 300 μm
- Diffusion D_i:
  - Einstein relation: $D_i = \frac{kT}{q} \cdot \mu_i$

    → spread of charge after time t: $\sigma^2 = 2 \cdot D_i \cdot t$ (1-d proj.)

    → 6 μm for 10 ns diffuse of electrons
- Resistivity ρ: defined by $\vec{E} = \rho \cdot \vec{J}$ (J the current density)
  - for Si with both electrons (n) and holes (p) as carriers: $\rho = \frac{1}{q(\mu_n \cdot n + \mu_p \cdot p)}$

  → resistivity of intrinsic Si at room temperature: 230 kΩ·cm

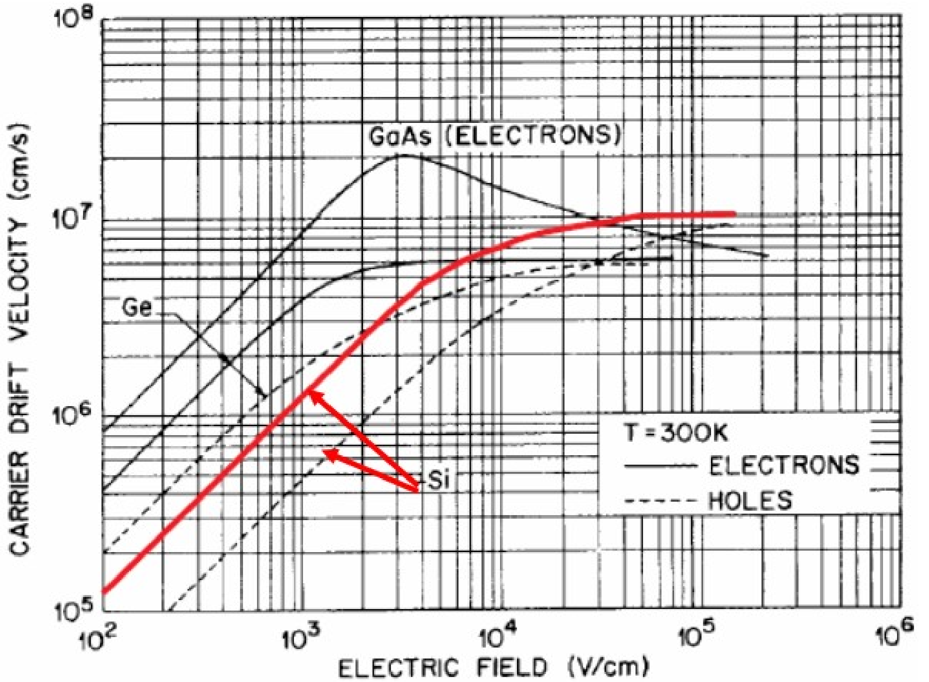

The Silicon ionization chamber - pn junction

- Thermal diffusion drives electrons and holes across pn junction
  - Generates depletion regions (no free charge carriers) with fixed space charge
  - Potential and electric field obtained from Poisson's equation: $-\frac{d^2V}{dx^2} = \frac{dE}{dx} = \frac{\rho(x)}{\epsilon}$
  - Diffusion potential (built-in potential V_{bi}) obtained by E_{Fermi} = const over junction
  - One-sided abrupt junction V_{bi}~0.65 V for n doping $1.4\cdot10^{12}$ cm^{-3} (3 kΩ·cm)
    → depth of depletion region: d ~ 25 μm
- A simple detector is a large surface diode with guard ring(s)

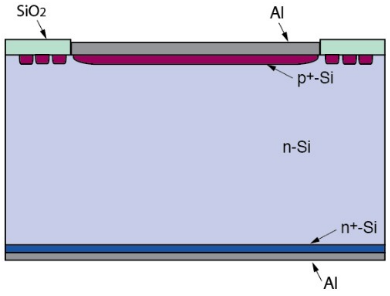

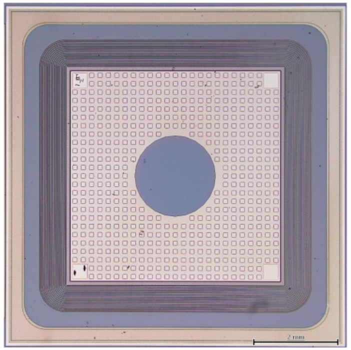

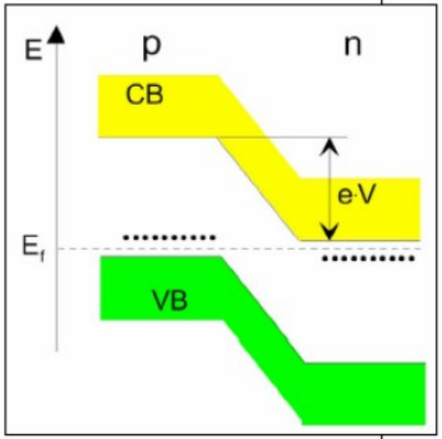

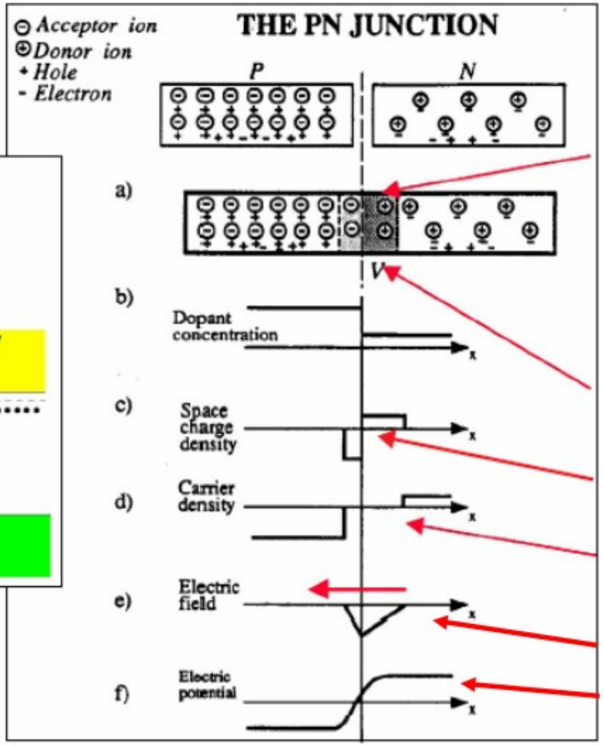

diffusion of e^- into p-zone

diffusion of h^+ into n-zone

depletion zone

asymmetry due to different level of doping

zone without free charge carriers

field linear in x

potential quadratic in x

pn junction

- **pn junction with reverse bias:**

  - apply bias voltage V_b to increase the depletion width W

  - poisson's equation (1-d, constant charge density): $V_b + V_{bi} = \frac{q}{2\varepsilon}(N_D x_n^2 + N_A x_p^2)$

  - charge neutrality: $N_D x_n = N_A x_p$

  → depletion width: $W = x_n + x_p = \sqrt{\frac{2\varepsilon(V_b + V_{bi})}{q}(\frac{1}{N_A} + \frac{1}{N_D})}$

- **For detectors highly asymmetric junctions are chosen, eg p+n (NA≫ND):**

  - depletion region xn ≫ xp, and $W \approx x_n = \sqrt{\frac{2\varepsilon(V_b + V_{bi})}{q\,N_D}} = \sqrt{2\varepsilon\mu_n\rho_n(V_b + V_{bi})}$ **(usually $V_b \gg V_{bi}$ ~ 0.65 V in Si)**

  - detector capacitance given by region of mobile charges (method to investigate N) $C = \varepsilon\frac{A}{W} = A\sqrt{\frac{\varepsilon\,q\,N_D}{2V_b}}$

- **If W ≥ detector thickness D**

  → Fully depleted detector (entire volume sensitive)

- **For D = 300 μm, n-type, ρ = 3 k·Ωcm**

  → V_b = V_D = 100 V

  → $t_{drift}(e^-)$ = 3.5 ns, $t_{drift}(h^+)$ = 11 ns

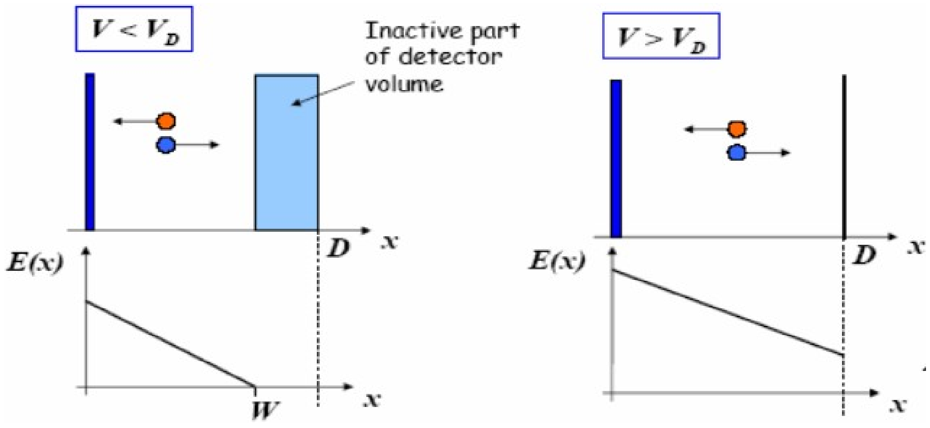

Outline and Overview

- Introduction: Examples of silicon detectors from the early days
- Interaction of particles with matter – detector parameters

  - Interaction of radiation/particles with detector material

  - Parameters characterising detectors
- Basics of silicon detectors

  - Principle of operation, material properties, the silicon ionization chamber (pn junction)

- **The ATLAS and CMS inner detectors**
- **Tracking detector requirements for the HL-LHC**
- **Layout of the new inner tracker (ITk)**

  - The concept of the ITk pixel and strip detector, pixel and strip sensors, strip modules

  - Radiation damage in silicon sensors
- **The High-Granularity Timing Detector in ATLAS**
- **New sensor technologies (LGADs, DMAPS etc)**
- **Summary**

The ATLAS inner detector

- **The current inner detector**

  - 3 pixel layers (PIX), 4 Si micro-strip layers (SCT) and straw tube quasi-continues tracker (TRT)

  - Additional pixel layer (IBL) was inserted in long shut-down 1 (LS1 – 2014)

  - Assumed pile up (μ) was 23 and bunch crossing 25 ns

  - 2T solenoidal magnetic field

- **Radiation damage**

  - PIX: designed to withstand 10^{15} 1 MeV n_{eq}/cm^2 (or $400fb^{-1}$)

  - IBL: designed to withstand 800 fb^{-1}

  - SCT: designed to withstand $2 \cdot 10^{14}$ 1 MeV n_{eq}/cm^2 (or $700fb^{-1}$)

- **Bandwidth limitation**

  - Both SCT and PIX apply zero suppression to accommodate

  <μ> up to 50

- **Occupancy limits**

  - SCT in the HL-LHC environment will not be able to resolve close by tracks in the core of high P_T jets

  - TRT will approach 100% occupancy and tracking efficiency will suffer

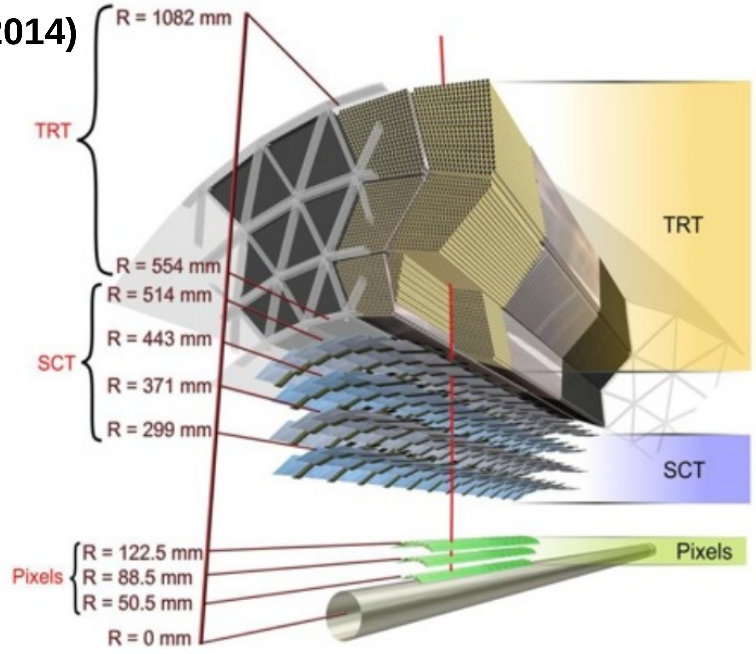

Phase-II upgrade of the Large Hadron Collider

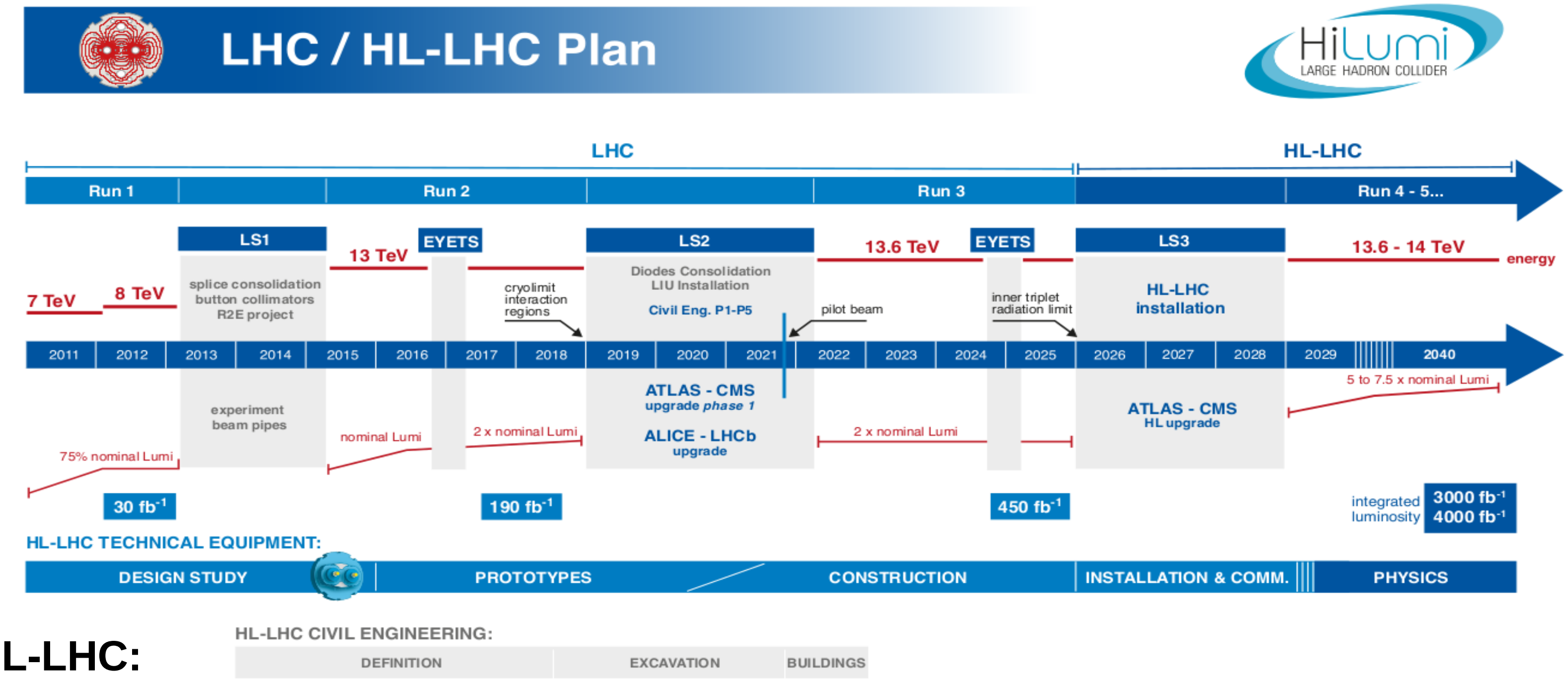

- **From LHC to HL-LHC:**
  - **- proton-proton collisions with up to 14 TeV at higher intensity**
  - **- instantaneous nominal luminosity x5 - 7.5 → Increased particle densities**
  - **- integrated luminosity x10 → Increased radiation damage and increase of overlapping proton-proton events (pile-up)**

For Phase-II upgrade: new all silicon tracker for ATLAS

Layout of the new Inner Tracker (ITk)

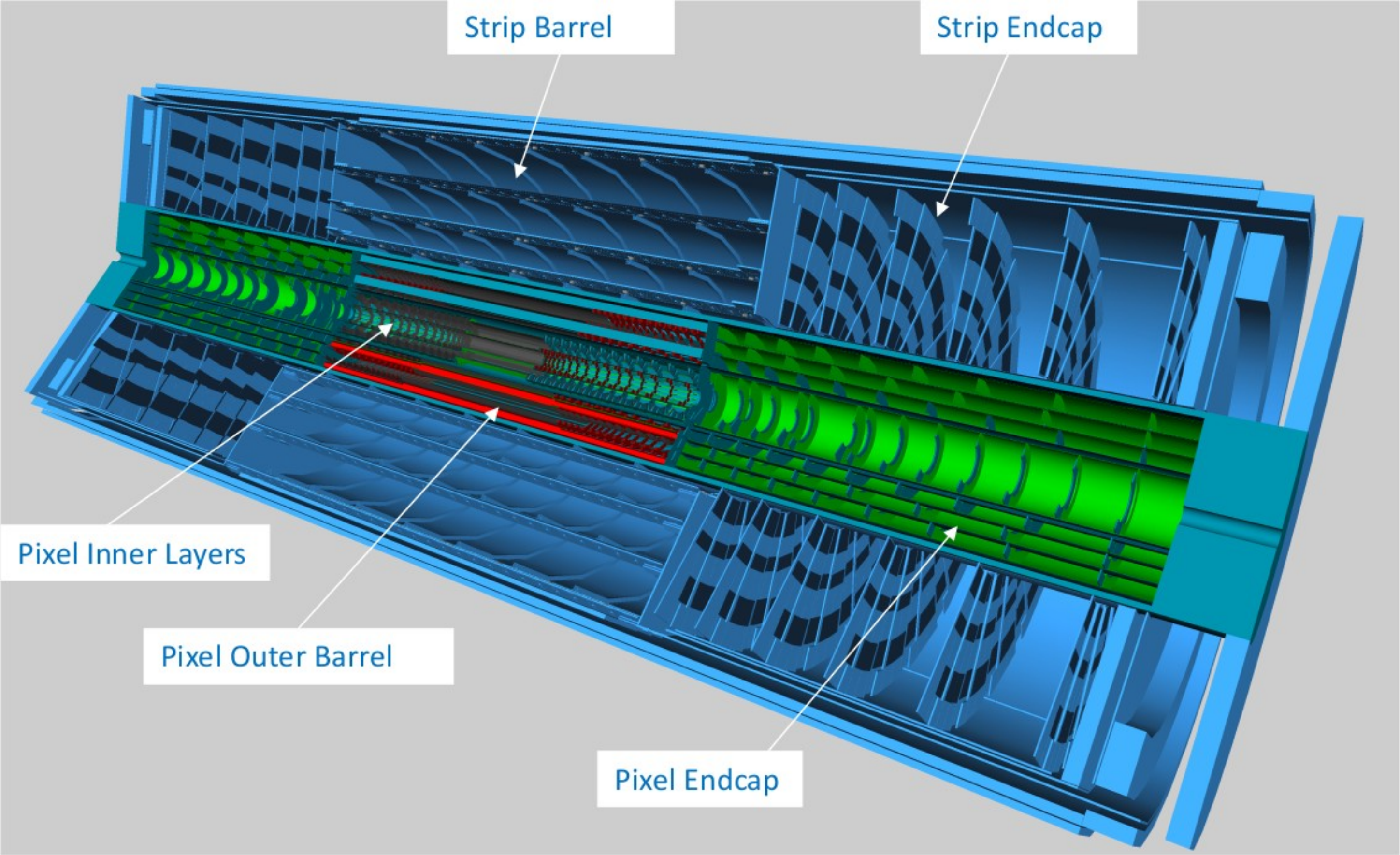

The ATLAS – pixel detectors

- **The read-out chip is mounted on top of the pixels (bump bonding)**
- **Each pixel has its own readout amplifier**
- **Can choose proper process for sensor and readout separately**
- **Fast readout and radiation-tolerant**
- **However, high material budget and high power dissipation**

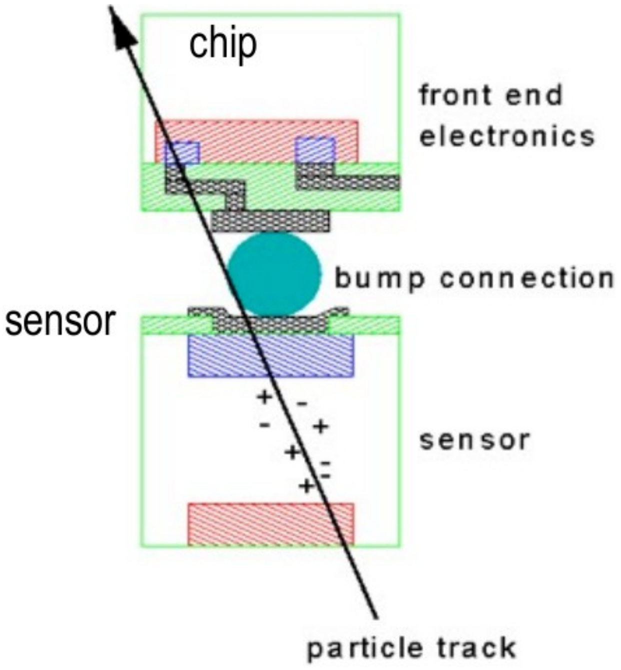

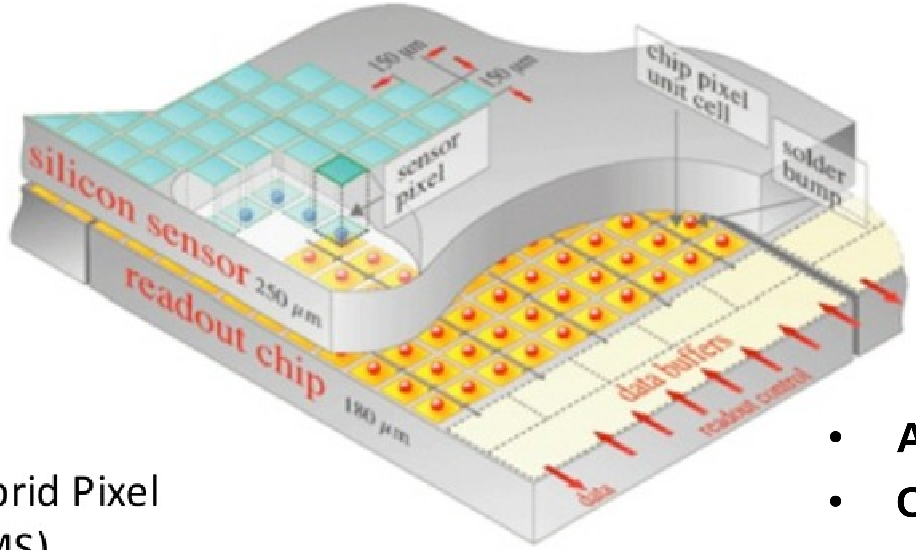

Hybrid Pixel
(CMS)

- **ATLAS pixels (IBL): ~80 M channels (150x150 μm^2)**
- **CMS pixels: ~65 M channels (50x400 μm^2)**

Pixel sensors: hybrid planar technology

- **Thin n-in-p planar sensors**
  - **- Dies of 4x4 cm^2, 100/150 μm thick, bias voltage up to 600 V**
  - **- Signal ~10 ke$^-$ and ~6 ke$^-$ after HL-LHC dose**
  - **- Test beam result for 50x50 μm^2 planar module irradiated at 3·10^{15} n$_{eq}$/cm^2**

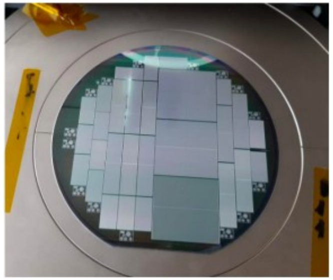

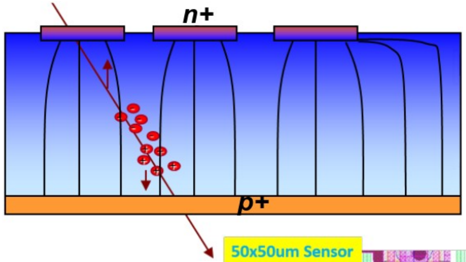

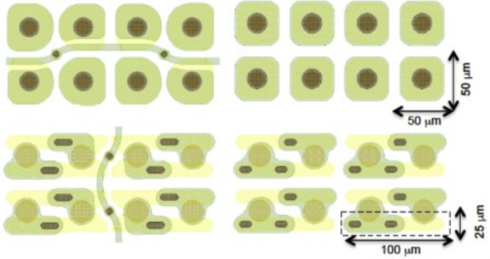

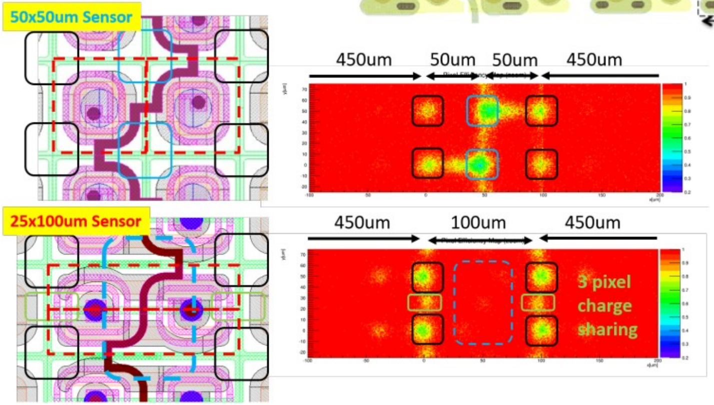

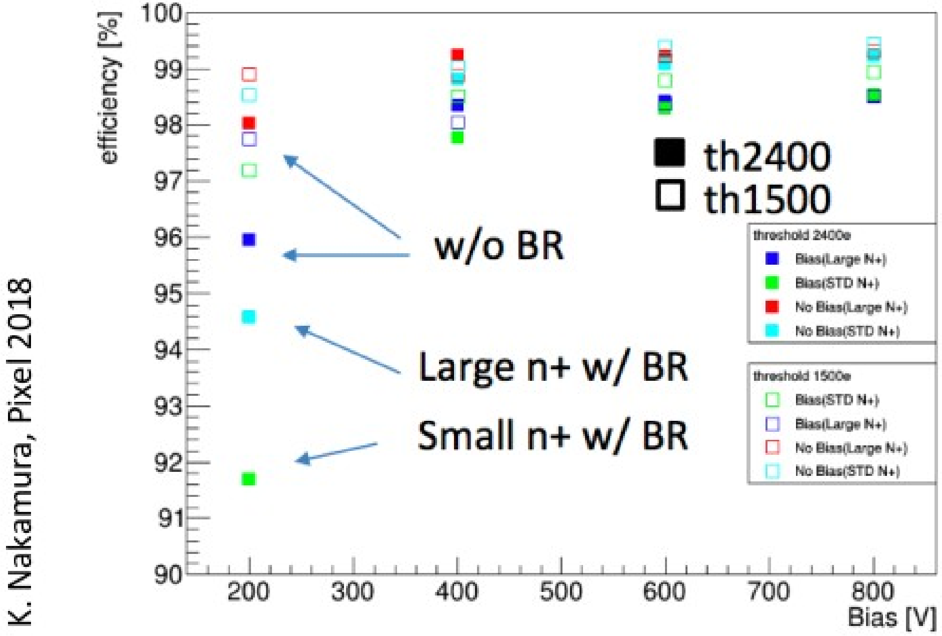

Pixel sensors: hybrid 3D technology

- **3D sensors**
  - **- For innermost layer: $1.3\cdot10^{16}$ n_{eq}/cm^2 for 2000 fb^{-1}**
  - **- Dies of 2x2 cm^2, 150 μm thickness plus 100-200 μm support wafer**
  - **- Pixel size of 25x100 μm^2 challenging for radiation hardness and only in part of L0 foreseen**
  - **- Efficiency >97% at perpendicular track incidence**

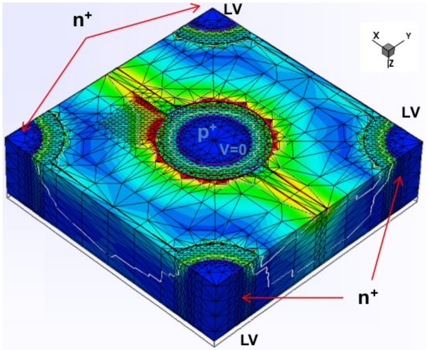

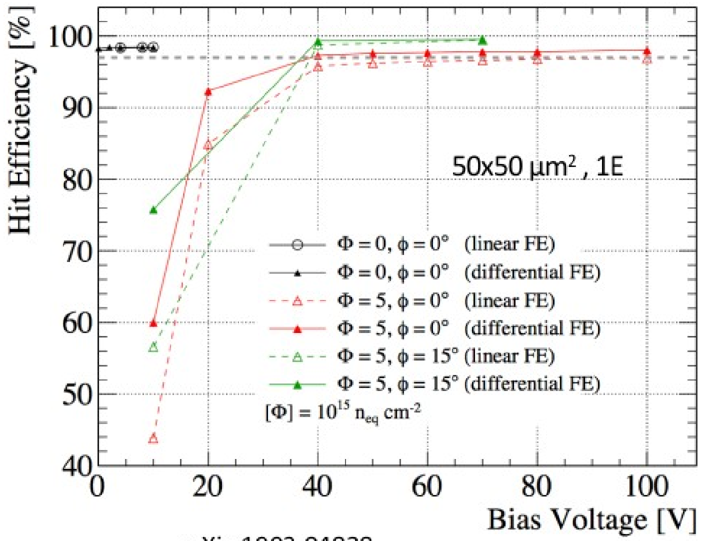

arXiv:1903.04838

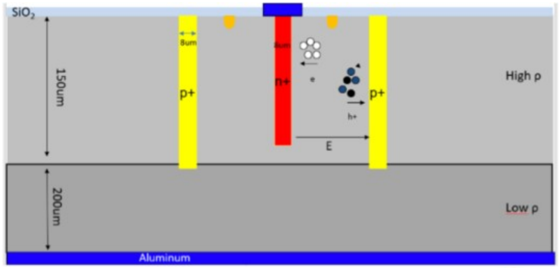

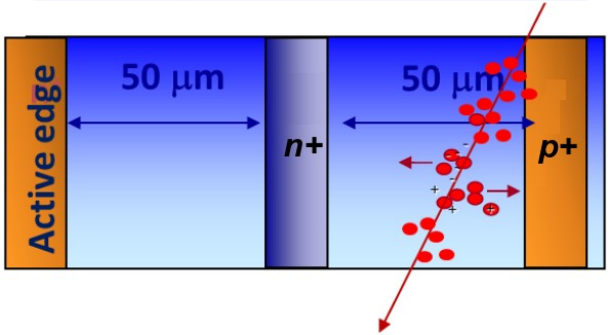

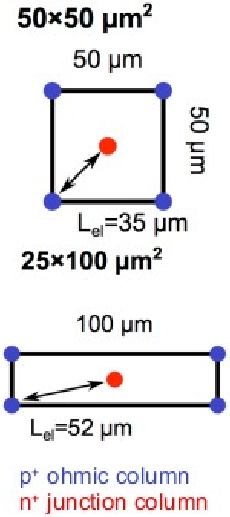

Strip sensor QA/QC program for ATLAS ITk

- **n-in-p float-zone sensors with p-stop isolation and ~320 μm thickness**
  - Strip length 8-50 mm depending on region, all sensors received from HPK for pre-production, production sensors are qualified now by the institutes
  - QA and QC methods exercised at production sites, sensor PRR has been completed successfully, setups commissioned etc

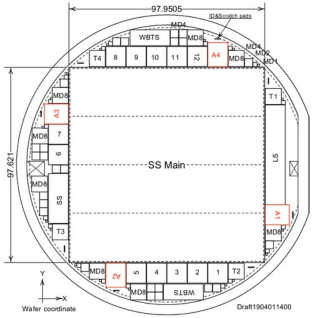

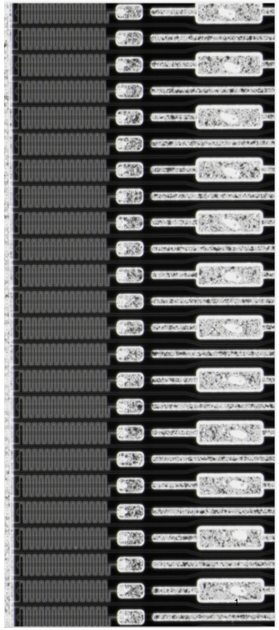

Short Strip sensor

Parameter	Specification
Length	97621 (± 20 μm dicing error)
Width	97950 (± 20 μm dicing error)
Edge distance ("slim edge")	450 (longitudinal), 550 (lateral) (± 20 μm dicing error)
#Strips	1282 (=128 ch/chip*10 chips+2xfield shaping strip)
- pitch	75.5 μm
- implant width	16 μm
- metal width	22 μm (AC coupling to implant)
- identification	(•) every 10th, 1st and last

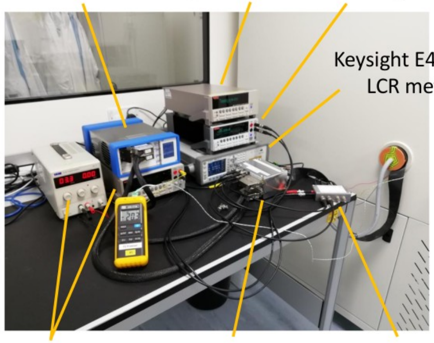

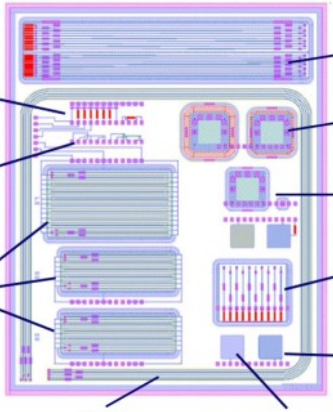

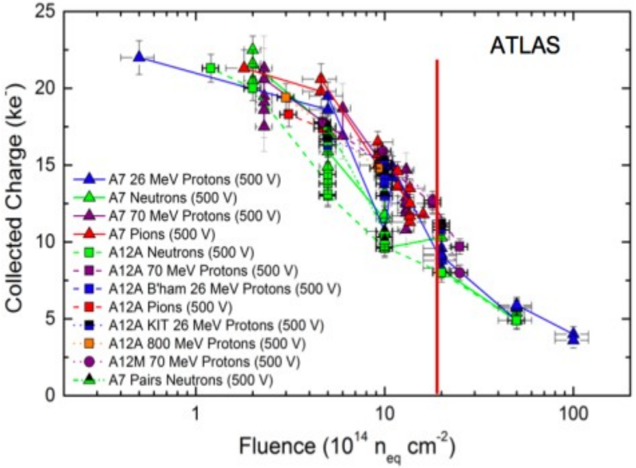

Strip modules assembly for ATLAS ITk

- Several modules assembled and evaluated before and after irradiation to HL-LHC fluences
- During module assembly, the hybrids and power boards are glued directly to the sensor
- Tooling finalised for mass production
- Module production site qualification will be completed soon

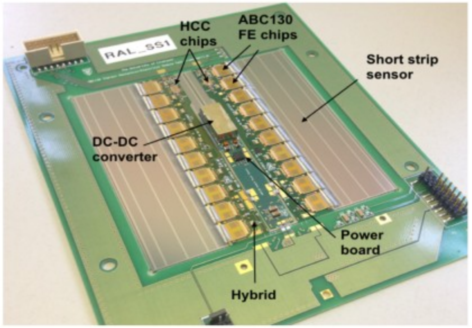

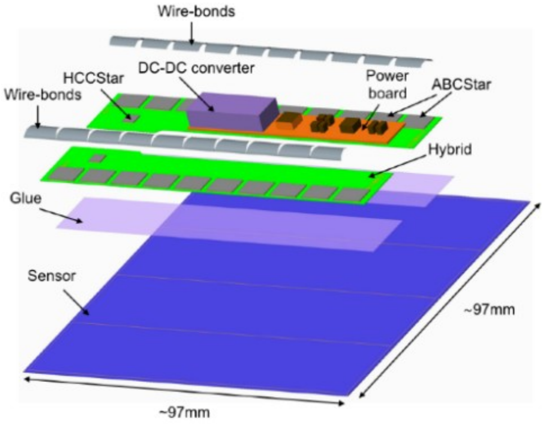

- Electrical tests of short strip stave with 5 modules and tests of a petal


Barrel 5 Short Strip Module Stave

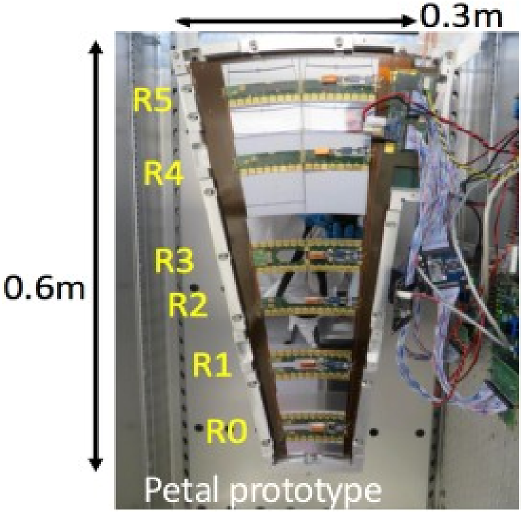

Tracking detector requirements for the HL-LHC

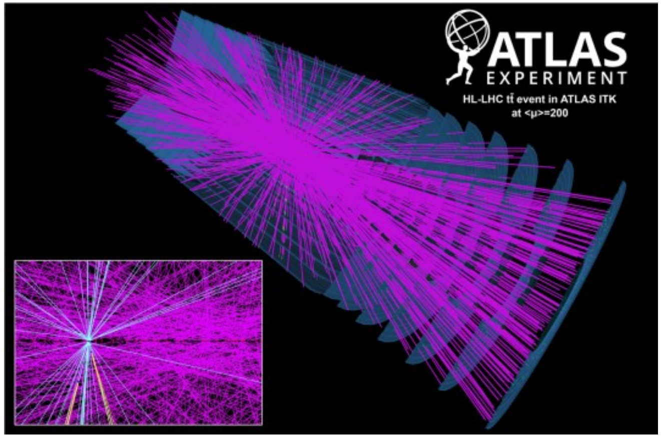

- Luminosity of up to $7.5 \cdot 10^{34}$ $cm^{-2}s^{-1}$, on average 200 interactions per bunch crossing → Keep occupancy at 1% level
- High particle fluence → Radiation damage
  - up to $1.3 \cdot 10^{16}$ n_{eq}/cm^2 and 900 Mrad for the pixel detector
  - up to $1.6 \cdot 10^{15}$ n_{eq}/cm^2 and 70 Mrad for the strip detector
- Low material budget, fast and reliable readout, high charge collection efficiency, high vertex and track position resolution
- Silicon strip and pixel detector in 2T magnetic field
- 4 central strip layers and two endcaps with 6 disks each
- 5 pixel layers in the central and forward sections
- Cooling with CO_2

PLOT-ITKD-2020-02

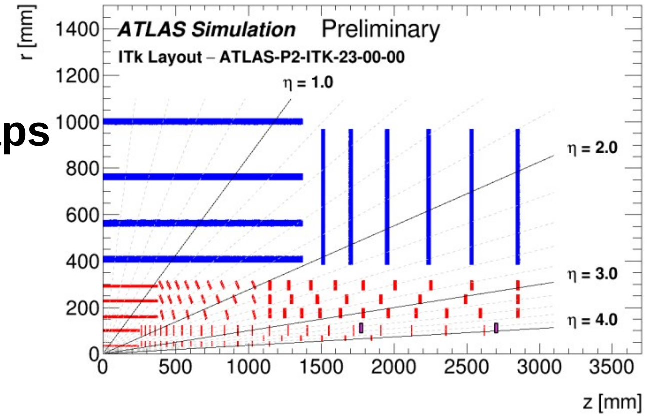

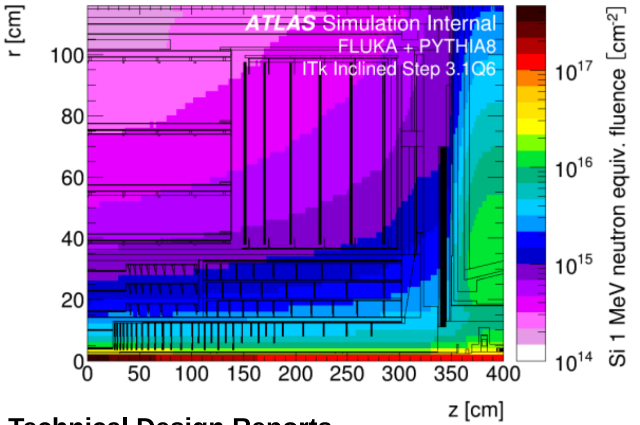

Technical Design Reports

Strip detector CERN-LHCC-2017-005

Pixel detector CERN-LHCC-2017-021

Bulk radiation damage in silicon sensors

- **Bulk damage (Non Ionizing Energy Loss)**
  - **- Point and cluster defects**
  - **- Increase of leakage current**
  - **- Change of the space charge in the depletion region, increase of full depletion voltage**
  - **- Charge trapping**
- **Signal to Noise ratio decreases**

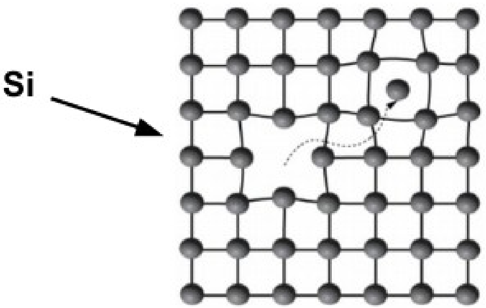

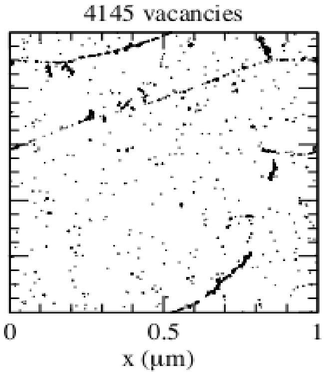

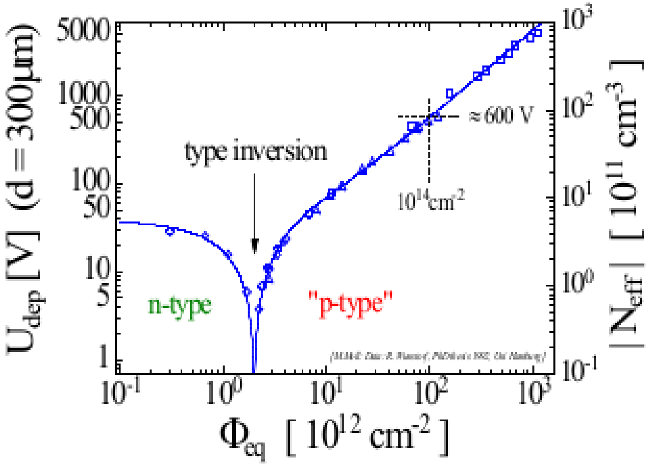

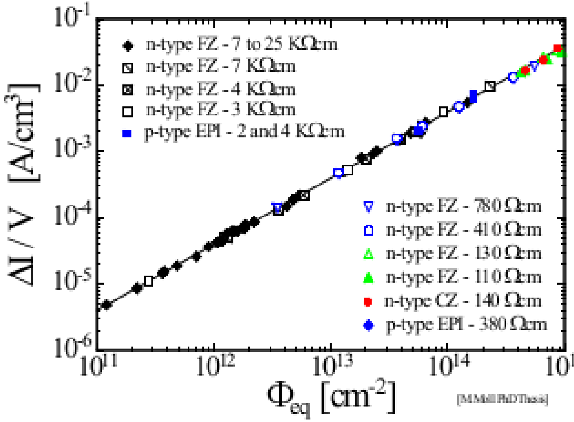

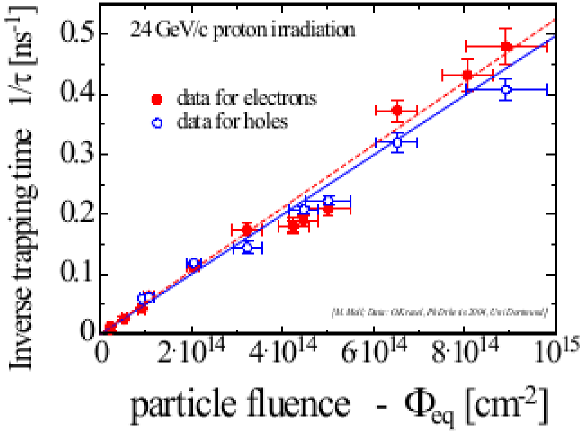

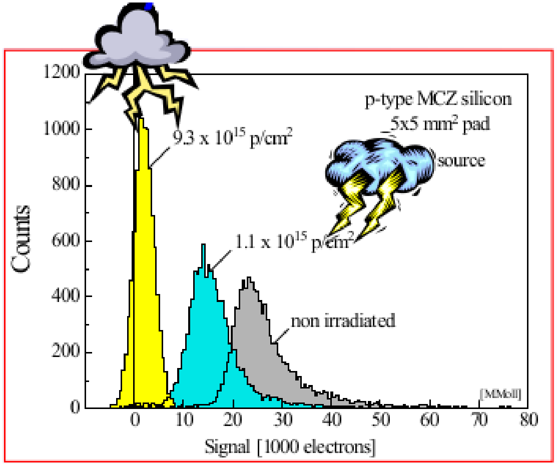

Bulk radiation damage in silicon sensors

- **Impact of defects on detector properties**

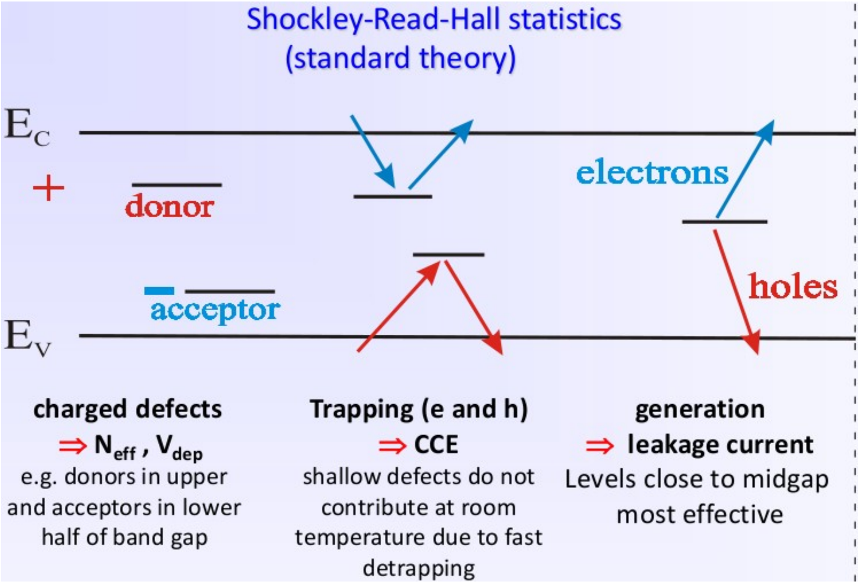

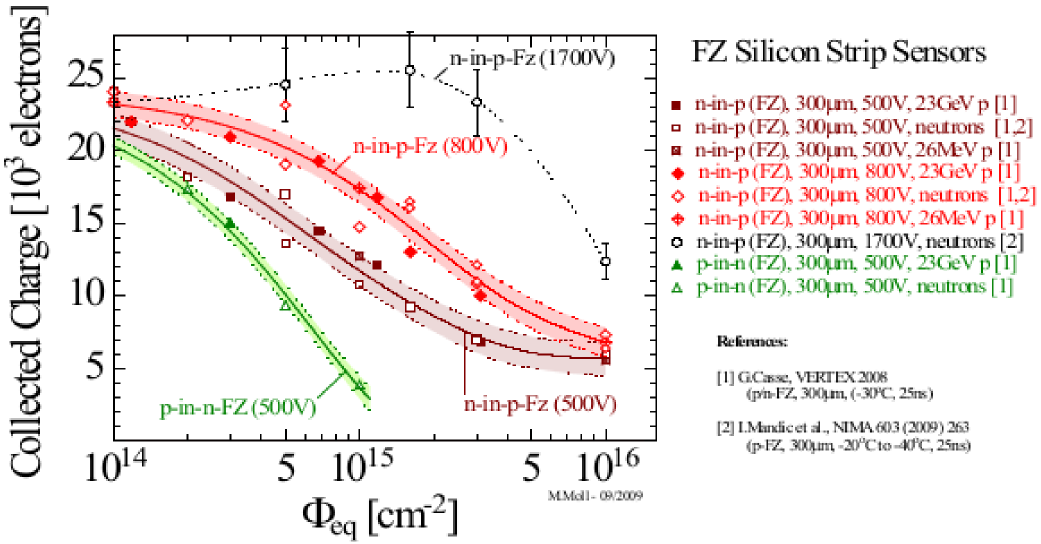

- **Detector properties can be simulated if all defect parameters are known**

  - $\sigma_{n,p}$: cross sections, ΔE: ionization energy,

  N_t: concentration

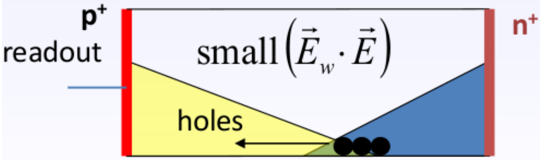

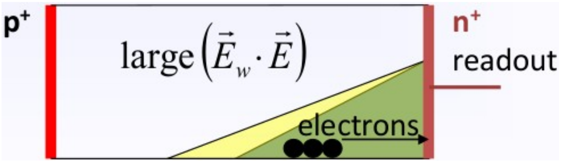

P-type silicon sensors demonstrate better performance than n-type after radiation damage at high fluence

Surface radiation damage in silicon sensors

- **Surface damage (Ionizing Energy Loss)**

  - Increase of oxide charges and Si-SiO_2 interface traps → influence on charge collection

  - Interface traps contribute to the leakage current as function of the transverse E_{field} and change the mobilities of holes and electrons at the Si-SiO_2 interface

Strip sensor CMS tracking detector

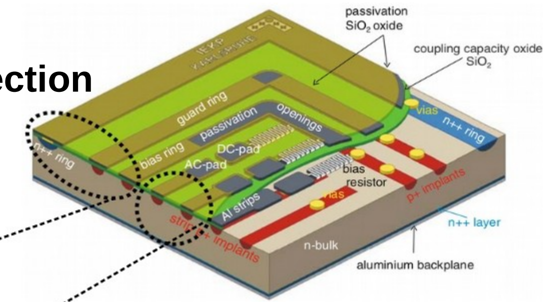

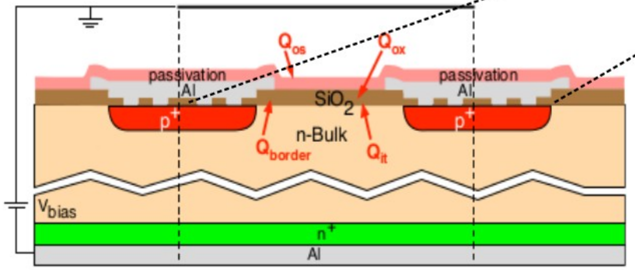

- Q_{os}: outer surface charge distribution
  - o.s. resistivity $R_{\square}$ → time depend.
- Q_{ox}: oxide charge
- Q_{border}: border trapped charge
- Q_{it}: interface trapped charge
  - Technology + surface radiation damage + time + E_{field} + E_{fermi} @ Si-SiO_2 interface

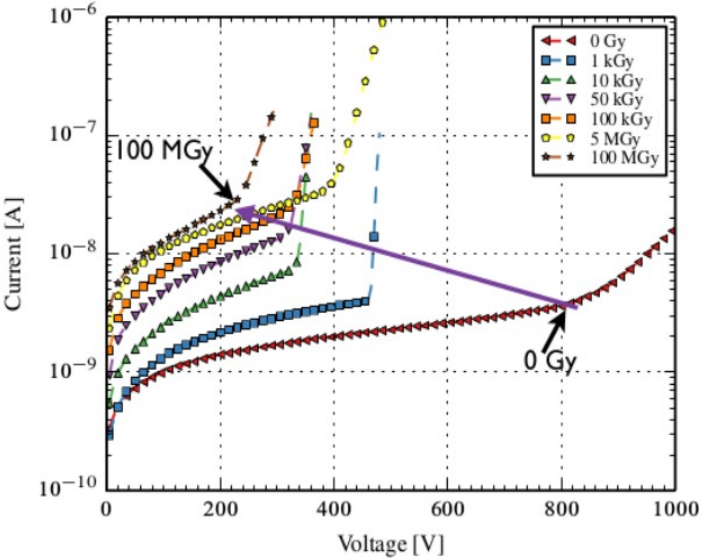

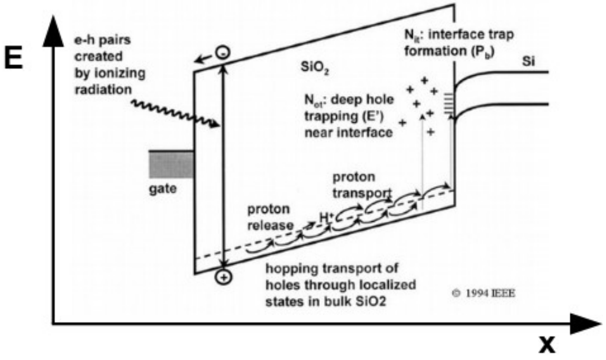

Surface charges influence breakdown behavior

Performance of silicon sensors in ATLAS

- **The importance of including radiation damage effects in the performance of silicon sensors at the current ATLAS tracking detector**

- **Simulation of the cluster charge of the 2nd pixel layer using the "Hamburg" radiation damage model**

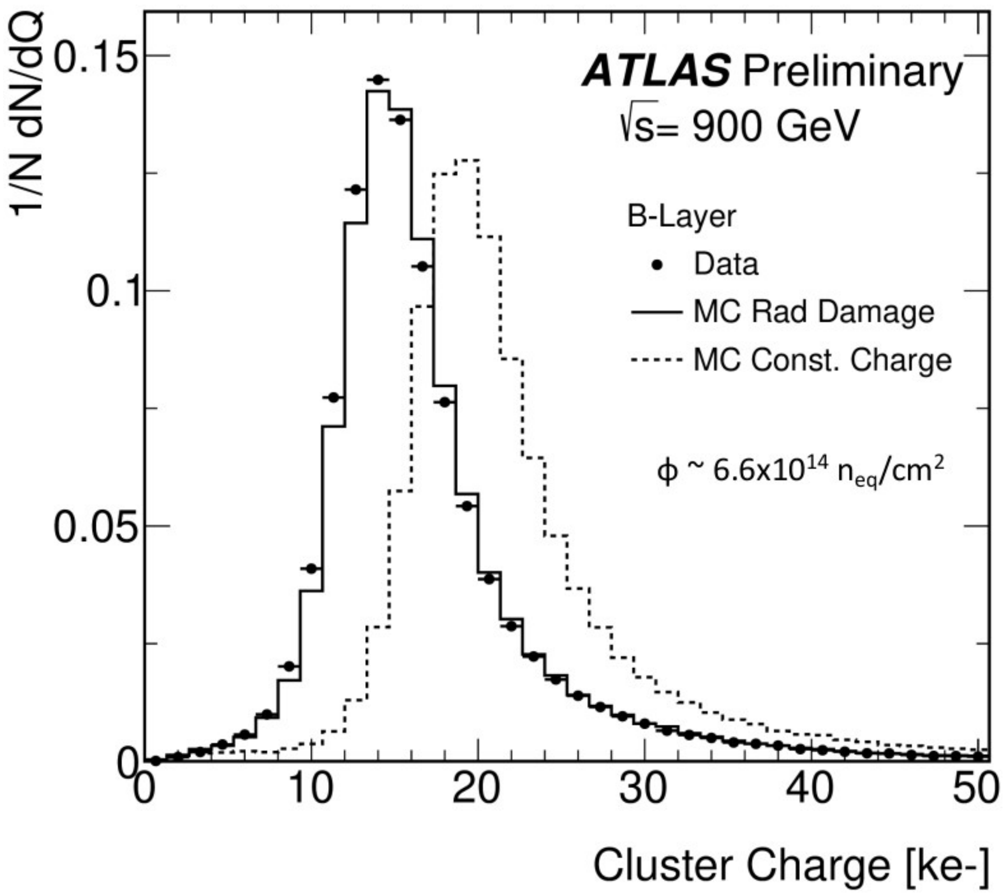

The High-Granularity Timing Detector in ATLAS

- The HGTD will provide time measurements for objects in the forward regions of the ATLAS detector
- General parameters
  - 2.4 < |η| < 4.0
  - Active area of 6.3 m^2 (total)
  - Design based on 1.3x1.3 mm^2 silicon pixels (2x4 cm^2 sensors)
  - Optimised for <10% occupancy and small capacitance
  - Radiation hardness up to $2\cdot10^{14}$ 1 MeV n_{eq}/cm^2 and 4.7 MGy
  - Number of hits per track: 2 in 2.4 < |η| < 3.1 and 3 in 3.1 < |η| < 4.0
  - Inner ring to be replaced at half life-time of HL-LHC
- Goal
  - Resolve close-by vertices (small timing resolution ~few 10s of psec.)
  - Impove pile-up rejection
  - Provide minimum bias trigger and instantaneous and unbiased luminosity measurement

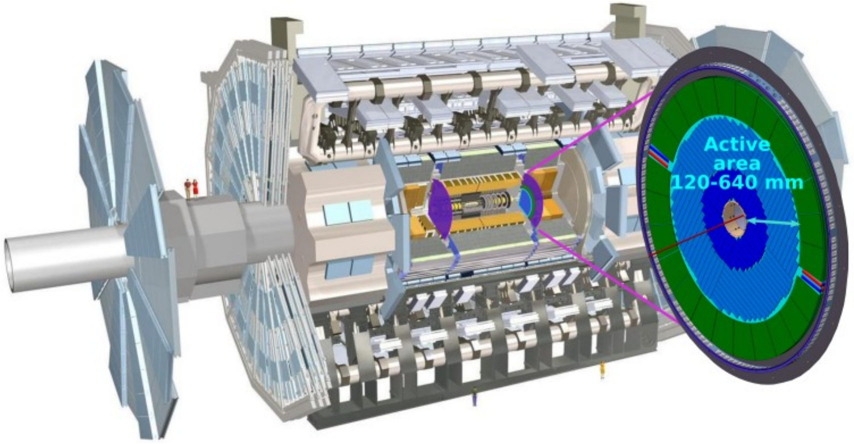

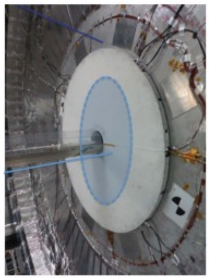

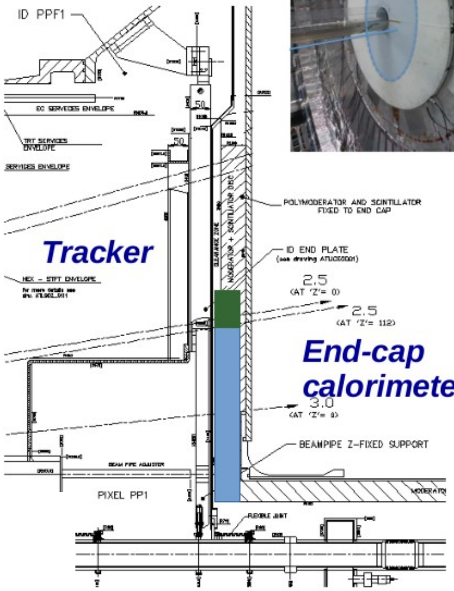

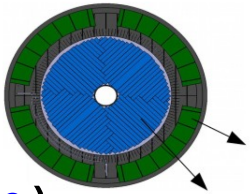

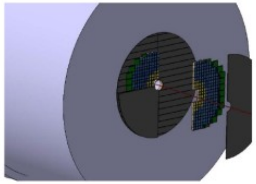

A time-tagging detector

- Time is set when the signal crosses the comparator threshold
- The timing capabilities are determined by the characteristics of the signal at the output of the pre-amplifier and by the TDC binning

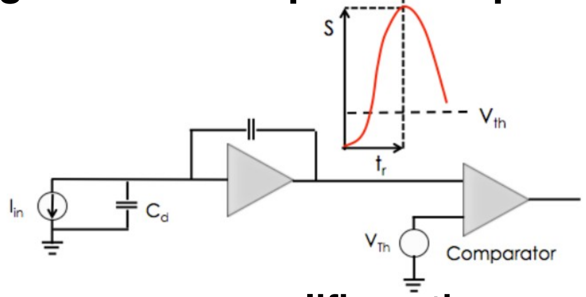

sensor **pre-amplifier** **time measuring circuit**

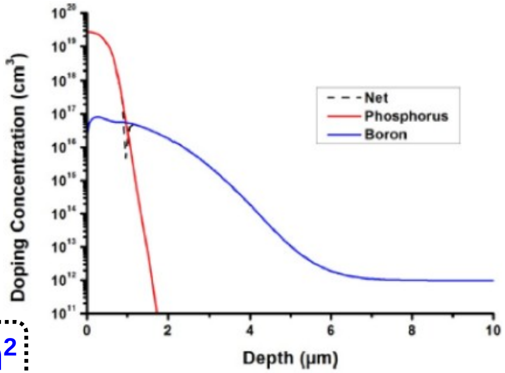

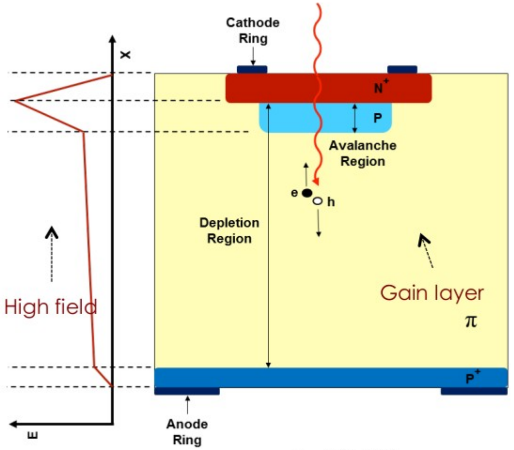

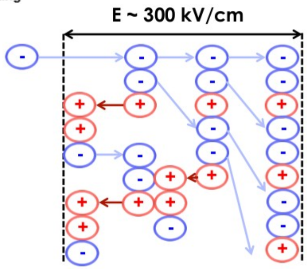

Radiation hardness overview at $2.5\cdot10^{15}\ n_{eq}/cm^2$

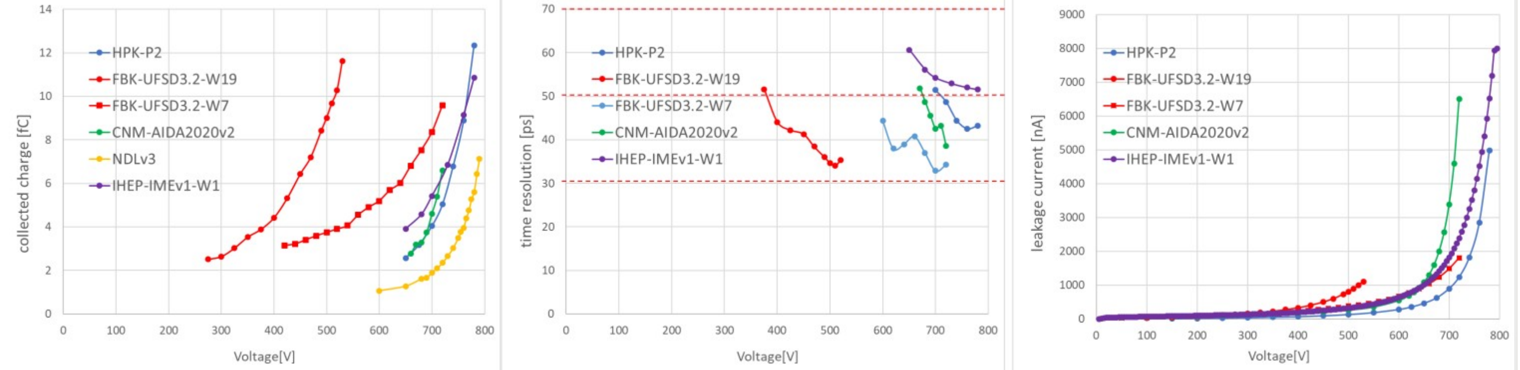

High electric field is obtained by adding an extra doping layer

Silicon detectors: LGADs R&D with Te2V & RD50

- **Design and testing of LGADs fabricated by Te2V and RD50 for the HGTD in ATLAS**

LGADs fabricated by Teledyne e2V

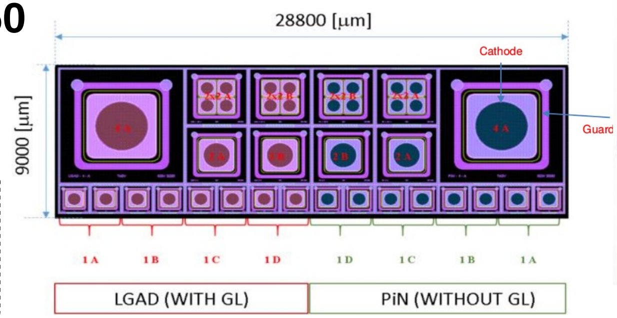

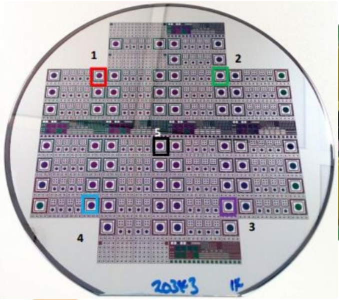

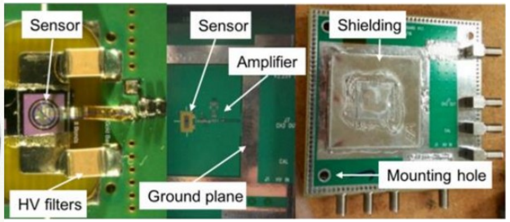

Highly segmented strip timing sensor designed and fabricated by CERN RD50/FBK

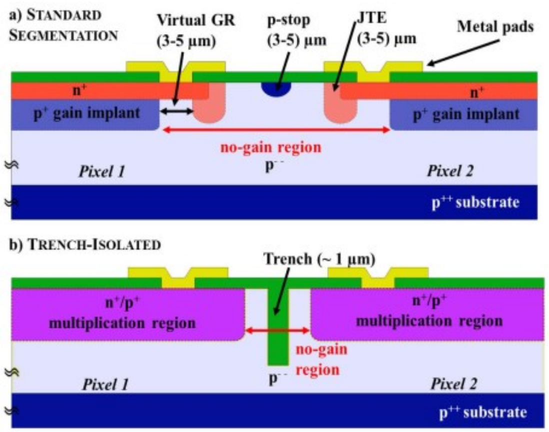

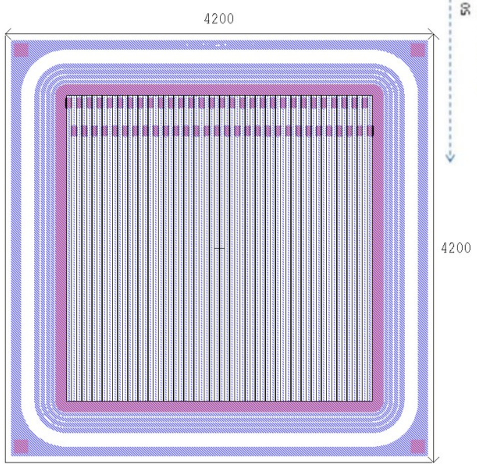

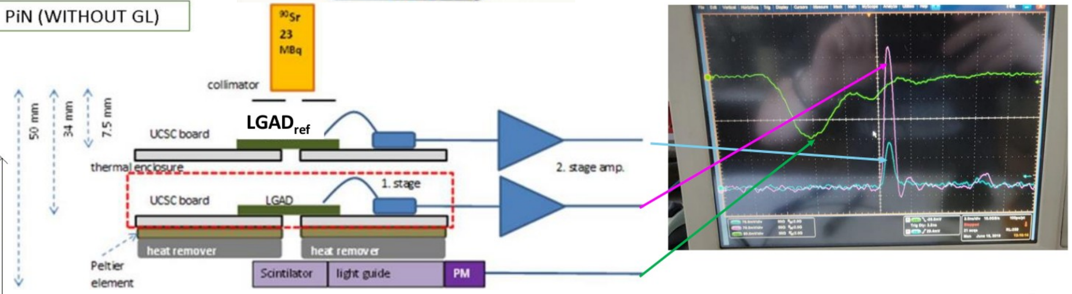

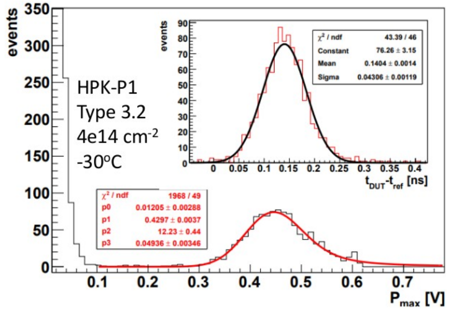

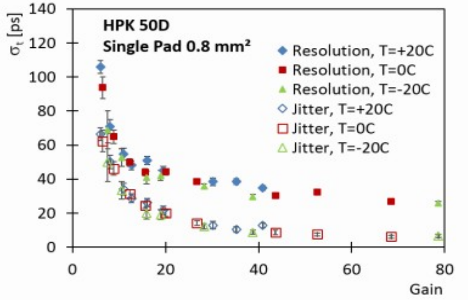

Low Gain Avalanche Detectors

- **Available vendors for LGAD sensor mass production**

HPK-P2

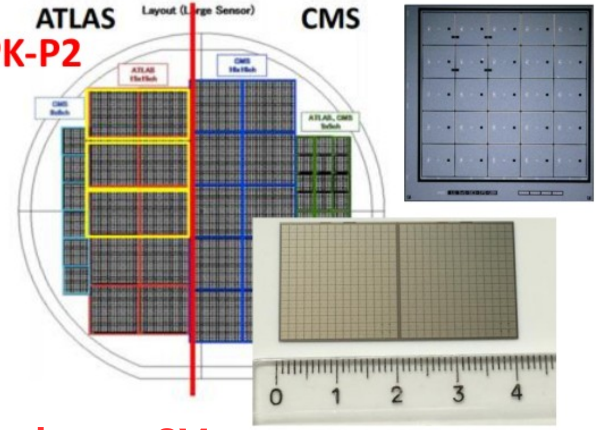

CNM-12916

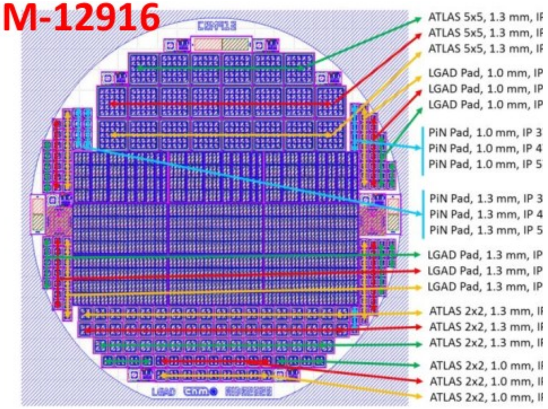

FBK-UFSD 3.2

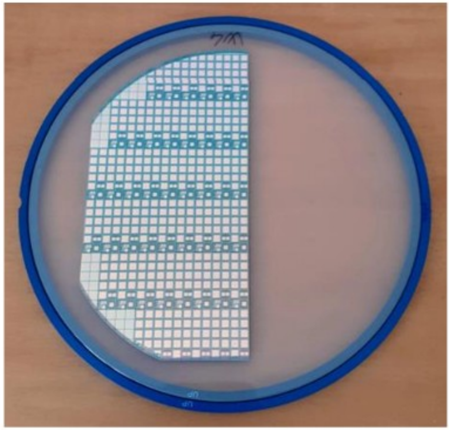

Teledyne e2V

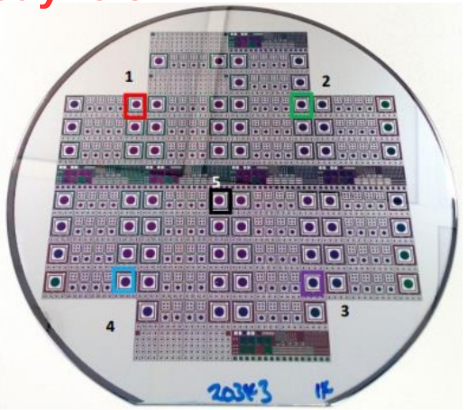

IHEP –IMEv1

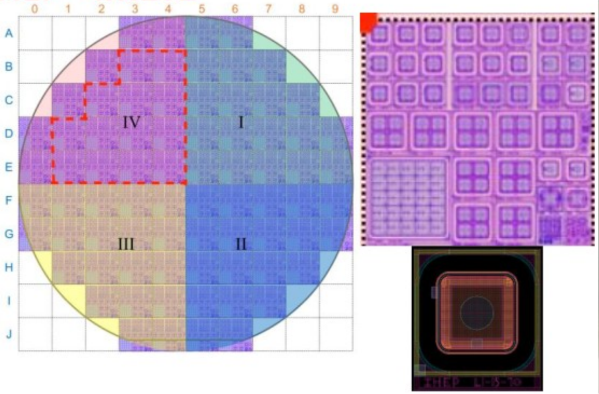

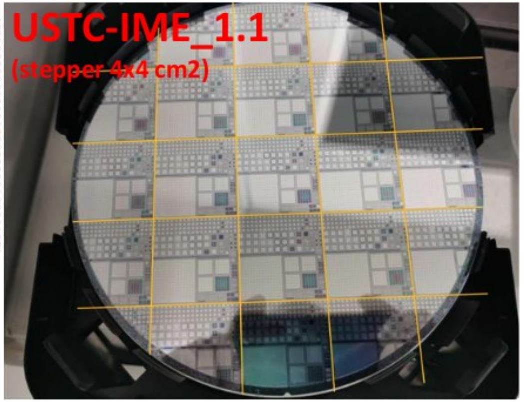

NDLv3

Technology development - long term concept

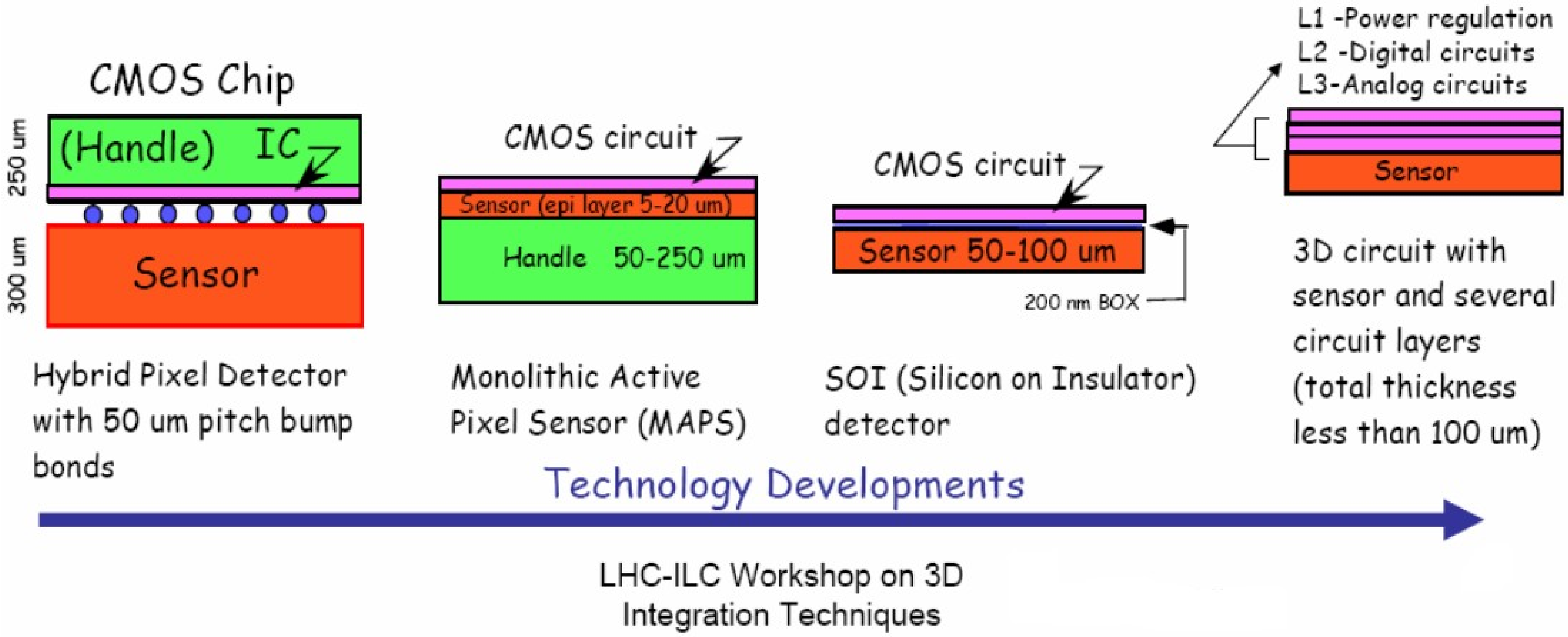

DMAPS for tracking & digital calorimetry

- **Development of a reconfigurable Depleted Monolithic Active Pixel Sensor for outer tracking and digital electromagnetic calorimetry (designed & tested by Bham and RAL groups)**
  - **- Basic idea of digital SiW EM calorimetry with the aim to count the number of pixels above threshold to estimate the shower energy**
  - **- Sensor prototypes (64x64 pixels) fabricated in the TowerJazz 180 nm CMOS imaging process**

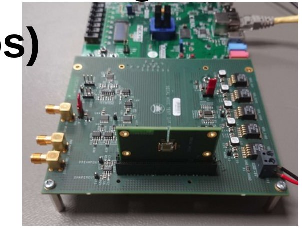

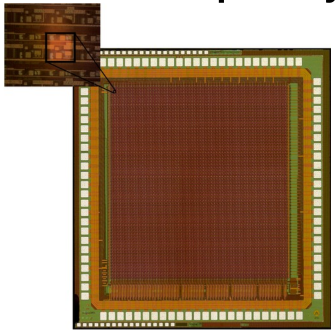

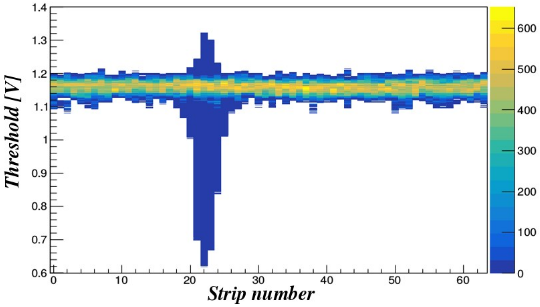

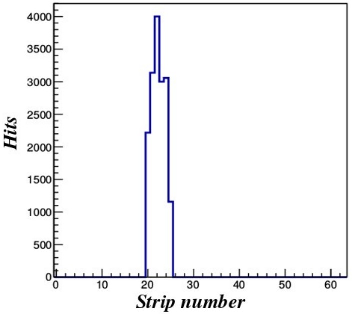

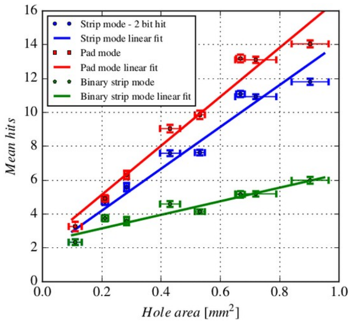

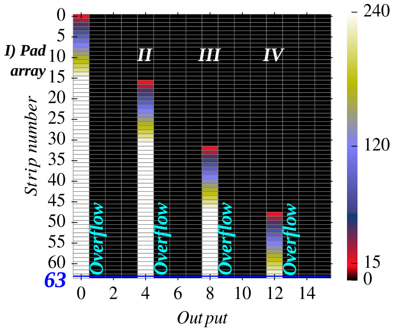

- **ALICE FoCAL (MAPS based) R&D to assemble a calorimeter**
  - **- Objective two-photon separation at few mm distance**
  - **- Low and High Granularity (CMOS MAPS) layers**
  - **→ Single shower particle measurement, 3D shower shapes**

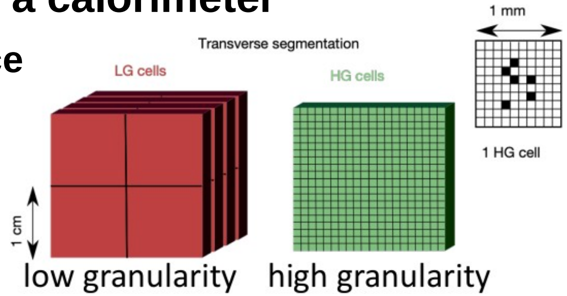

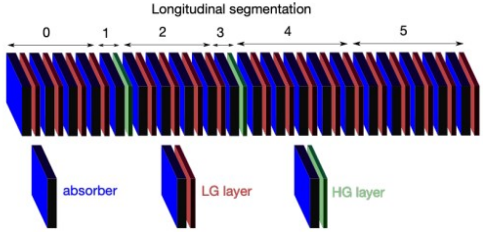

The DECAL Fully Depleted sensor

- TowerJazz 180 nm CMOS modified process
  - The first version is referred to as an addition continuous n^{-} layer design for each pixel
  - The second version of two variants (gap in the n- layer and extra deep p-well) which expected to shape the electric field so the charge carriers produced are steered more directly towards the collection electrode in the pixel center
- The second version and the variant with gap in the n^{-} layer was chosen for the DECAL FD
- Pixel timing response has been simulated (by CERN groups) with 3D TCAD simulation for a MIP traversing the pixel corner
- Faster charge collection has been simulated for the second version (two variants of the modified process)

H. Pernegger, Depleted CMOS sensors for HL-LHC, Proceeding of Science, (VERTEX 2018), (041), 2018

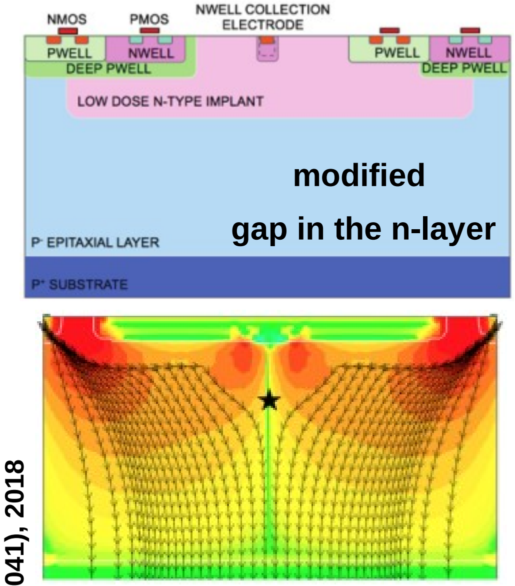

Collected charge for different versions of the modified process

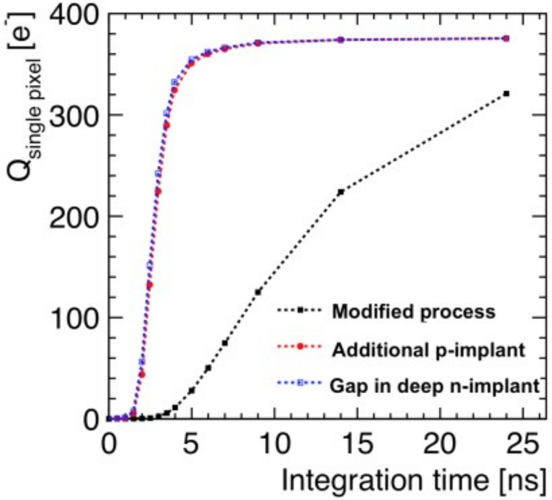

DECAL FD digital functionality

- With the DECAL FD possibility of configuration of all pixel columns and full depletion of the sensor under bias voltage on p-epi
- Threshold scan in single pixels → threshold pixel map and in principle threshold trimming of the pixel matrix
- 5 bits pixel trimming with a maximum shift of ≈150 mV
- Example of trimming of a single row for all columns at threshold of 1.17 V

Threshold voltage as a function of pixel configuration

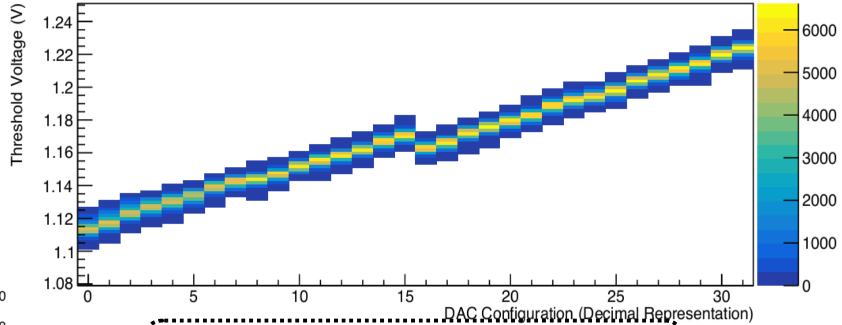

Threshold voltage before & after trimming of a single pixel row

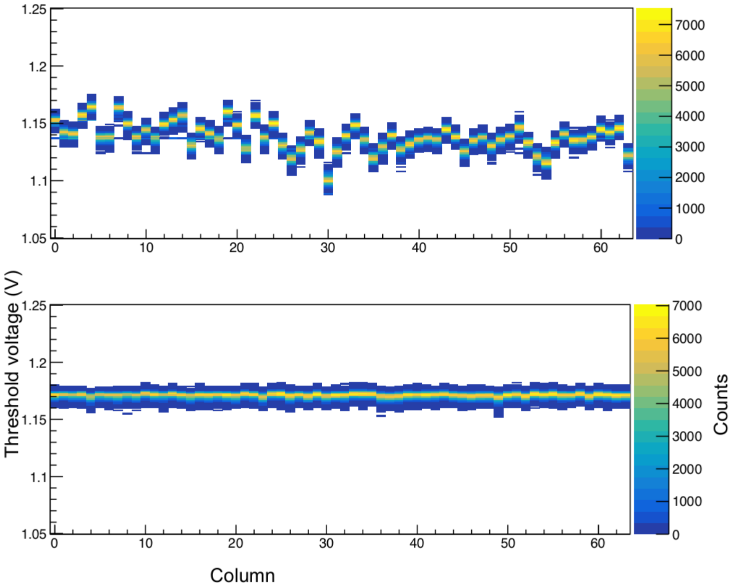

Threshold distribution of a single pixel

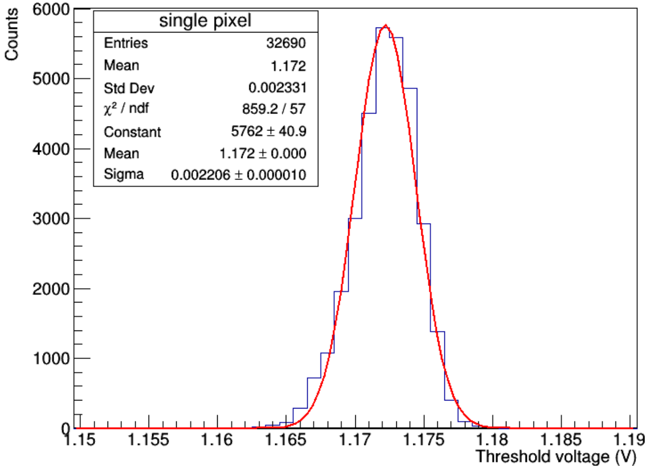

DECAL FD test with monochromatic X-rays

- **Uniform threshold voltage of the pixel matrix and long term threshold scan of a single row**

Threshold uniformity under X-ray illumination

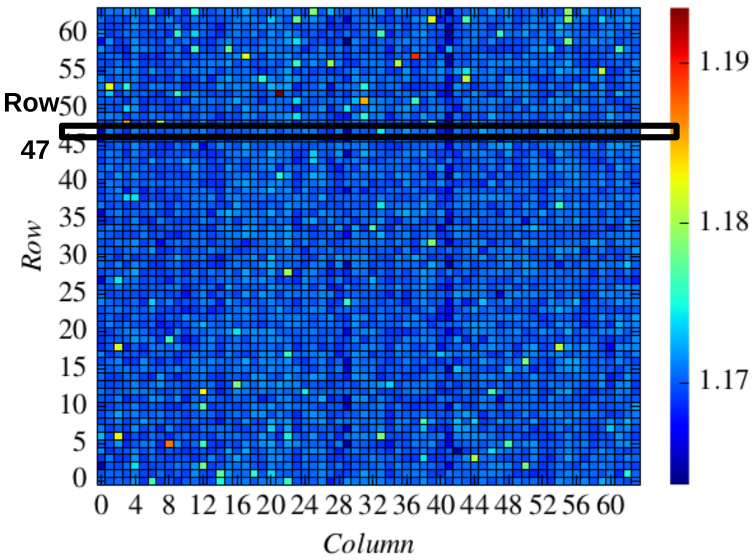

Long term threshold scan pixel row 47

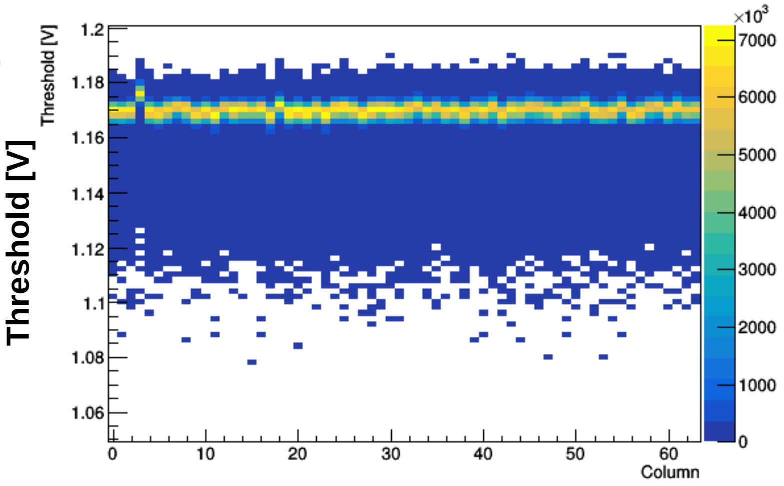

Pixel row threshold distribution

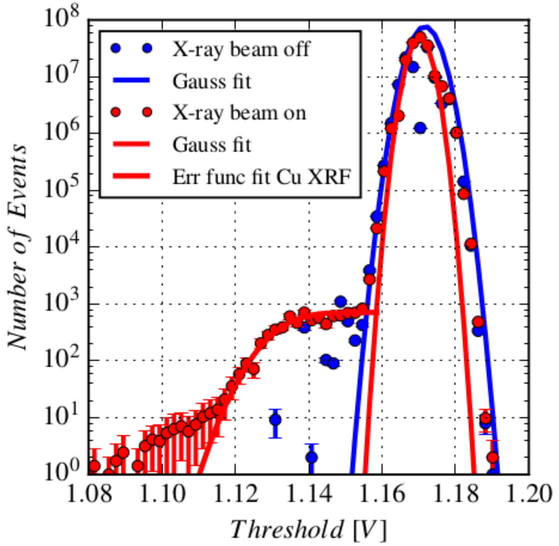

- Error function fit in the signal detected below the global threshold

- Conversion gain, f = 59 [e^-/mV]

	Mean [V]	Sigma [mV]
Beam off Gauss	1.172	3.3
Beam on Gauss	1.170	2
Beam on Err func	1.132	10.2

DECAL FD energy calibration

- Fitting corrected and smeared HEXITEC spectra, different target materials

raw HEXITEC spectrum
25 μm Si corrected spectrum
additional Gaussian smearing

- Convert from E (keV) to voltage V (mV): $V = \alpha \cdot E$
- Conversion factor obtained $\alpha = 5.55 \pm 0.37$ mV/keV
- Relative energy resolution $\sigma_E/E = 13.7 \pm 3.6\%$

Relative energy resolution

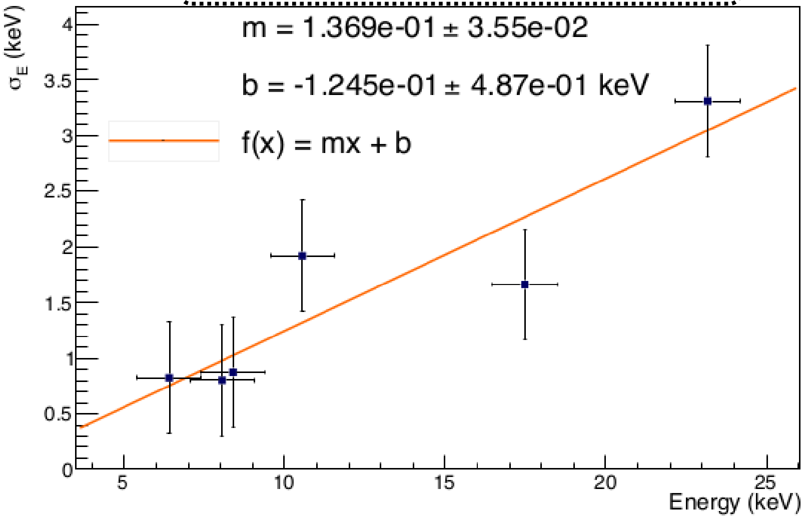

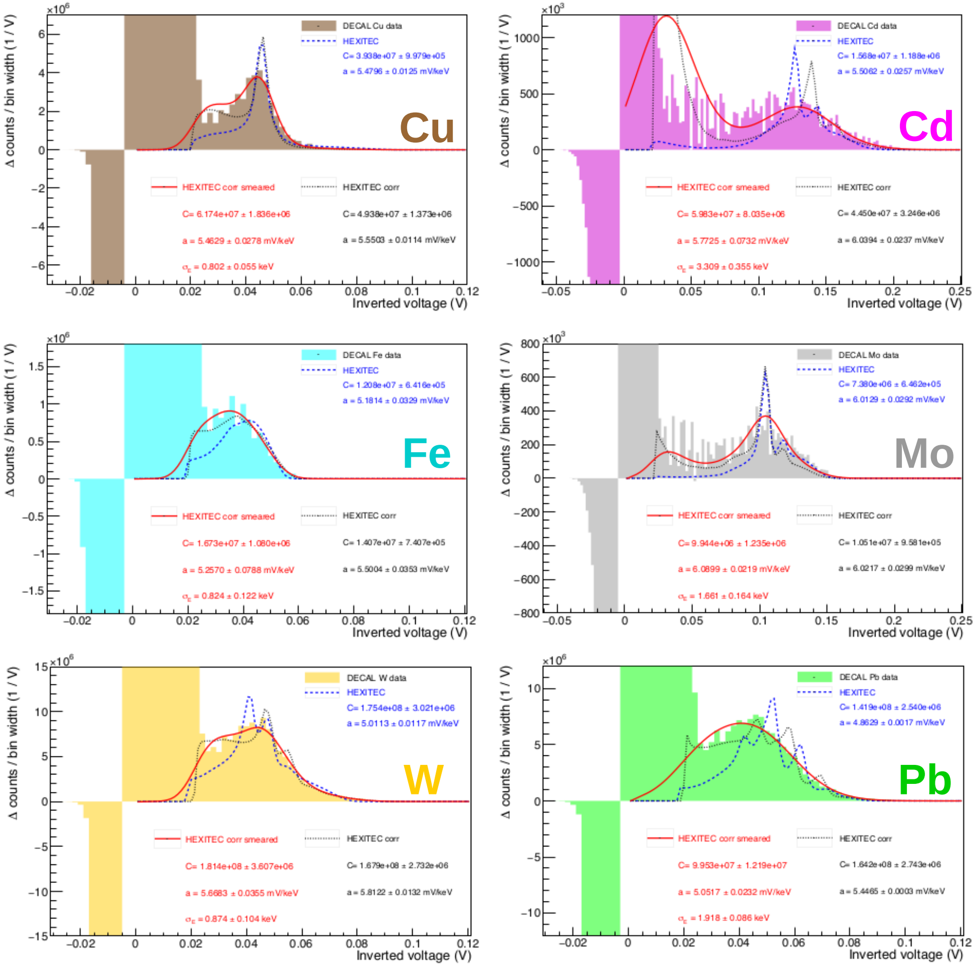

Summary

- Looking back on > ½ century of fascinating detector developments

  - Silicon detectors enabled important discoveries + precision measurements → No Si – no Higgs!
- Well understood performance: pulse height distribution, "Landau" dE/dx, position resolution, charge sharing, charge collection, Lorentz force, resolution vs track angle, effect of δ-rays on resolution, electronic noise + dE/dx fluctuations, optimal reconstruction algorithm (η)
- New inner tracker in preparation for the ATLAS experiment in the High Luminosity era

  - 5 layer pixel detector with about 10000 pixel-hybrid modules (~x6 of current pixel detector)

  - 4 layer strip detector with about 18000 strip modules

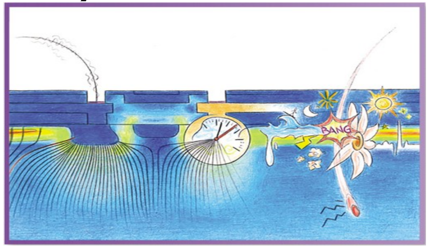

- HGTD detector promises to improve pile-up rejection for HL-LHC:

  - significant improvements on reconstruction performance at high-η values

  - LGAD sensor technology: provide timing, occupancy, radiation hardness, challenging <30 ps resolution obtained before irradiation and 30 – 50 ps after $2.5 \cdot 10^{15}$ n_{eq}/cm^2
- Depleted MAPS (DMAPS) provide the advantage of a monolithic detector design with improved radiation tolerance, fast charge collection → qualified as suitable candidate technology for tracking and calorimetry in future systems

"New directions in Science are launched by new tools much more often than by new concepts." F. J. Dyson

Thank you for your attention

Acknowledgments

Special thanks for the material used from

P. Allport, M. Bomben, D. Bortoletto, N. Cartiglia,

C. Damerrel, E. Fretwurst, I.M. Gregor, R. Klanner,

G. Kramberger, M. Krammer, S. Kuehn, S. McMahon,

M. Moll, G. Lutz, H. Spieler, R. Yarema

Back up

Silicon properties

- Absorption of photon → breaks bond → excite electron in conduction band and vacant “hole” in valence band
- Electrons and holes move quasi freely in lattice (hole filled by nearby electron, thus moving to another position)

Property		Si	Ge	GaAs	Diamond
Atomic Number		14	32	31/33	6
Atomic Mass	[amu]	28.1	72.6	144.6	12.6
Band Gap	[eV]	1.12	0.66	1.42	5.5
Radiation Length X_0	[cm]	9.4	2.3	2.3	18.8
Average Energy for Creation of an Electron-Hole Pair	[eV]	3.6	2.9	4.1	~ 13
Average Energy Loss dE/dx	[MeV/cm]	3.9	7.5	7.7	3.8
Average Signal	[$e^-/\mu m$]	110	260	173	~ 50
Intrinsic Charge Carrier Concentration	[cm^{-3}]	$1.5 \cdot 10^{10}$	$2.4 \cdot 10^{13}$	$1.8 \cdot 10^{6}$	$< 10^{3}$
Electron Mobility	[cm^2/Vs]	1500	3900	8500	1800
Hole Mobility	[cm^2/Vs]	450	1900	400	1200

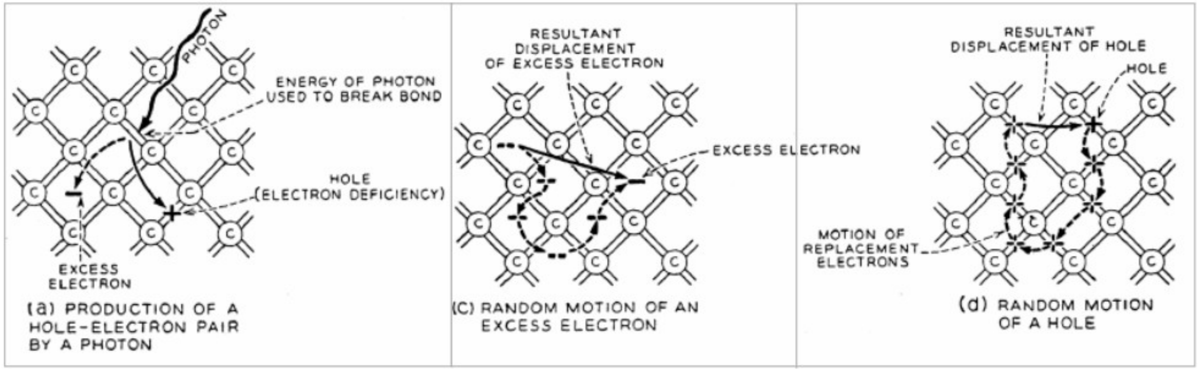

- Number of thermally excited charge carriers ($n_{intrinsic}$):

$$n_i = \sqrt{n_V n_C} \cdot exp(-\frac{E_{Gap}}{2kT})$$

  - Si at room temperature (kT ~ 26 meV): $1.5 \cdot 10^{10} cm^{-3}$

Doping in silicon – change of conductivity

- **Doping with elements from group III (Acceptor, eg B)**
  p-type Si is formed
  - One valence bond remains open and attracts electrons from neighbor atoms
  - The energy level of the acceptor e^- is above the edge of the valence band
  - At room T, most levels are occupied by e^- leaving h^+ in the valence band

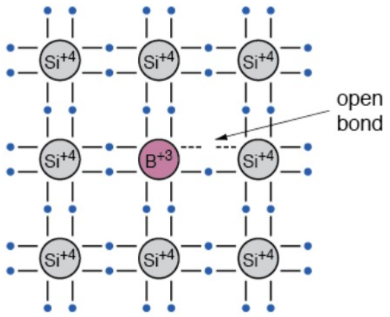

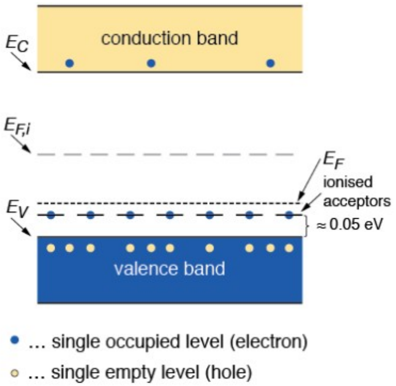

- **Doping with elements from group V (Donor, eg As)**
  n-type Si is formed
  - The 5th valence is weakly bound
  - The energy level of the donor e^- is below the edge of the conduction band
  - At room T, most electrons are raised to the conduction band
  - The E_F level moves up

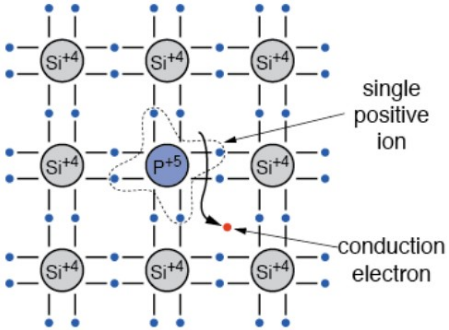

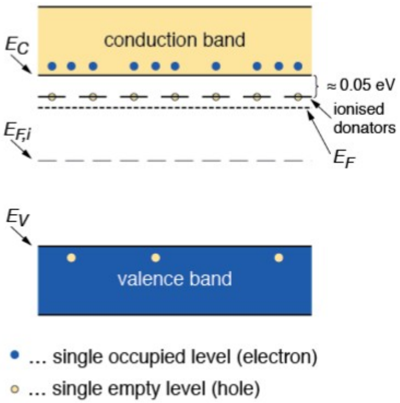

- **Resistivity dominated by majority charge carriers $n = N_{D,A}$:**

$$\rho = \frac{1}{q \cdot \mu_i \cdot n_i}$$

- typical Si detector doping, few 10^{12} cm^{-3} → ρ = 1 … 5 kΩ·cm

Silicon detector fabrication

- **Steps in fabrication of planar silicon detectors**

  - polishing and cleaning

  - oxidation at 1300 K

  - deposition of photosensitive polymer, UV illumination

  - creation of pn junction via implantation/diffusion

  - annealing: implanted ions occupy lattice sites

  - deposition of Al

  - patterning of electric contacts

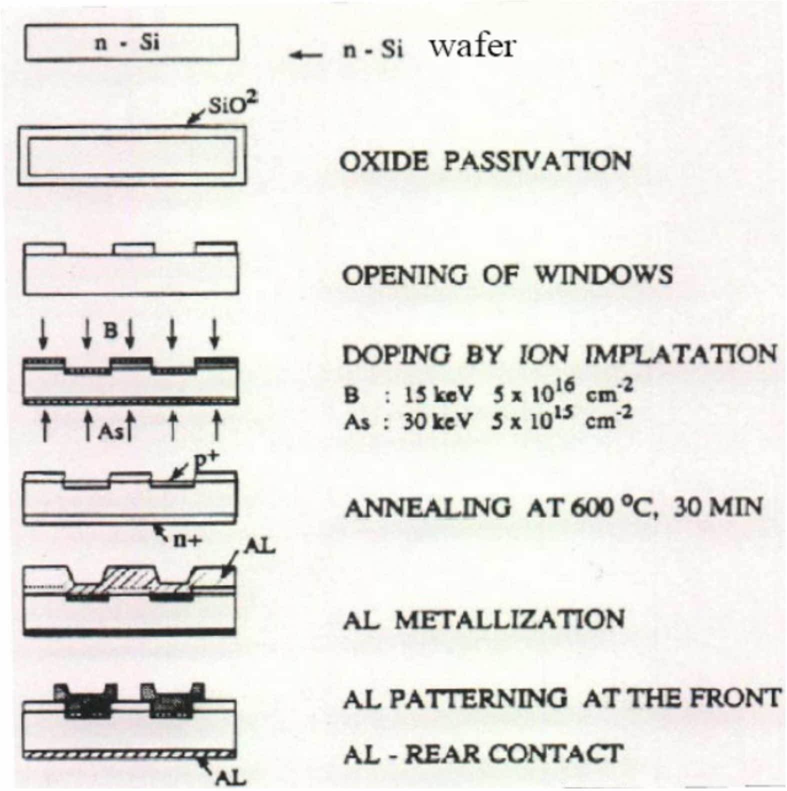

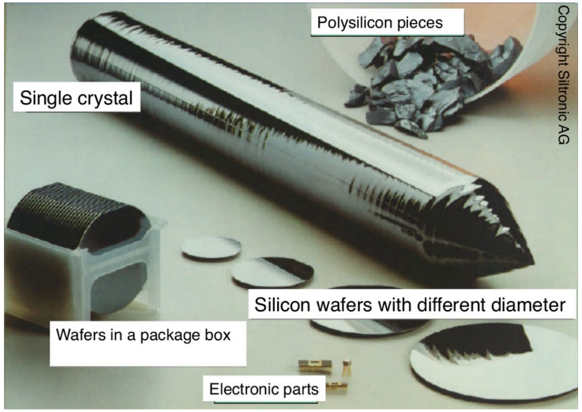

The ATLAS inner detector

Inner Detector (ID)
Tracking

- Silicon Pixels 50 x 400 μm^2
- Silicon Strips (SCT)
  80 μm stereo
- Transition Radiation Tracker (TRT) up to 36 points/track
- 2T Solenoid Magnet

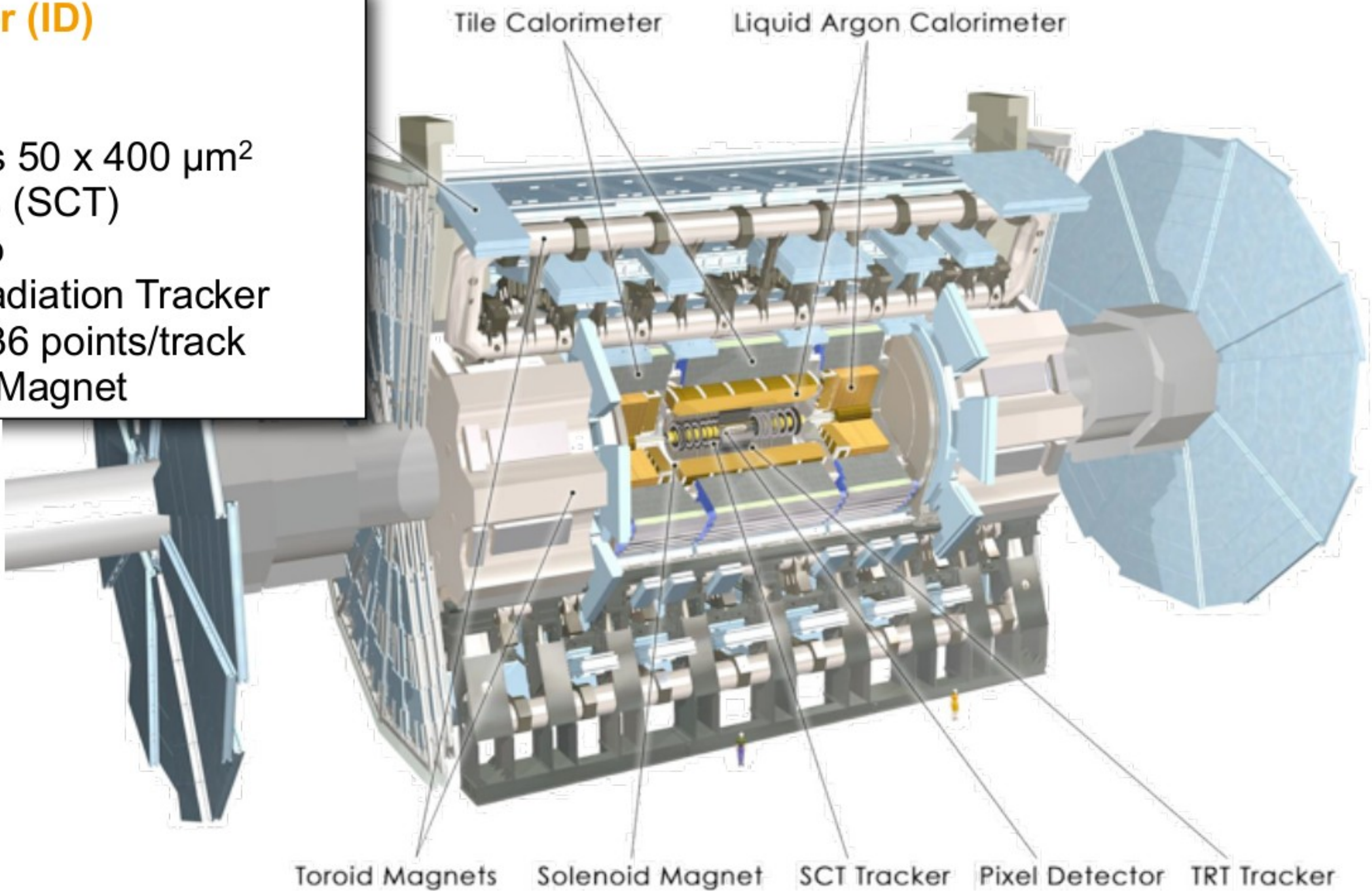

The ATLAS inner detector

- **Designed to precisely reconstruct charged particles trajectories**
  - 7- points silicon (pixels + strips)
  - straw tube quasi-continues tracker with electron identification capability
  - 2 T solenoidial magnetic field

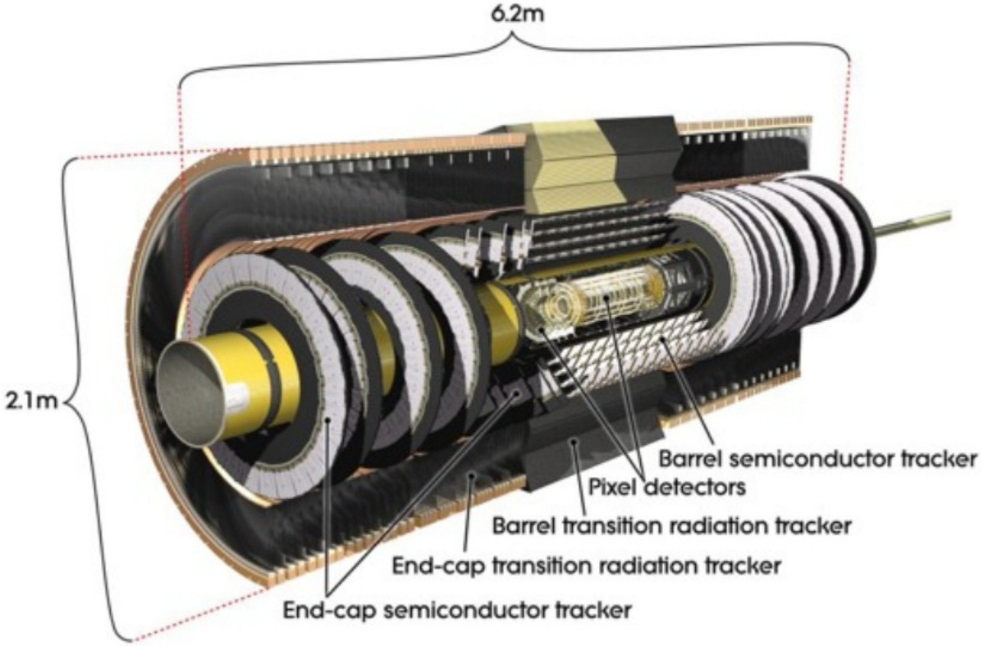

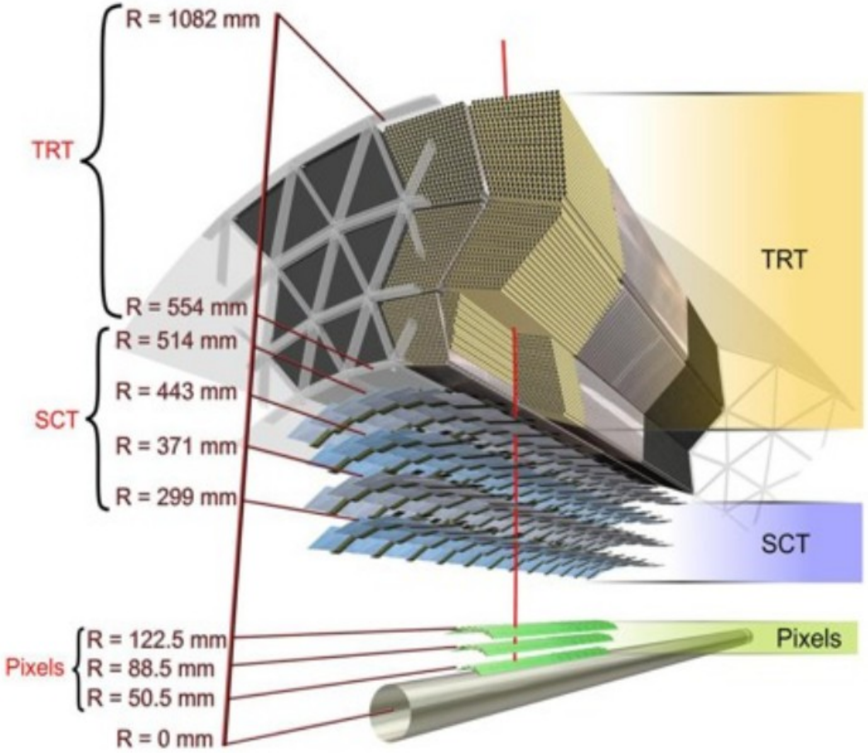

The ATLAS SemiConductor Tracker

- **61m² of silicon micro-strip detectors**
  - 20,000 separate sensors ordered

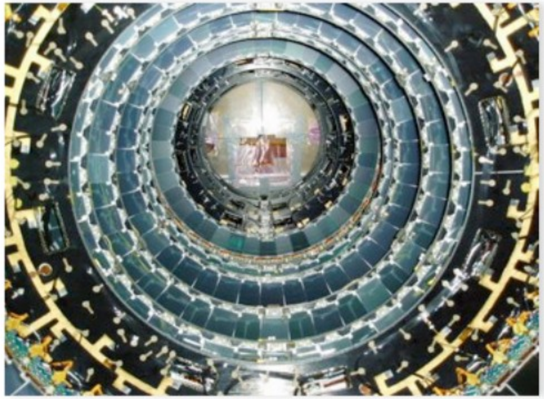

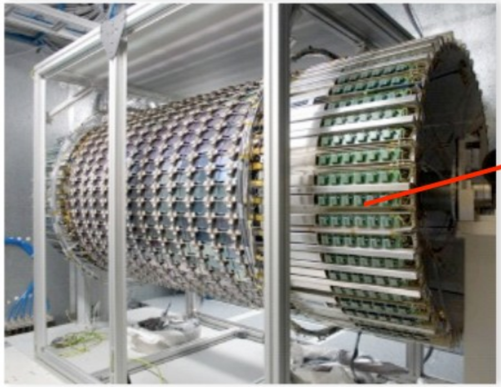

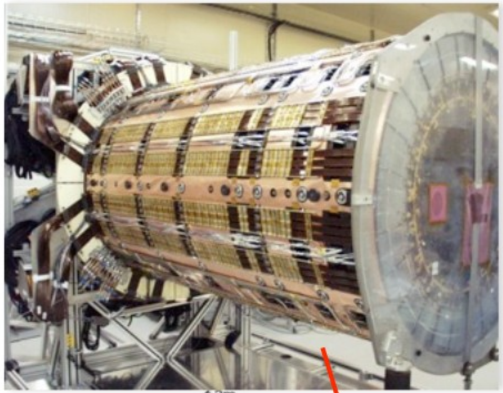

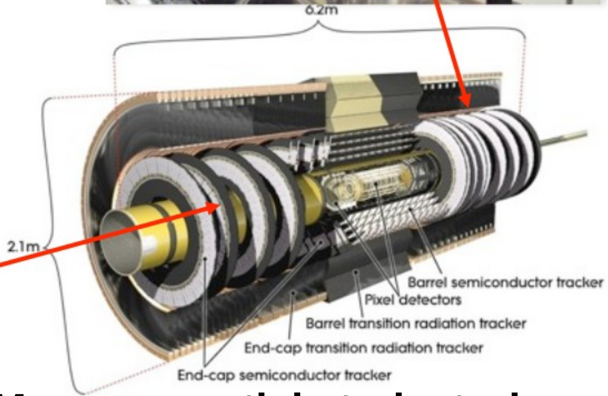

- **Measure particle trajectories with ~10 μm precision (7 Mio ch.)**
  - withstand radiation levels of up to 100 kGy

The ATLAS SCT – strip detectors

- The SCT consists of 4 barrel layers, built with 2112 modules, and disk endcaps build of 1976 modules
  - The total number of strips is $6.3 \cdot 10^6$
- The barrel module consist of 4 single sided p-on-n strip detectors
  - Pitch 80 μm
  - Strip length 120 mm
  - Stereo angle 40 mrad
- The end-caps are built with three different modules
  - Pitch 57 - 95 μm
  - Strip length 55 - 120 mm

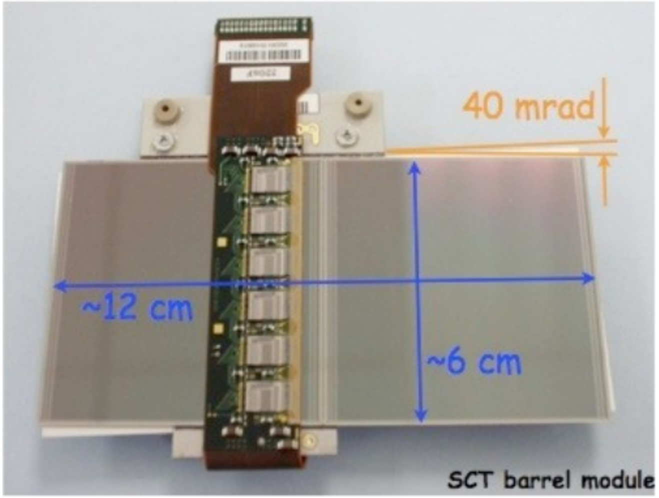

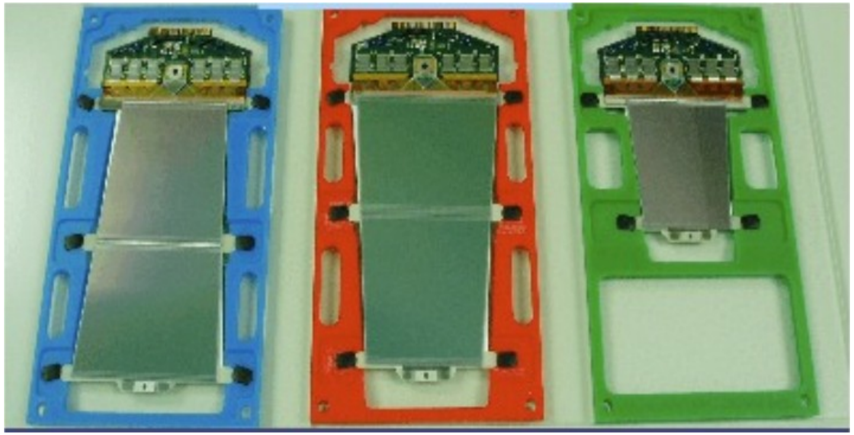

Readout chip of the strip sensor

- **Binary readout chip (130nm CMOS technology)**
  - ABCStar with 256 channels, operated at 1.5 V
- **Pre-production of ABCStar chips being tested with better single-event effects (SEE) tolerance**
- **Design of hybrid controller chip (HCC)**

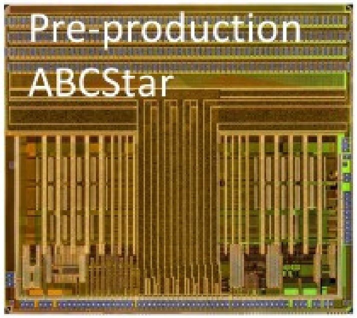

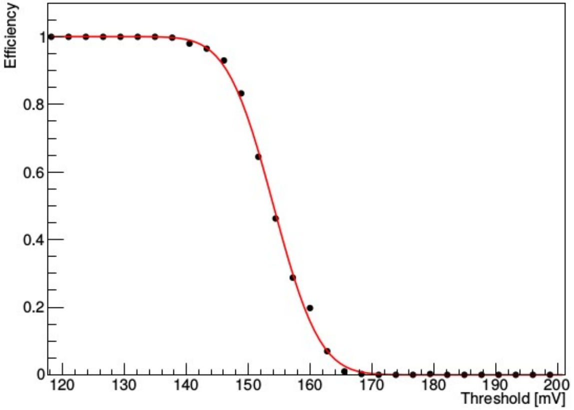

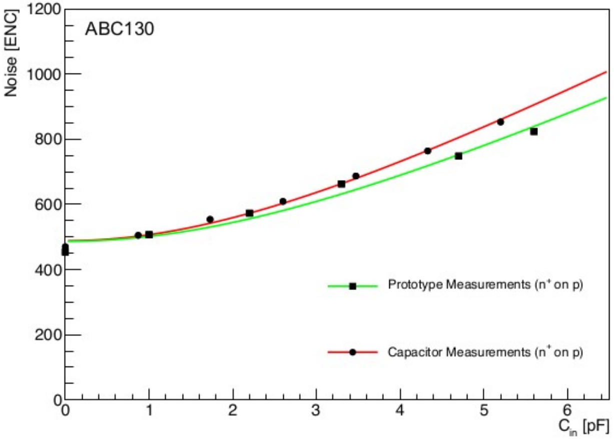

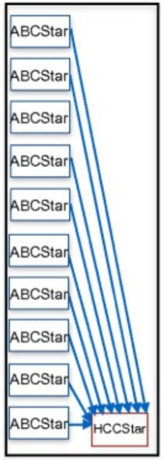

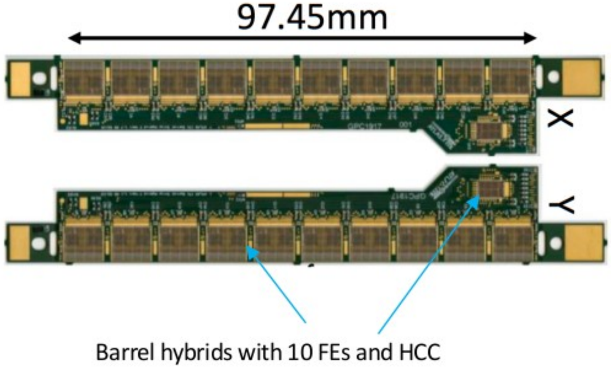

$$\mathrm{ENC} = \frac{\sigma[\mathrm{mV}]}{\mathrm{gain}[\mathrm{mV/fC}]}$$

Module performance in test beam and irradiation

- **Several test beam campaigns at the DESY-II test beam facility of non-irradiated and irradiated star modules**
  - Sensors have been irradiated to max. expected fluence and annealed
  - Hybrids irradiated to the max. expected X-ray dose
- **Measured signal-to-noise ratio values above required value of 10 for all evaluated modules at operation bias voltages**

- **Results show efficiency >99% and <0.1% noise occupancy requirement**

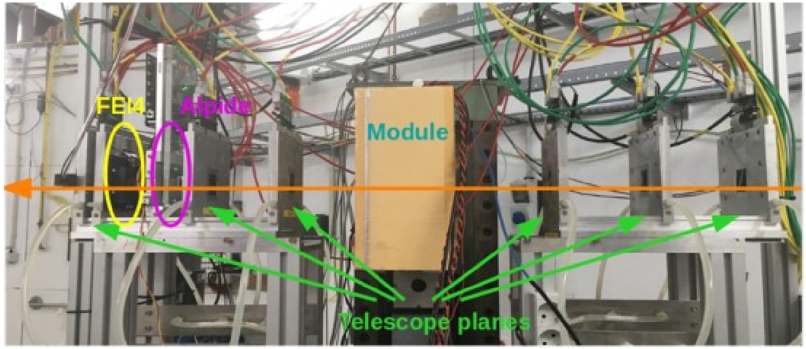

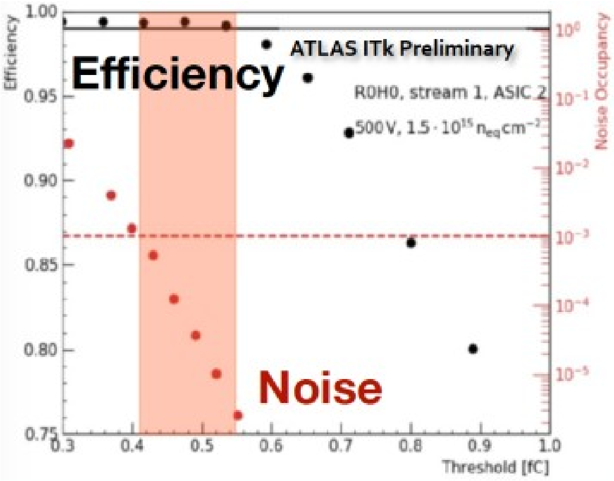

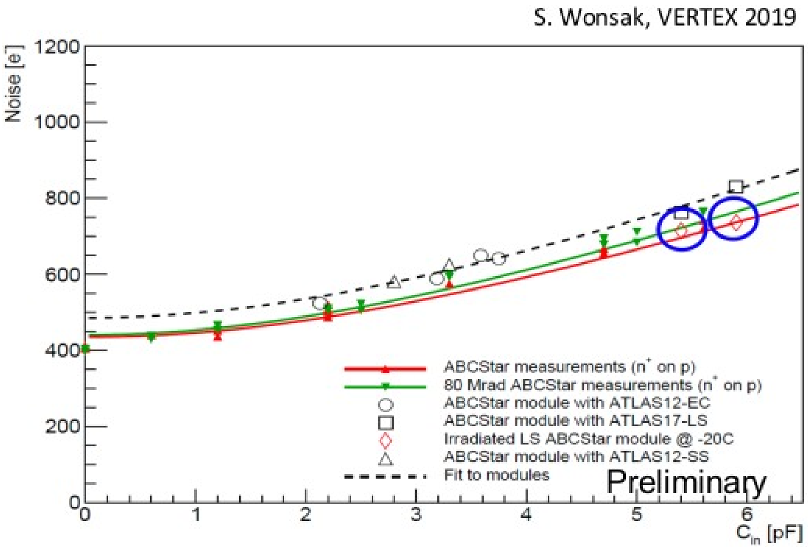

The pixel detector

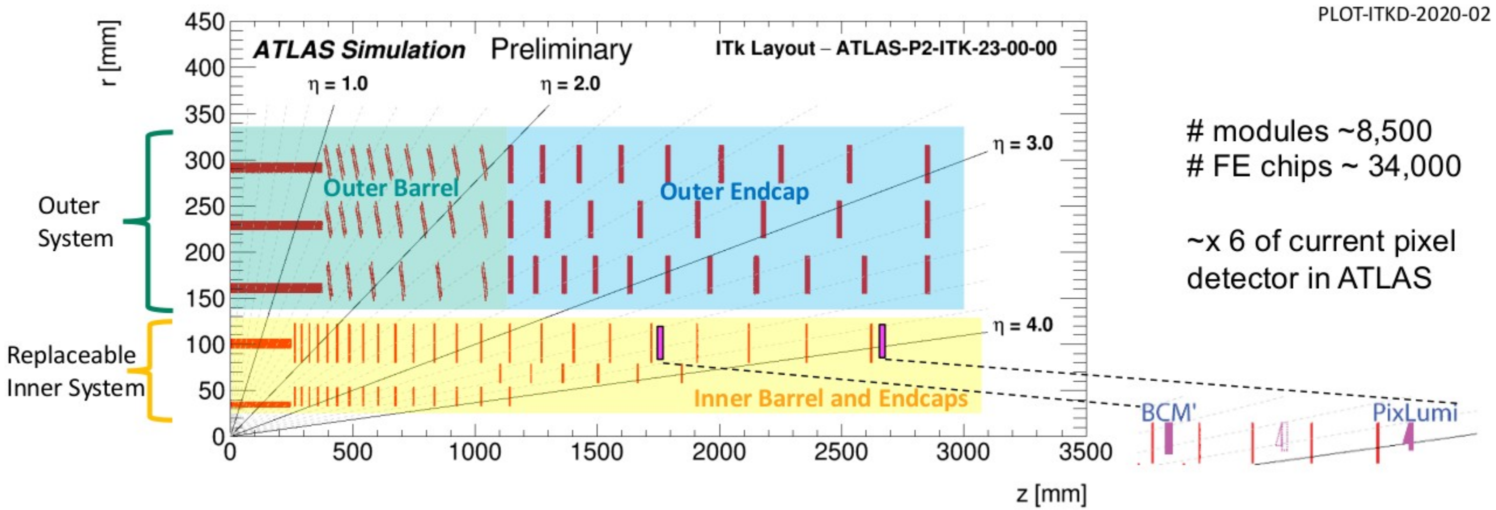

- **Different sensor types and technologies depending on distance from the interaction point**

  - 3D sensor technology in triplet assemblies (Layer 0) and planar sensor technology of 100 μm thickness (Layer 1) and 150 μm thickness (Layers 2,3,4)

  - Pixel size 50x50 μm^2 (L1-L4, rings of L0), 25x100 μm^2 (flat part of L0)
- **Luminosity monitoring and beam abort modules recently added**
- **Fast readout with max. 1 MHz trigger rate**
- **Reduction of material by deploying serial powering and CO_2 cooling**

Readout chip of the pixel sensor

- RD53 Collaboration: joint R&D of ATLAS and CMS to design the pixel front-end chip
- ASIC: 65nm CMOS technology fabricated by TSMC
  - 4 data lines at 1.28 Gbps, low threshold ~600 e^-, design power 0.7 W/cm^2, up to 8A supply current for four-chip module, radiation hardness up to 500 Mrads
  - 154k pixels per chip, expecting up to 250 hits/chip/bunch crossing

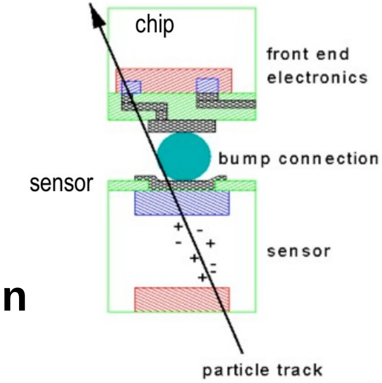

- RD53A FE prototype investigated → comparable performance within specification
  - Wafer probing performed, two readout systems for testing available, radiation damage depends on dose rate, operation in serial powering chain confirmed
- ATLAS ITkPixV1 FE prototype
  - Differential FE of RD53A FE with a few changes (under current and over voltage protection)
  - Confirms the desired behavior
  - Issue with high digital current, it will be solved in the next version

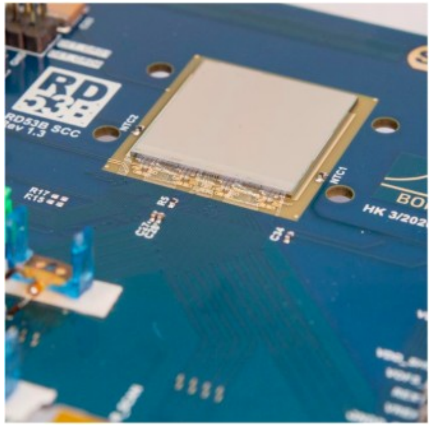

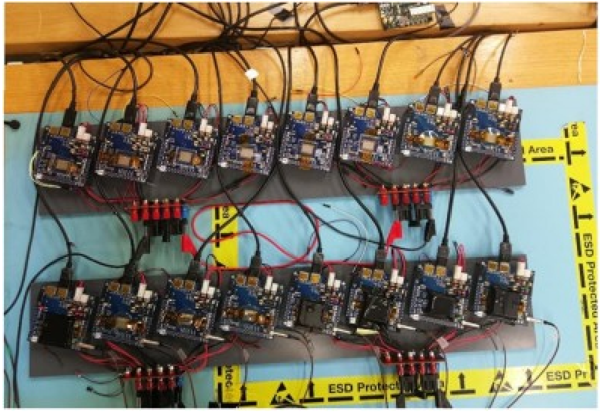

Surface radiation damage in silicon sensors

- **Observations on charge collection***
  of p-spray n^+-p strip sensor for Vbias = 600 V

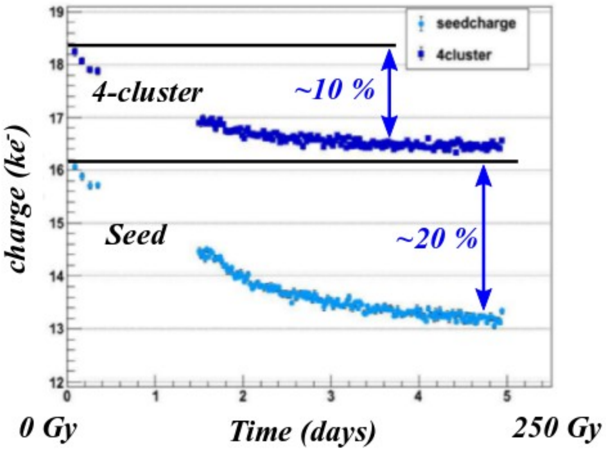

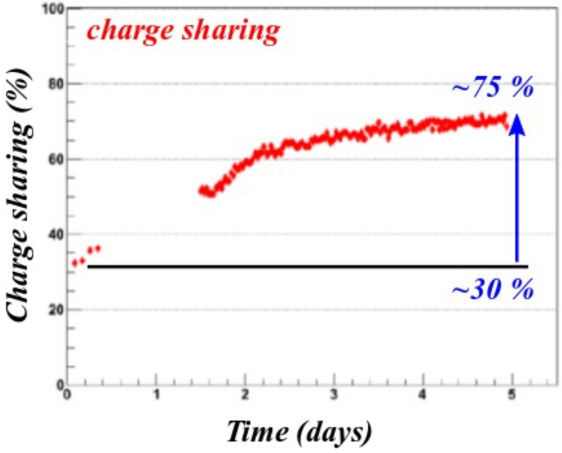

*CMS TRACKER GROUP collaboration, *Impact of low-dose electron irradiation on n^+-p silicon strip sensors*, Nucl. Instrum. Meth. A 803 (2015) 100 [arXiv: 1505.02672]

Surface charges influence charge collection

- **Simulation of N_{ox}^{eff} dependence on charge collection**

- n^+-p sensor with p-spray ($N_{p\text{-}spray}$ = $2.5 \cdot 10^{11}$ cm^{-2})

$N_{ox}^{eff} = 10^{10}$ cm^{-2}

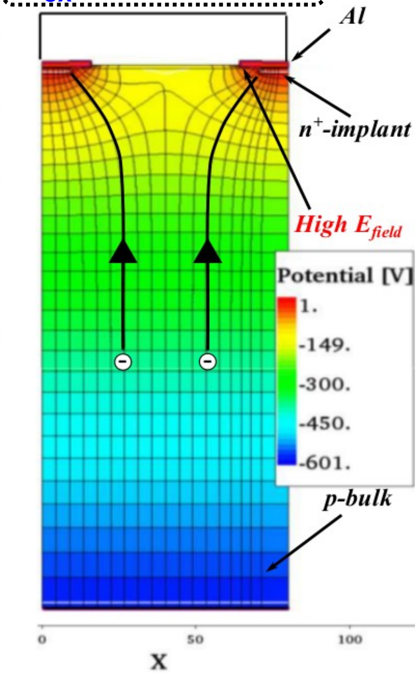

$N_{ox}^{eff} = 5 \cdot 10^{11}$ cm^{-2}

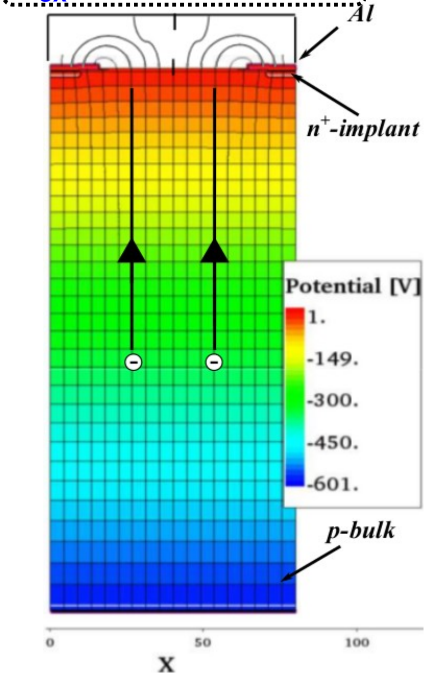

Noise source in silicon sensors

- **Noise source: time walk and time jitter**
- **Time walk: the voltage value V_{th} is reached at different times by signals of different amplitude**
- **Time jitter: the noise is summed to the signal, causing amplitude variations**

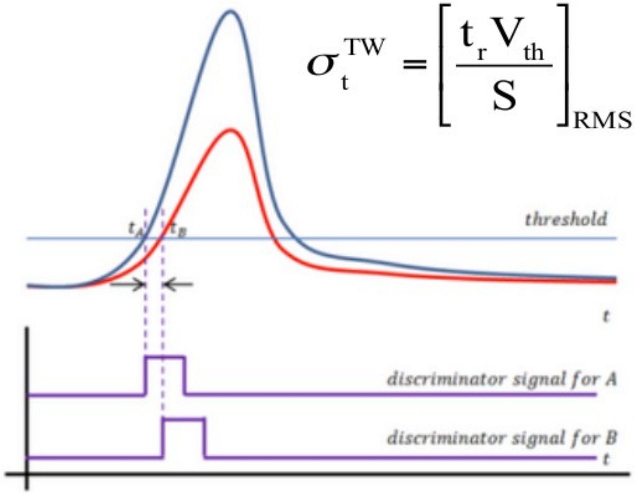

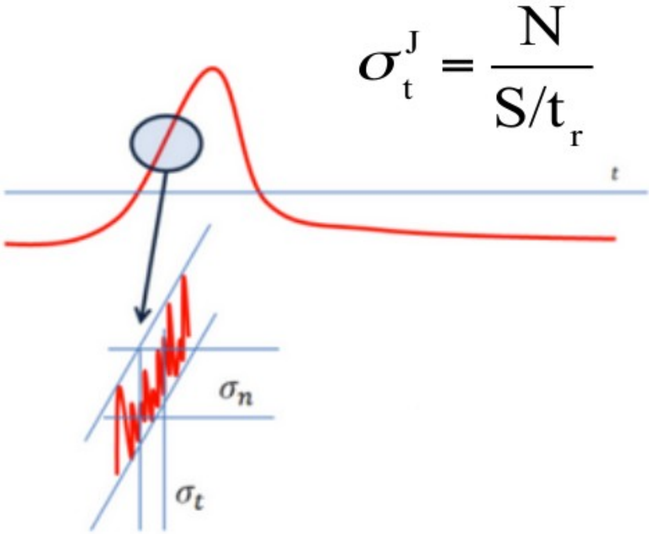

Due to the physics of signal formation

Due to electronic noise

$$\sigma_{Total}^2 = \sigma^2_{Time\ Walk} + \sigma_{Jitter}^2 + \sigma_{TDC}^2$$

Time resolution in signal formation

- **Time resolution and slew rate**

$$\sigma_t^2 = \left(\left[\frac{V_{th}}{S/t_r}\right]_{RMS}\right)^2 + \left(\frac{N}{S/t_r}\right)^2 + \left(\frac{TDC_{bin}}{\sqrt{12}}\right)^2$$

- **Where: S/t_r = dV/dt = slew rate, N = system noise, V_{th} = 10 N**
- **Assuming constant noise maximizing the S/t_r term → minimize the time resolution**
- **How the signal is formed in a sensor?**

  - A particle creates charge carriers, the carriers start moving under the influence of an external field

  - The charge carrier motion induces a current on the electrodes

  - The signal ends when the charges reach the electrodes
- **Signal shape is determined by Ramo's theorem:** $i \propto qvE_w$

  → Highest possible E_{field} to saturate velocity

  → Large pad to have uniform weighting field

  → A lot of charge

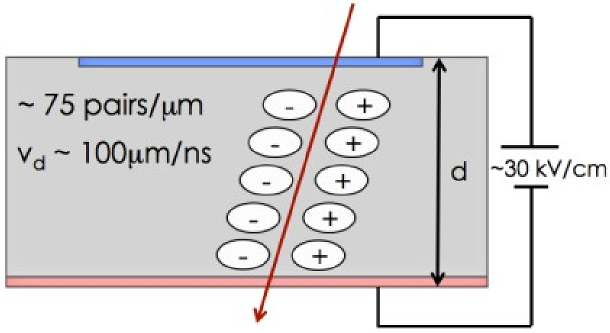

Low Gain Avalanche Detectors

- **LGADs: silicon sensors with gain ~ 10, minimize N, moderate S**
  - Low gain to avoid shot noise and excess noise factor
- **Ideal characteristics: 750 e/h pair per micron instead of 75 e/h, segmented, radiation hard, no dead time, very low noise, no cross talk**
- **Gain in silicon its based on the avalanche mechanism and starts in high electric fields, E~300 kV/cm**
- **Charge multiplication $N(l) = N_0 \cdot e^{\alpha \cdot l}$, $G = e^{\alpha \cdot l}$, α depends on E_{field},**
  α ~ 0.7 for electrons and 0.1 for holes [pair/μm]

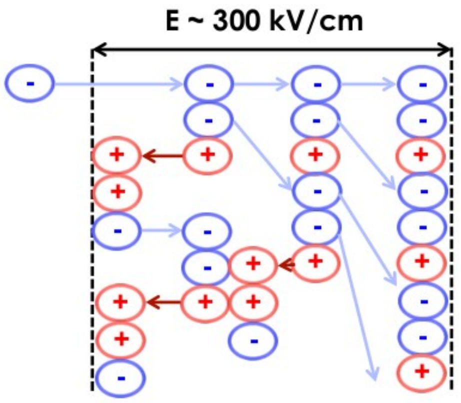

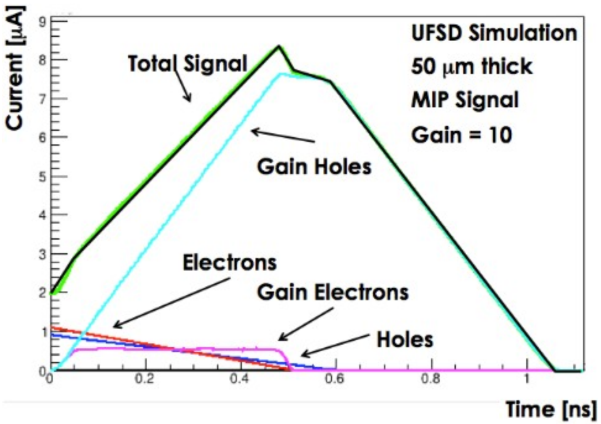

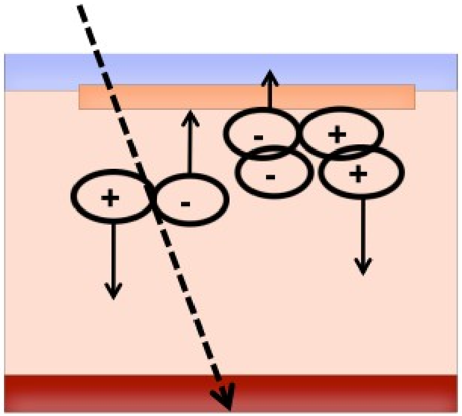

DECAL: Data acquisition system and software

- The data acquisition is done using a NEXYS Video board from Digilent and a specific made DECAL motherboard
- Ethernet based readout system using the ATLAS ITSDAQ data acquisition software

DECAL Hardware

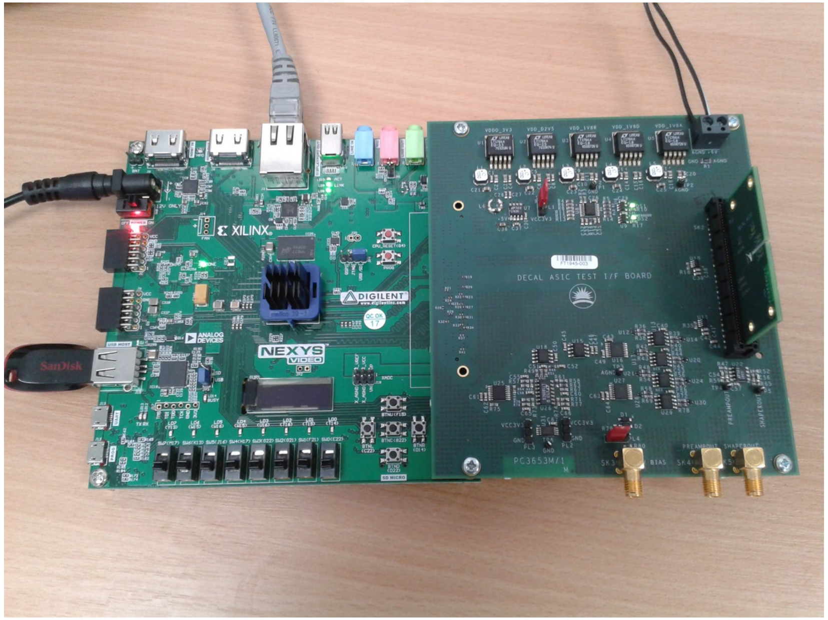

DECAL ASIC plugged in the motherboard

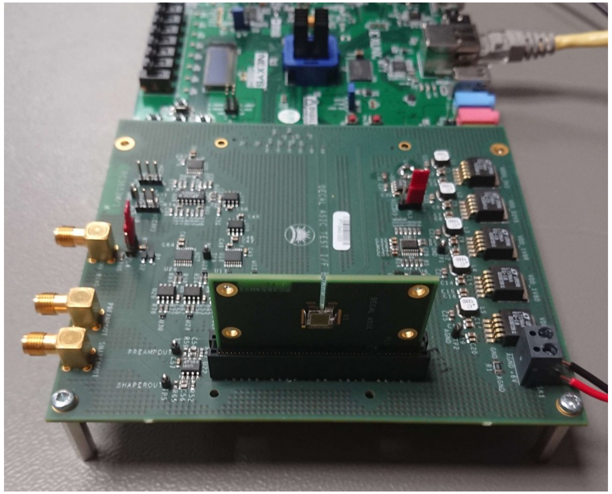

DECAL ASIC & MAPS sensor

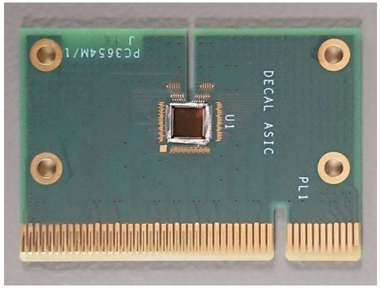

DECAL sensor test using monochromatic X-rays

- **Target material Cu used**
  - **- High voltage 60 kV and tube current 50 mA**
  - **- Alignment is performed using a laser**

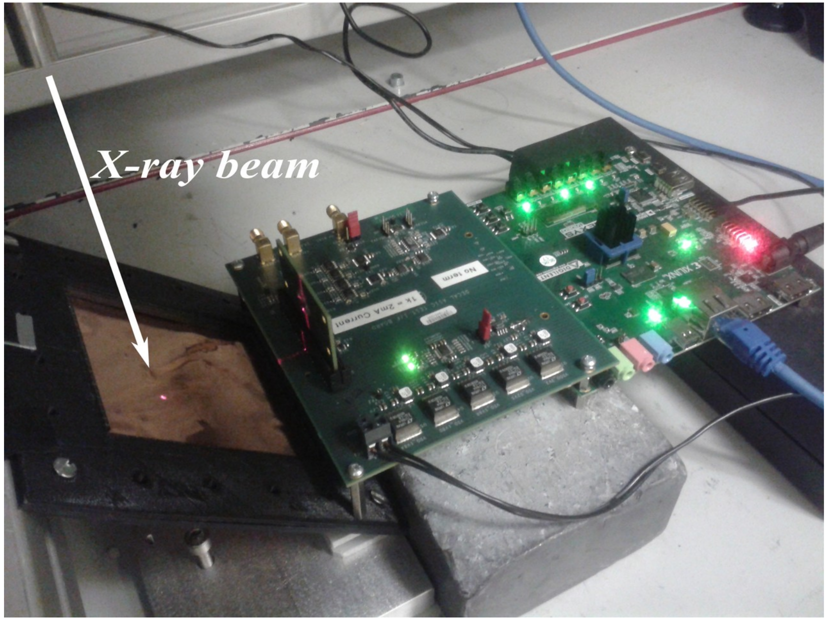

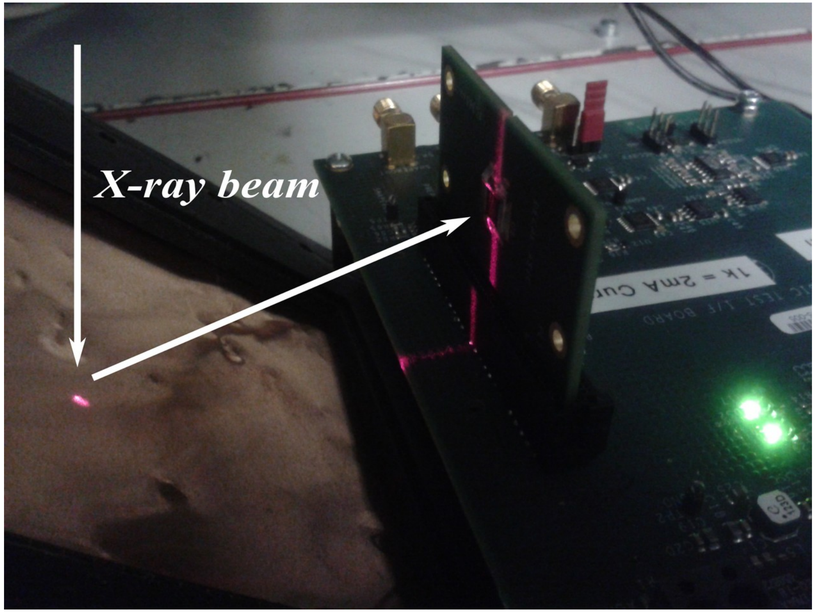

DECAL FD test with Sr90 source

- Uniform threshold voltage of the pixel matrix and long term threshold scan of a single row with a Sr90 source of 160 MBq activity

Threshold uniformity under Sr-90 exposure

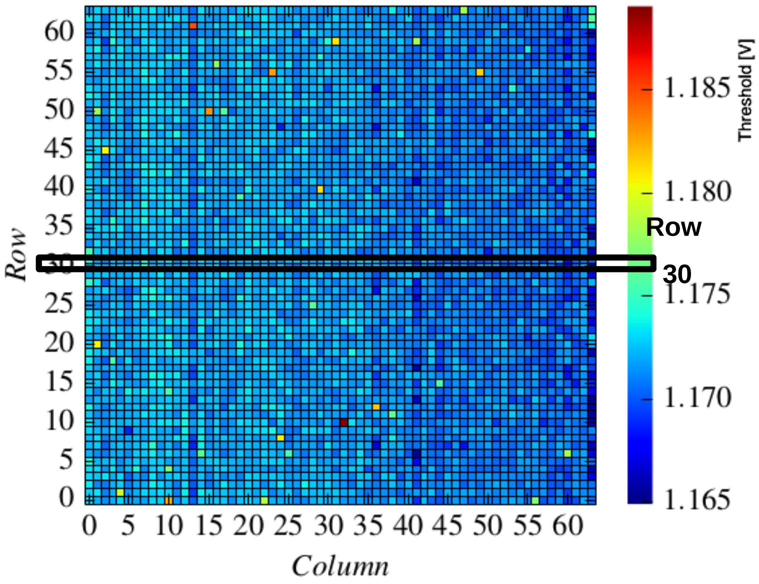

Long term threshold scan pixel row 30

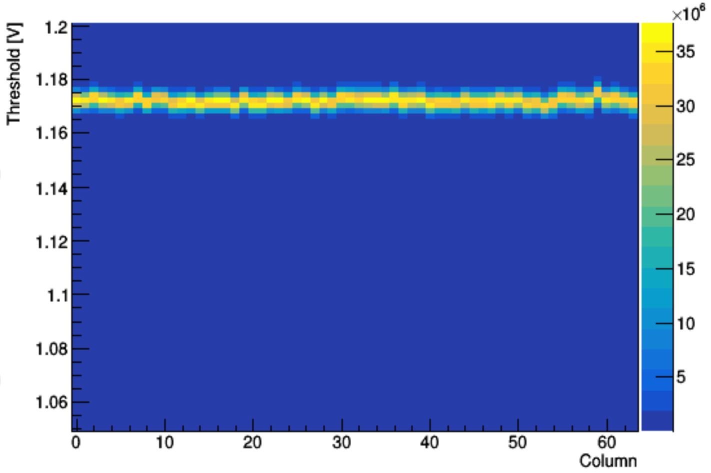

Pixel row threshold distribution

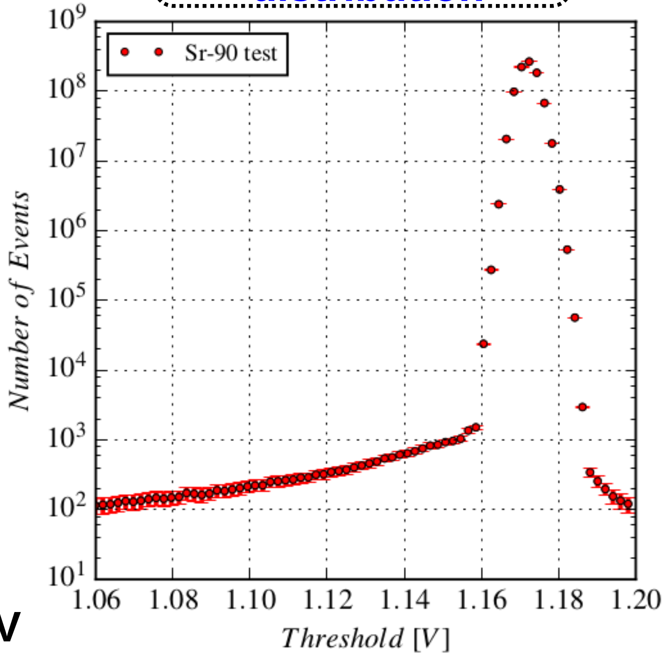

- Events recorded for thresholds below the global threshold ~ 1.17 V

- Evidence of MIP detection sensitivity

HR-CMOS sensor development

- **HR-CMOS R&D for digital calorimetry and tracking**

  - OVERMOS: A CMOS MAPS project demonstrator

  - DECAL sensor: DMAPS for digital electromagnetic calorimetry, pre-shower and outer tracking

  - TowerJazz Investigator chip & characterisation of the TowerJazz modified process

OVERMOS pixel

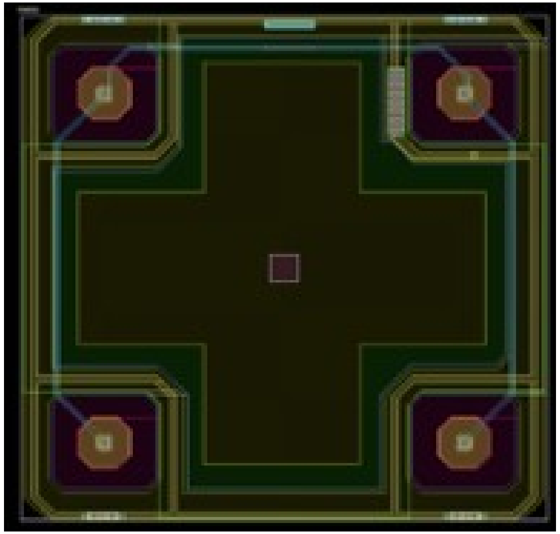

OVERMOS sensor matrix

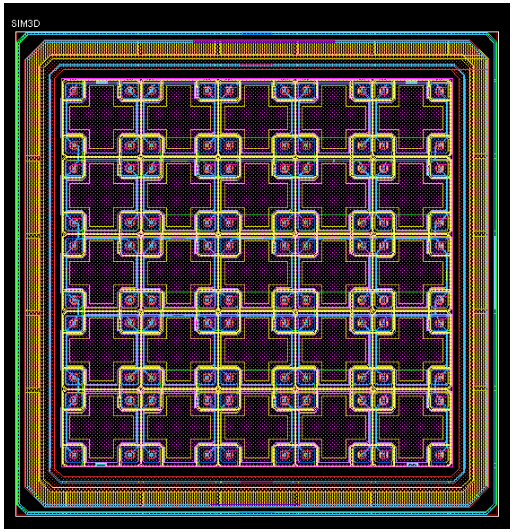

DECAL sensor matrix

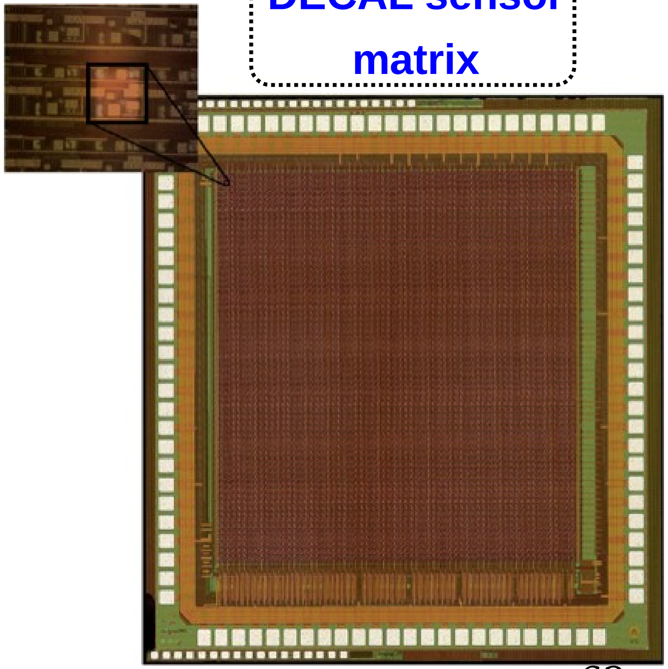

OVERMOS: A CMOS MAPS project demonstrator

- **OVERMOS 1.0 & 1.1 (project support from UKRI – STFC)**

  - Designed and fabricated in the standard TowerJazz 180 nm CMOS imaging process on 8 µm epitaxial Si, sensor matrix consists of 5x5 pixels with a pitch of 40x40 µm, multi diode arrangements within pixel, CMOS DPW originally proposed for DECAL of ILC

  - Neutron irradiations from $1 \cdot 10^{13}$ up to $1 \cdot 10^{15}$ n_{eq}/cm^2 at Ljubljana

- **OVERMOS characterisation results**

  - Measurement campaign and TCAD simulations to understand detailed device response

  - Charge collection results using IR laser illumination on non-irradiated/irradiated structures and comparison with optical TCAD simulations

Pixel cross section with individual doping layers

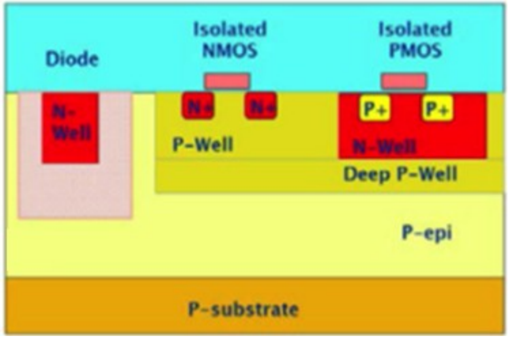

Simulated fabrication process in TCAD

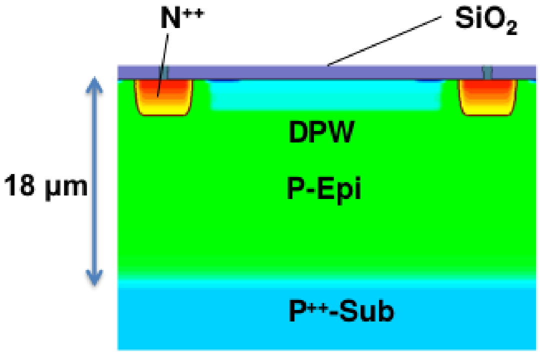

OVERMOS: A CMOS MAPS project demonstrator

- **OVERMOS 1.1 (TCAD simulation of Current vs Voltage as a function of fluence)**

  - Using the Hamburg Penta Trap Model (HPTM) presented in the RD50 workshop, Hamburg (4-6/6/18)

Current vs Voltage results before and after irrad. from data and TCAD simulation

E.G. Villani, TCAD process and device simulation of OVERMOS, a CMOS 180nm MAPS detector, 34th RD50 Workshop, Lancaster (12-14/6/19)

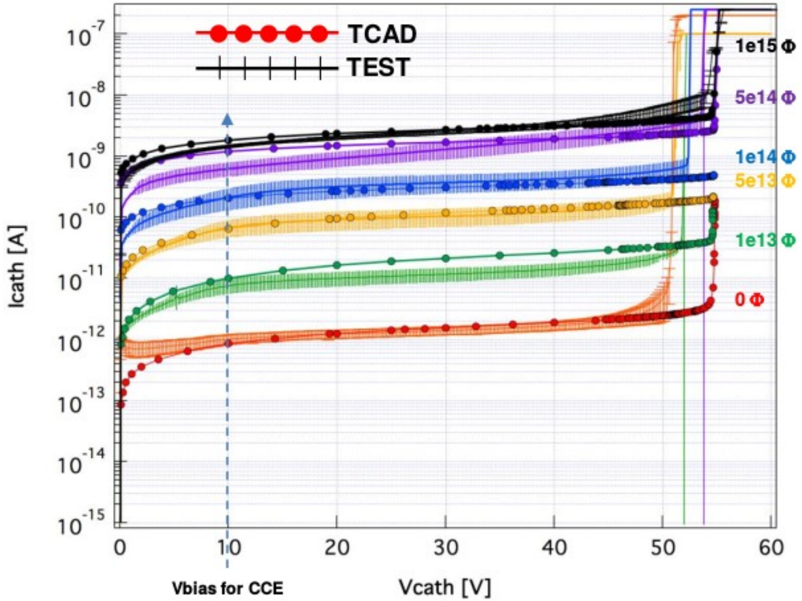

Φ	I_{leak_μ}[A] @10V	I_{leak_TCAD}[A] @10V	Δ%	aBV$_{\mu}$[V]	BV$_{TCAD}$[V]
0	1.0e-12	0.85e-12	15	50.8	54.79
1e13	7.5e-12	1e-11	-33.3	52	54.6
5e13	6.72e-11	7.47e-11	-11.1	51.2	54.7
1e14	2.1e-10	2.06e-10	1.9	52.4	54.7
5e14	6.21e-10	1.18e-9	-90	53.6	54.8
1e15	1.43e-9	1.83e-9	-28	54.4	54.8

Good agreement between data and TCAD simulation

OVERMOS: A CMOS MAPS project demonstrator

- **OVERMOS 1.1 (TCAD simulation of Charge Collection)**

CC results before irrad. from data and TCAD simulation for 3 pixel hit positions 7, 10, 25

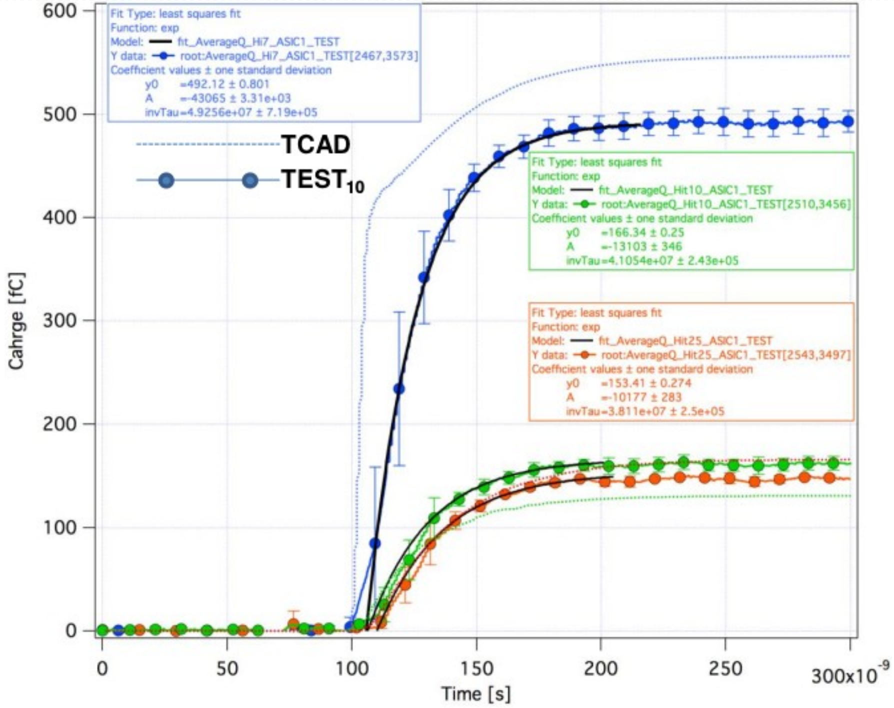

E.G. Villani, TCAD process and device simulation of OVERMOS, a CMOS 180nm MAPS detector, 34th RD50 Workshop, Lancaster (12-14/6/19)

$TEST_{10}$: Average of 10 pixels before irrad.

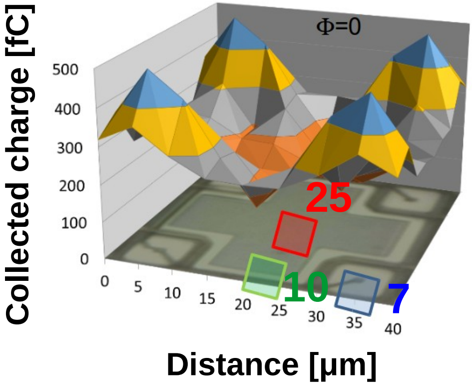

- **Pulse rise time differences between the data and TCAD simulation**
- **The effects of charge amplifier used during the measurements are under investigation**
- **After irradiation the results look similar and the total collected charge is lower for the same pixel hit positions**

Motivation digital EM calorimetry

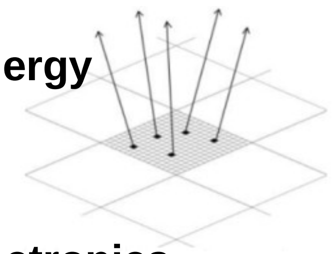

- **Digital SiW EM calorimetry with Monolithic Active Pixel Sensor**
  - Basic idea: count the number of pixels above threshold to estimate the shower energy
- **Small pixel size to avoid saturation (more than 1 hit/pixel) in high density showers**
- **Production costs of CMOS may decrease with growing market**
- **Full-system complexity and costs can be lower due to integration of sensor and electronics**

- **Potential to improve reconstruction if increased granularity can be exploited**
  (50 μm crossed strips vs 5 mm pads)
  - On-going simulation work with
  $\pi^0 \rightarrow \gamma\gamma$ reconstruction

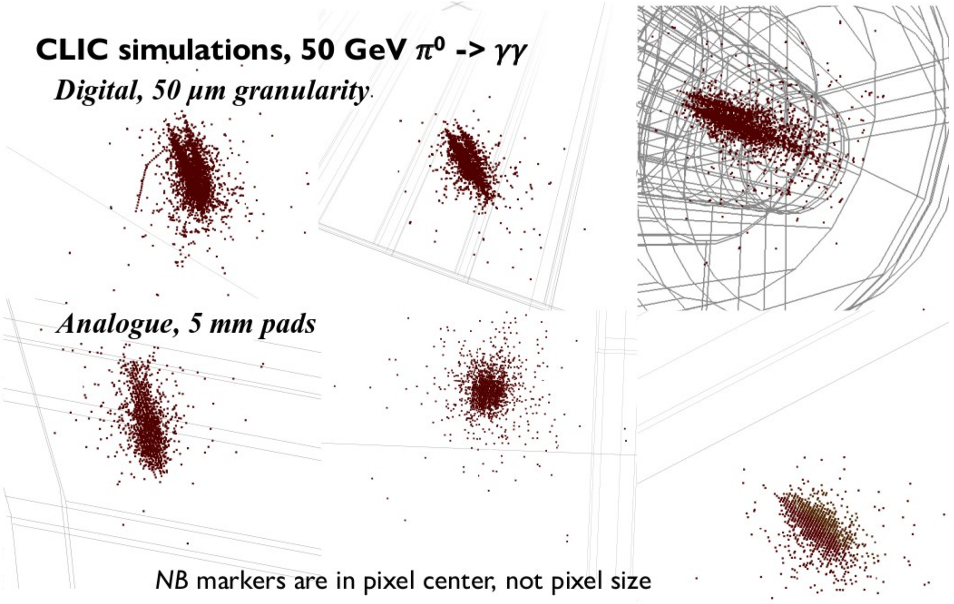

- **MAPS prototypes in 150 nm and 180 nm CMOS imaging process also demonstrate good radiation hardness**

The DECAL sensor

- Monolithic Active Pixel Sensor designed and fabricated in the standard TowerJazz 180 nm CMOS imaging process on 18/25 μm epitaxial Si
- Sensor matrix consists of 64x64 pixels with pitch of 55x55 μm
  - Four collection nodes, low capacitance, optimum cross talk reduction, expect good signal/noise
  - Operational with 1-2 V bias or higher voltage for faster charge collection
  - Pre-amplifier, shaper, comparator, discriminator and trimming logic
  - One pixel only with analogue output, data rate 40 MHz for the digital pixels
- The digital pixel

Simulated pixel in TCAD

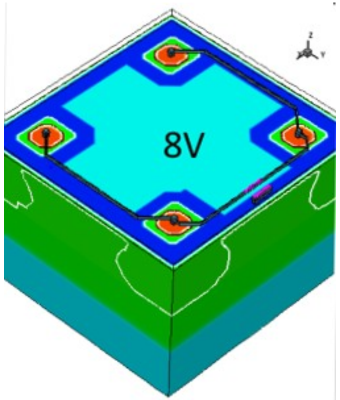

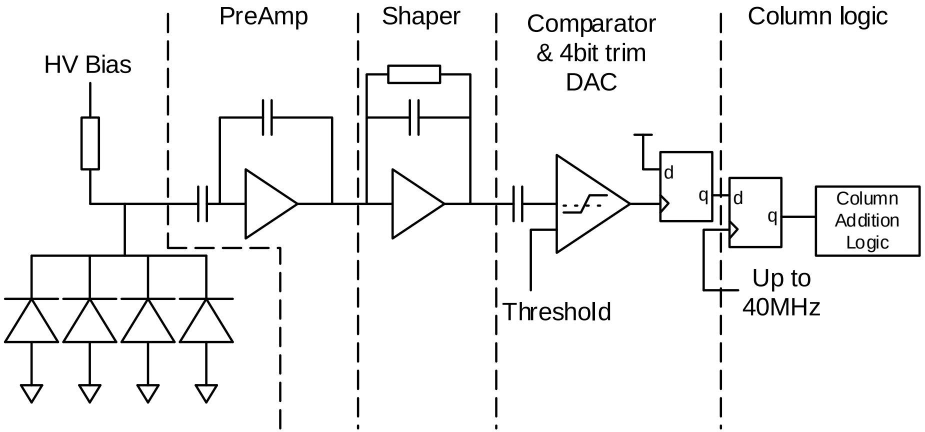

Single pixel gds picture

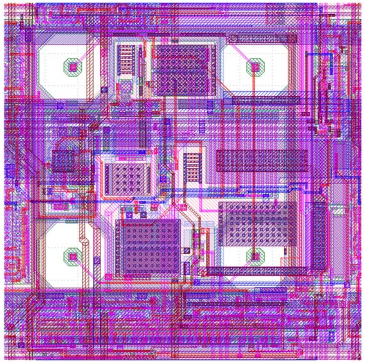

Data acquisition system & Analogue pixel test

- **The data acquisition is done using a NEXYS Video board from Digilent and a specific made DECAL motherboard**
  - Ethernet based readout system using the ATLAS ITSDAQ data acquisition software

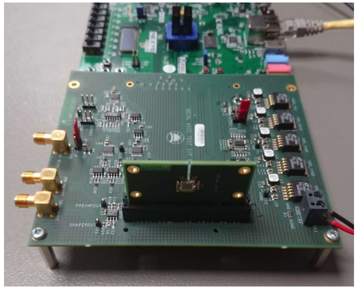

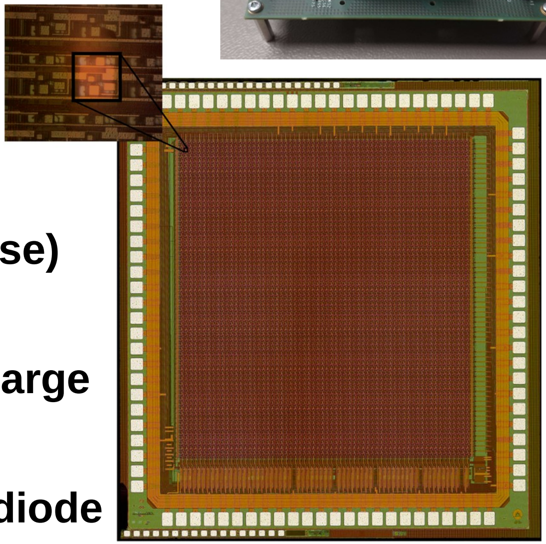

- **Laser illuminations with a TriLite (pJ/pulse) in the IR wavelength (1064 nm)**
- **Calculation of the equivalent injected charge in the 18 μm epi of the DECAL Si sensor for a laser spot of 10x10 μm² using a Si diode**

Shaper signal compared to Cadence simulations

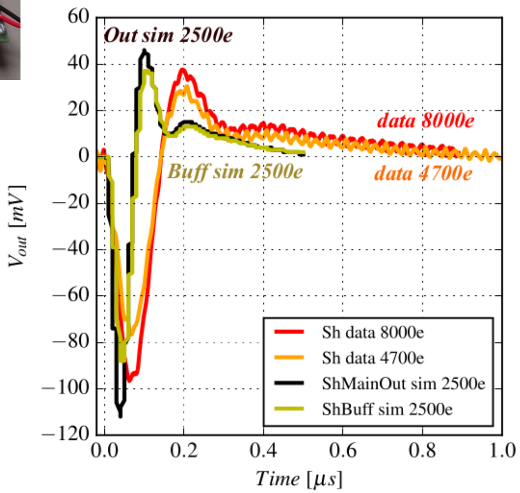

Agreement is observed in the rising time between the measured and simulated signal illuminating at the top left collection node of the analogue pixel
The injected charge estimated to be 2 or 3 times higher than the simulated charge value

Pixel & readout logic

- To achieve data rate of 40 MHz pixel column sum has to be complete within 25 ns
- The readout logic is configured either for strip or pad mode

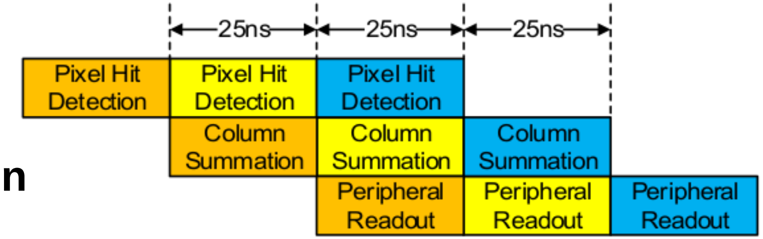

- Strip mode (1x64 pixel array) outputs per pixel column
  - Counts above threshold, max 3 hits per column
  - Data rate: 320 Mbits/s x 16 = 5.12 Gbits/s

- Pad mode (16x64 pixel array) outputs per pad area
  - 4 pad arrays, max 15 hits in each of four 16 column blocks (240 total counts)
  - Lower rate, about ¼ of the LVDS output channels

Overflow flag if max total counts exceeded

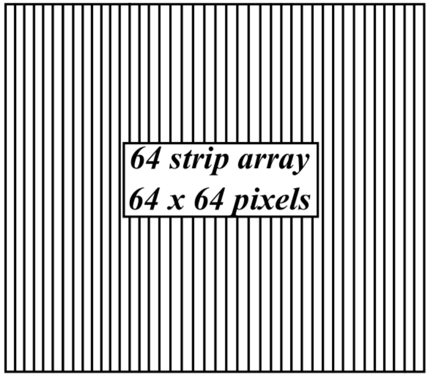

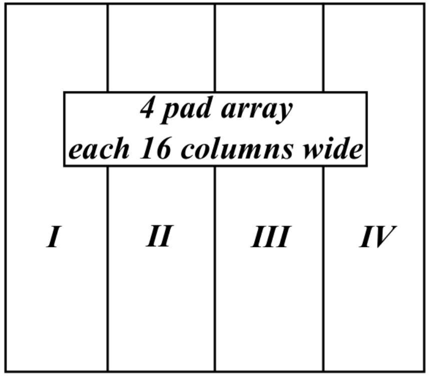

Testing of the digital functionality

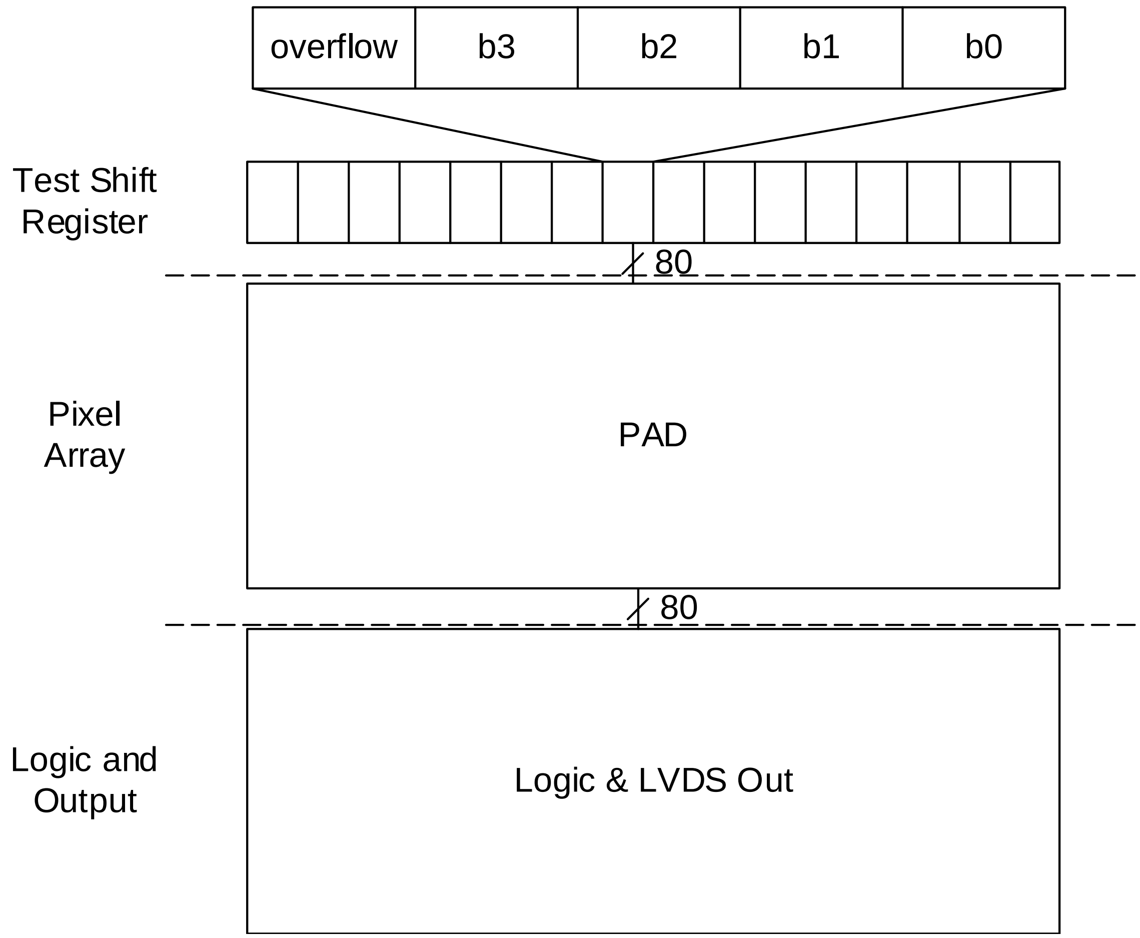

Digital functionality in strip and pad mode

- Testing pixel output by placing data in the test shift register, running the output, checking if output is correct, the test is complete for both strip and pad mode with the logic setup differently
- For pad mode, lower 4 bit of every column get added up, hence expected maximum is 240 for 16 column blocks, highest bits get summed in overflow

Inject_number(3) → 11 in the 1st strip

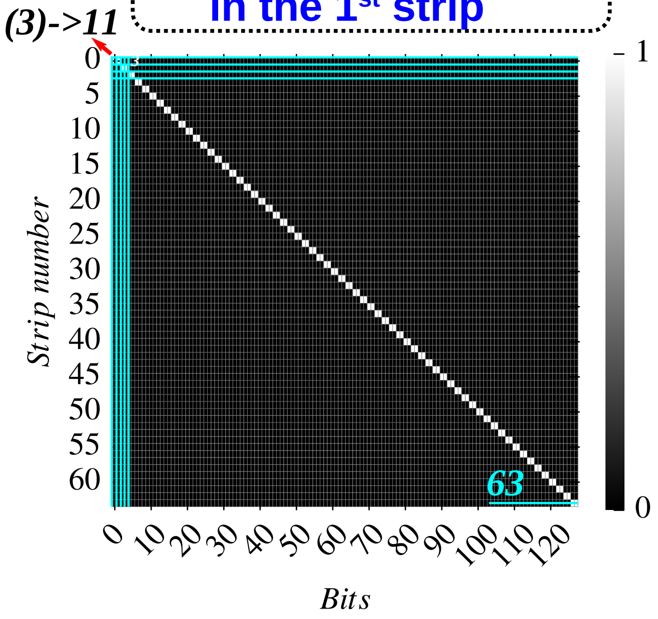

Inject_number(15) and total sum

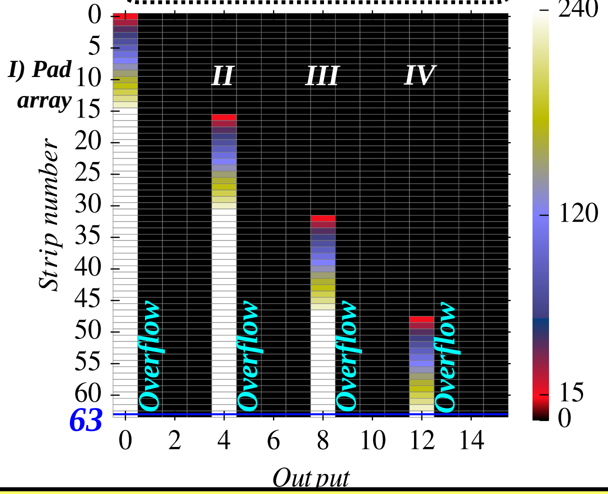

Inject_number(16) and total sum

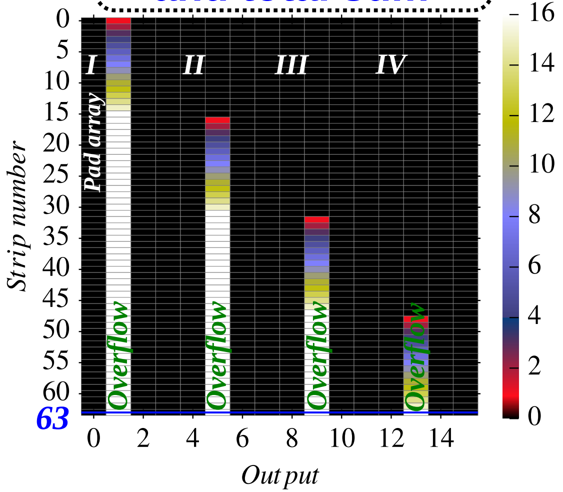

The observed maximum number is 240 and overflow is observed after the inject_number(16) with sum zero of the output blocks

Threshold scans: Digital functionality

- The performance of the digital pixels is evaluated performing threshold scans under laser illuminations with a diode laser and pulse frequency 100 kHz
  - Rate of hits in each pixel allows to test the full chain from analogue to digital
  - Threshold scan in strip mode with unmasked pixels and global chip configuration
- Defocused beam, hits recorded from around 10 strips, as the laser illumination causes the pixel shaper output voltage to drop
- Noise band and a clear signal response reflecting the Gaussian laser beam profile
- Using the laser trigger, the shaper response from a single strip is measured
- Time response of the order of 25 ns

Threshold voltage as a function of strip number

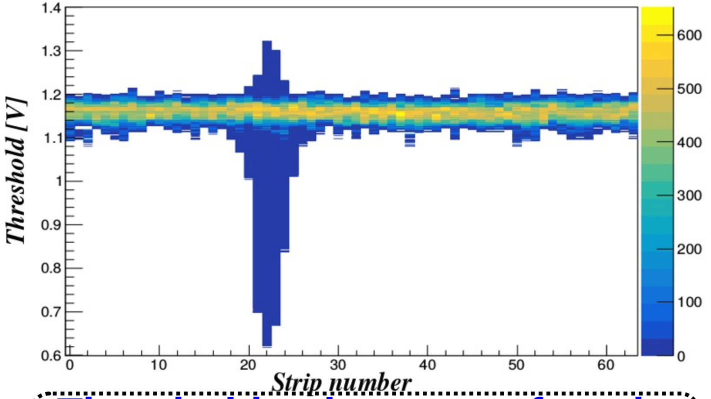

Threshold voltage as a function of bunch crossing number

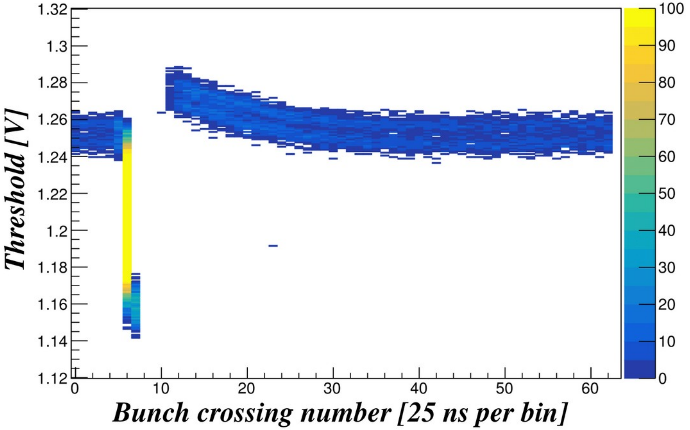

Threshold scans: Digital functionality

- Comparison of the summing logic in strip and pad mode under identical laser illumination conditions
  - With defocused laser beam 6 strips are fired at a global threshold value of 1 V

Strip mode

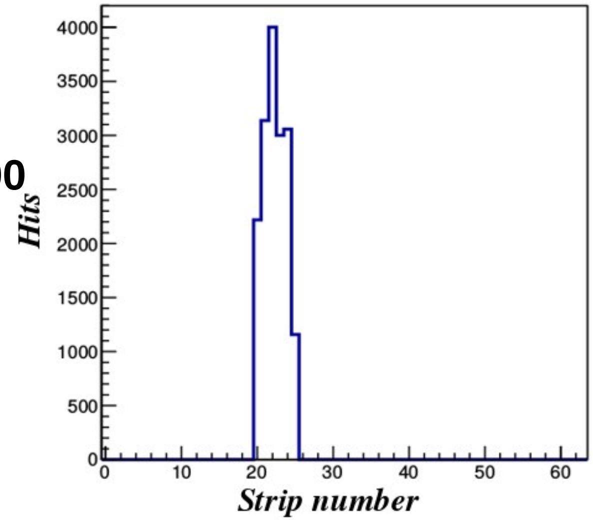

Pad mode

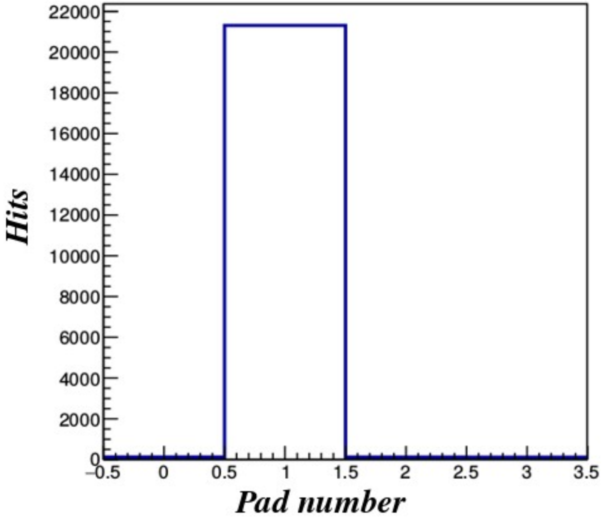

- The mean value of hits for each strip is approximately 3, the laser repetition was chosen 1000

- The strips, number from 20 to 25, fired in strip mode, correspond in pad number 1

The sum of hits for the 6 strips is smaller than the total number of hits in pad number 1, as in pad mode the max hits per strip can be up to 15. However in strip mode there is more information where each hit occurred due to higher granularity

Strip vs Pad mode as a function of illumination area

- **Laser illumination using an Al aperture with hole diameter in the range of 400 – 1100 μm**
- **Investigation of the dependence of the mean hits for strip and pad mode on the illumination area**

  - Linear behavior is observed as a function of hole area, as both strip and pad mode are operated below saturation

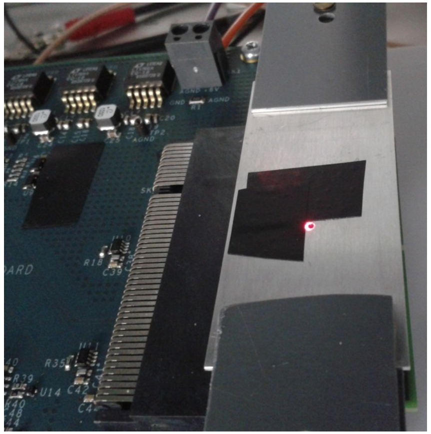

Mean value of hits as a function of threshold for hole diameter 1.1 mm

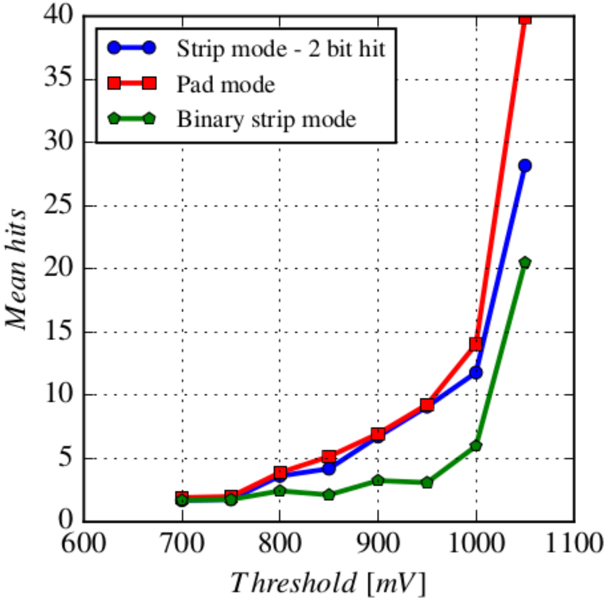

Mean value of hits for threshold 1V for different illumination hole area

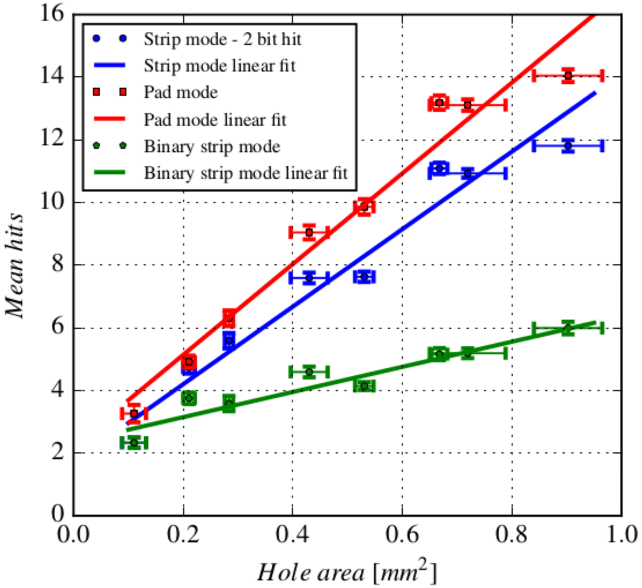

The TowerJazz 180 nm CMOS modified process

- The first version is referred to as an addition continuous n$^-$ layer design for each pixel
- The second version consists of two variants (gap in the n$^-$ layer and extra deep p-well) which expected to shape the electric field so the charge carriers produced are steered more directly towards the collection electrode in the pixel center

W. Snoeys et al., A process modification for CMOS monolithic active pixel sensors for enhanced depletion, timing performance and radiation tolerance, Nucl. Inst. and Meth. A 871 (2017) 90-96

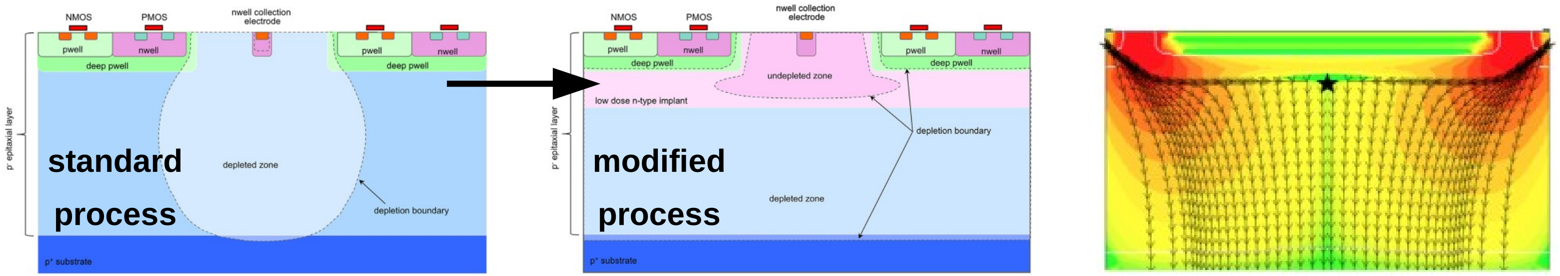

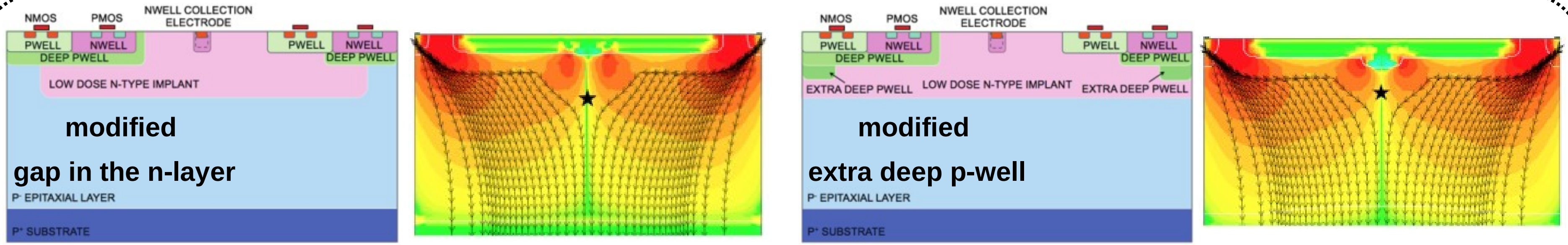

H. Pernegger, Depleted CMOS sensors for HL-LHC, Proceeding of Science, (VERTEX 2018), (041), 2018

M. Munker et al., Simulations of CMOS pixel sensors with a small collection electrode, improved for a faster charge collection and increased radiation tolerance, Journal of Instrumentation 14 (2019) C05013

Signal formation in planar pn diode

- Signal in electrodes by induction
- Electrodes (example parallel plates)
- Electrostatic problem can be solved by inf no. of image charges
- Moving charge changes charge profile
  → induces detectable signal
- Problem can best solved by method of weighting fields
- Example: charge pair +/-q produced at x_0

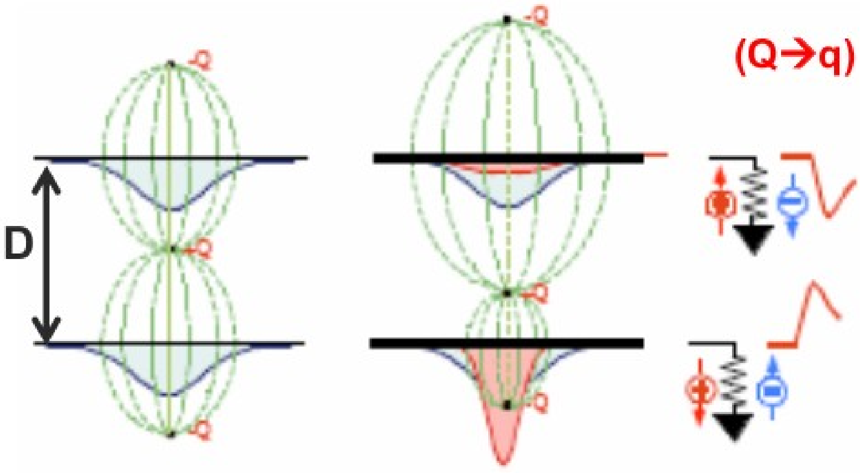

- induced current: $I = \frac{dQ}{dt} = -q\frac{v}{d}$

- total charge
  induced by -q $Q^- = -\frac{-q}{D}\int_{x_0}^{d} dx = -\frac{q}{D}x_0$
  induced by +q $Q^+ = -\frac{+q}{D}\int_{x_0}^{0} dx = -\frac{q}{D}(D - x_0)$

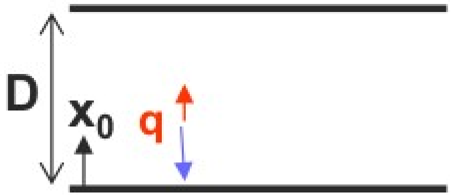

  sum $Q = Q^- + Q^+ = -q$

- Situation more complicated when electrodes are segmented (eg strip detectors)